

Effect of an Optimised Impact Pad on Molten Steel Quality in a 4 Strand Delta-shaped Tundish

by

Ahmed Kaiser Hamid

Department of Mining and Materials Engineering

McGill University, Montreal, Canada



July 2013

A thesis submitted to McGill University in partial fulfillment of the requirements of the degree of Masters of Engineering.

© Ahmed Kaiser Hamid, 2013

ABSTRACT

The tundish plays an important role to produce refined steel as well as acting in its traditional role as a steel distribution vessel. Presently, a tundish fitted with different flow control devices, such as an impact pad, dams, weirs, baffles, etc. is used to provide the maximum opportunity for carrying out various metallurgical operations such as inclusion separation, superheat control, reduced slag entrapment and to provide thermal and particulate homogenization. Modelling has shown that a correctly designed impact pad in a continuous casting tundish can significantly reduce the amounts of slag entrained into individual moulds during ladle change operations. It can also minimize non-metallic inclusions reporting to the final product by improving inclusion flotation efficiency.

Water can be used for the physical simulation, because the kinematic viscosities of liquid steel (at 1600°C) and water (at 20°C) are equivalent. In this one third scale water modeling work, the effects of an optimized impact pad on molten steel quality was evaluated in terms of “slag” entrainment during a ladle change, together with tracer dispersion studies and residence time distribution (RTD) analyses for isothermal and non-isothermal cases (temperature differences in between incoming fluid and existing fluid within the tundish) so as to visualize flow patterns developing within the tundish. Furthermore, the effect of increasing the molten steel capacity within the tundish by raising the liquid level, on the degree of slag entrainment during ladle changing operations, was also demonstrated.

RESUMÉ

Le Tundish joue un rôle important dans la production de l'acier raffiné ainsi que d'agir dans son rôle traditionnel d'un récipient de la distribution d'acier. Actuellement, un Tundish équipé de divers dispositifs de commande d'écoulement tels comme amortisseur d'impact, barrage, déversoirs, baffles, etc. est utilisé pour fournir le maximum de chances pour la réalisation de diverses opérations métallurgiques tels que la séparation d'inclusions, alliage rognage, réglage de la surchauffe, réduit piégeage de scories et pour fournir une homogénéisation thermique et de particules. La modélisation a montré que la conception d'un approprié amortisseur d'impact dans un Tundish de coulée continue permet de réduire de façon significativement les quantités de scories piégeage dans des moules individuels pendant les opérations de changement de louche. Cela réduit également les inclusions non métalliques et améliore le produit final en raison d'une plus grande efficacité de la flottation.

L'eau peut être utilisée pour la simulation physique, parce que la viscosité cinématique de l'acier liquide (1600°C) et de l'eau (20°C) sont équivalentes. A une échelle 1/3 du travail de modélisation, l'effet d'un optimale amortisseur d'impact sur la qualité d'acier fondu a été évaluée en termes de piégeage de scorie pendant le changement de "ladle", cette avec l'étude de la dispersion de traceurs et les analyses de la distribution des temps de séjour (RTD) pour les cas isothermique et non-isothermique (différence de température entre les flux de liquide d'entrée et sortie du Tundish) pour visualiser flux dans le Tundish. En plus l'affect d'augmenter la capacité d'acier fondue dans le Tundish par l'élévation du niveau du liquide, sur le grade du piégeage de scorie pendant les opérations de changement de louche ont aussi été démontré.

ACKNOWLEDGEMENTS

I would like to convey my sincere gratitude to my supervisor Professor R.I.L. Guthrie and Co-supervisor Dr. Mihaiela Isac for their advice, encouragement and support from the beginning to the end of my studies. This was a huge opportunity for me to be accepted as one of their graduate students. To me, the most crucial part was their encouragement. I felt more lively and energetic every time I met with them about my research works.

I would like to acknowledge the financial support received from the Natural Sciences and Engineering Research Council of Canada (NSERC) for research funding. I would also like to acknowledge the McGill Metals Processing Centre (MMPC) for providing the research facilities needed to carry out all the experiments.

I would like to thank all the group members of MMPC. I am gratefully indebted to Dr. Luis Calzado and Mr. Ken Morales for their help and support during water modeling experiments. My boundless thanks to my friend, Faisal Alghamdi, for his support, motivation and friendship, from the beginning to the end of my studies at McGill. I also express my heartfelt thanks to all of my friends, especially to Mr. Kaymul Islam, Senior Process engineer, KSRM steel plant limited, Bangladesh and Mr. Sajjad Hossain, Assistant Manager, Osmania Glass factory, Bangladesh for their encouragement and friendship during my research works.

Finally, I would like to express my sincere gratitude to the almighty God who gave me the ability to acquire and apply knowledge. There are no words for me to mention my acknowledgement to my father Nur Ahmed and my mother Ferdousi Begum, and my siblings Minhaz, Masud and Tasnim. It was their unconditional love, ultimate sacrifice and absolute motivation which made it possible for me to pursue my studies. I would also like to thank my paternal grandparents Late Siddique Ahmed & Late Ayesha Khatun, my maternal grandparents Abul Bashar & Late Nur Nahar Begum and my uncles including Nasir, Shahab, Gayas, Moin, Taslim & Yasin, for their helpful motivation for my studies.

NOMENCLATURE

L_m	: Length of model tundish	m
L_p	: Length of prototype tundish	m
λ	: Geometry scale factor	-
Q_w	: Reduced scale water flow rate	liter/minute
Q_s	: Molten steel flow rate	liter/minute
g	: Acceleration due to gravity	m/s^2
u	: Mean velocity of fluid through the cross section of the Tundish	m/s
Bu, Tu	: Buoyancy Number, $\frac{\beta\rho\Delta TgL^3/u^2}{Re^2}$	-
Gr	: Grashof number, $\beta\rho\Delta TgL^3/\nu^2$	-
Re	: Reynolds number, $\frac{\rho UL}{\mu}$	-
Fr	: Froude number, $\frac{U^2}{gL}$	-
Wb	: Weber number, $\frac{\rho U^2 L}{\sigma}$	-
Bo	: Bond number, $\frac{\rho g l^2}{\sigma}$	-
β_w	: Coefficient of thermal expansion of water, $\frac{1}{V} \frac{dV}{dT}$	K^{-1}
β_s	: Coefficient of thermal expansion of steel, $\frac{1}{V} \frac{dV}{dT}$	K^{-1}
μ	: Molecular Viscosity	kg/m.s
ρ	: Density	kg/m^3
ν	: Kinematic Viscosity, $\frac{\mu}{\rho}$	m^2/s
σ	: Surface Tension	N/m
F_i	: Inertial force	N

F_{μ}	: Viscous force	N
V, v	: Velocity	m/s
V^*	: Dimensionless velocity	-
x, L	: Length	m
t^*	: Dimensionless time	-
p, P_0	: Pressure	N/m ²
P^*	: Dimensionless Pressure	-
d_{in}	: Diameter of inclusion	μm
d_p	: Diameter of the simulant particle	μm
ρ_{in}	: Density of inclusion	kg/m ³
ρ_p	: Density of the simulant particle	kg/m ³
A	: Cross-sectional area of the ingot	m ²
ΔT	: Temperature difference between incoming steel and existing steel within tundish	K
$\Delta \rho$: Density difference between molten steel and simulated water	kg/m ³
\bar{t}	: Theoretical or nominal residence time	s
θ	: Dimensionless time	-
θ_c	: Dimensionless average time, up to $\theta=2, \frac{\sum_{\theta=0}^2 C_i \theta_i}{\sum_{\theta=0}^2 C_i}$	-
t_m	: Mean residence time, up to $\theta=2$	s
$\Delta \theta$: Dimensionless time difference	-
Q_a	: Volumetric flow rate through the active region of a tundish	m ³ /s
V_d	: Volume of dead region in a tundish	m ³

V_{dp}	: Volume of dispersed plug flow region in a tundish	m^3
V_m	: Volume of mixed flow region in tundish	m^3
θ_{min}	: Dimensionless time for the first appearance of tracer at the tundish exit	-
θ_{max}	: Dimensionless time for the maximum concentration of tracer in the tundish exit	-
ΔV	: Change in voltage	Volt
D	: Orifice diameter	μm
I	: Imposed DC current	Amp.
U_s	: Terminal rising velocity	m/s
Gu	: Guthrie Number, $\frac{Residence\ time, \tau_{Residence}}{Inclusion\ float\ out\ time, \tau_{Float\ Time}}$	-
N_{inlet}	: Number of inclusion at inlet	No. inlet/ m^3
N_{outlet}	: Number of inclusions at outlet	No. outlet/ m^3
C_D	: Drag coefficient	-
Bare tundish	: Tundish without any flow modifiers	-
MSIP	: Tundish fitted with McGill Standard Impact Pad(MSIP)	-
MIIP	: Tundish fitted with proposed McGill Improved Impact Pad(MIIP)	-
SEN	: Submerged entry nozzle	-

LIST OF FIGURES

Chapter-1

Figure 1.01: Schematic diagram of a continuous casting machine

Chapter-2

Figure 2.01: C-curve and F-curve for plug flow and well mixed flow system

Figure 2.02: A typical residence time distribution curve for flow in a tundish

Figure 2.03: Flow models and theoretical C-curves (a) Mixed model, and (b) Modified mixed model

Figure 2.04: Typical RTD curves for different widths of the tundish (Inlet Froude number 0.74, bath height 260mm and inlet exit distance of 780mm)

Figure 2.05: Simulated average residence time, dead volume, plug volume and mixed volume for different equivalent water levels in tundish

Figure 2.06: Vortex formation in a water model for different tundish equivalent steel levels in tundish, a) 30 ton, b) 35 ton, c) 37 ton and d) 40 ton

Figure 2.07: Schematic top view of curved tundish (symmetrical half) with flow control devices (pouring chamber)

Figure 2.08: Tundish geometry with weir and dam arrangement

Figure 2.09: Change in Stokes Rise Velocity with inclusion size

Figure 2.10: Trajectories of inclusions in the water flow: (a) Isothermal conditions and particle sizes from 1 to 10 μm , (b) Non-isothermal and particles sizes from 1 to 10 μm , (c) Isothermal conditions and particle sizes from 10 to 50 μm , (d) Non-isothermal conditions and particles sizes from 10 to 50 μm

- Figure 2.11: Tundish geometry with first chamber and second chamber
- Figure 2.12: Fluid flow in a round tundish with flow control devices after injecting blue ink: (a) 20s; (b) 30s; (c) 50s
- Figure 2.13: Comparison of RTD curve for isothermal and non-isothermal tundish

Chapter-3

- Figure 3.01: Three dimensional schematic illustration of tundish fitted with impact pad
- Figure 3.02: Orthographic projection of a 4 strand delta shaped tundish fitted with impact pad
- Figure 3.03: Schematic view of McGill standard impact pad (MSIP)
- Figure 3.04: Schematic view of McGill improved impact pad (MIIP)
- Figure 3.05: Schematic representation of tundish during slag entrainment test
- Figure 3.06: Schematic representation of tundish during tracer dispersion test
- Figure 3.07: Schematic view of tundish during residence time distribution (RTD) analysis

Chapter-4

- Figure 4.01: Schematic diagram of tundish during slag entrainment experiments
- Figure 4.02: Simulated slag layer (oil-sudan IV dye) on the top surface of tundish
- Figure 4.03: Slag movement in tundish fitted MIIP during ladle changing operations
- Figure 4.04: Slag movement in tundish fitted MSIP during ladle changing operations

- Figure 4.05: Attached Watman-5 filter paper in the SEN to collect entrained slag
- Figure 4.06: Comparative chart of weight of “slag” entrained during a ladle change simulation, for different FCD’s
- Figure 4.07: Comparative bar chart of weight of “slag” entrained during a ladle change simulation, with varying capacity of the tundish
- Figure 4.08: Effect of tundish capacity in reducing the amount of entrained slag
- Figure 4.09: Tracer distribution within the tundish under isothermal conditions, $\Delta t = 5s$, using different flow arrangements
- Figure 4.10: Tracer distribution within the tundish under isothermal conditions, $\Delta t = 8s$, using different flow arrangements
- Figure 4.11: Tracer distribution within the tundish under isothermal conditions, $\Delta t = 15s$, using different flow arrangements
- Figure 4.12: Tracer distribution within the tundish under isothermal conditions, $\Delta t = 32s$ with different flow arrangements
- Figure 4.13: Tracer distribution within the tundish under isothermal conditions, $\Delta t = 58s$, using different flow arrangements
- Figure 4.14: Tracer distribution within the tundish under isothermal conditions, $\Delta t = 120s$, using different flow arrangements
- Figure 4.15: Tracer distribution within the tundish under non-isothermal conditions after 10s, for different flow arrangements for a step up of $\Delta T = +10^{\circ}C$
- Figure 4.16: Tracer distribution within the tundish under non-isothermal conditions after 20s, for different flow arrangements for a step up of $\Delta T = +10^{\circ}C$

- Figure 4.17: Tracer distribution within the tundish under non-isothermal conditions after 32s, for different flow arrangements for a step up of $\Delta T = +10^{\circ}\text{C}$
- Figure 4.18: Tracer distribution within the tundish under non-isothermal conditions after 60s, for different flow arrangements for a step up of $\Delta T = +10^{\circ}\text{C}$
- Figure 4.19: Tracer distribution in the tundish under non-isothermal conditions after 10s, for different flow arrangements for a step down of $\Delta T = -10^{\circ}\text{C}$
- Figure 4.20: Tracer distribution in the tundish under non-isothermal conditions after 25s, for different flow arrangements for a step down of $\Delta T = -10^{\circ}\text{C}$
- Figure 4.21: Tracer distribution in the tundish under non-isothermal conditions after 42s, for different flow arrangements for a step down of $\Delta T = -10^{\circ}\text{C}$
- Figure 4.22: Tracer distribution in the tundish under non-isothermal conditions after 120s, for different flow arrangements for a step down of $\Delta T = -10^{\circ}\text{C}$
- Figure 4.23: $Bu(U_o^2/u_p^2)$ vs. temperature difference in a liquid steel tundish steel, for a 12 tonne capacity when a new ladle containing fresh liquid steel is employed
- Figure 4.24: $Bu(U_o^2/u_p^2)$ vs. temperature difference in a liquid steel tundish, for a 20 tonne capacity when a new ladle containing fresh liquid steel is employed
- Figure 4.25: RTD curves for a bare tundish under isothermal conditions
- Figure 4.26: RTD curves for tundish fitted with MSIP under isothermal conditions

- Figure 4.27: RTD curves for tundish fitted with MIIP under isothermal conditions
- Figure 4.28: RTD curves for a bare tundish under non-isothermal conditions with a step up temperature of $\Delta T = +10^{\circ}\text{C}$
- Figure 4.29: RTD curves for tundish fitted with MSIP under non-isothermal conditions with a step up temperature of $\Delta T = +10^{\circ}\text{C}$
- Figure 4.30: RTD curves for tundish fitted with MIIP under non-isothermal conditions with a step up temperature of $\Delta T = +10^{\circ}\text{C}$
- Figure 4.31: RTD curves for a bare tundish under non-isothermal conditions for a step down temperature of $\Delta T = -10^{\circ}\text{C}$
- Figure 4.32: RTD curves for tundish fitted with MSIP under non-isothermal conditions for a step down temperature of $\Delta T = -10^{\circ}\text{C}$
- Figure 4.33: RTD curves for tundish fitted with MIIP under non-isothermal conditions for a step down temperature of $\Delta T = -10^{\circ}\text{C}$

LIST OF TABLES

- Table 1.01: Properties of Water and Steel
- Table 4.01: Slag entrainment in tundish with different flow modifiers
- Table 4.02: Calculation of average particle rise velocity through a cross section of Tundish
- Table 4.03: $Bu(U_o^2/u_p^2)$ calculation in liquid steel tundish varying the size of tundish(full scale)
- Table 4.04: $Bu(U_o^2/u_p^2)$ calculation in water model tundish varying the size of tundish (full scale)
- Table 4.05: $Bu(U_o^2/u_p^2)$ calculation in water model tundish varying the size of tundish (1/3 scale)
- Table 4.06: RTD parameter for different configurations of tundish under isothermal conditions

LIST OF CONTENTS

Chapter 1. INTRODUCTION

- 1.1 Introduction
- 1.2 Continuous Casting Process and Tundish metallurgy
- 1.3 Motivation of the Present Work
- 1.4 Objectives

Chapter 2. LITERATURE REVIEW

- 2.1 Introduction
- 2.2 Physical Modeling Principles
- 2.3 Similarity Factors and Modeling Criteria Study
- 2.4 Dimensional Analysis
- 2.5 Metallurgical Performance Studies of the Continuous Casting Tundish
 - 2.5.1 Residence Time Distributions (RTD)
 - 2.5.2 Inclusion Separation
 - 2.5.3 Slag Entrainment during Ladle Changing Operations
- 2.6 Final Remarks

Chapter 3. EXPERIMENTAL PROCEDURES

- 3.1 Introduction
- 3.2 Slag Entrainment Experiments
- 3.3 Tracer Dispersion Studies
- 3.4 Residence Time Distribution (RTD) Analyses

Chapter 4. RESULTS AND DISCUSSION

4.1 Slag Entrainment Experiments

4.1.1 Tundish without Flow modifier (Bare Tundish)

4.1.2 Tundish fitted with McGill Improved Impact Pad (MSIP)

4.1.3 Tundish fitted with McGill Improved Impact Pad (MIIP)

4.1.3 Effect of Tundish Capacity on Slag Entrainment

4.2 Tracer Dispersion Studies

4.2.1 Isothermal conditions of Tundish with Different Flow modifiers

4.2.2 Non-isothermal conditions of Tundish with Different Flow modifiers

4.2.2.1 Step up temperature ($\Delta T = +10^{\circ}\text{C}$)

4.2.2.1 Step down temperature ($\Delta T = -10^{\circ}\text{C}$)

4.3 Residence Time Distribution (RTD) Analysis

4.3.1 Isothermal conditions in Tundish with different flow modifiers

4.3.2 Non-isothermal conditions in Tundish with different flow modifiers

4.3.2.1 Step up temperature ($\Delta T = +10^{\circ}\text{C}$)

4.3.2.2 Step down temperature ($\Delta T = -10^{\circ}\text{C}$)

Chapter 5. CONCLUSIONS AND FUTURE WORK

Conclusions

Future Work

References

CHAPTER-1

INTRODUCTION

1.1 Introduction

Steel is the favored material for the construction of structures, automobiles, ships, pipelines, mining equipments, offshore construction, aerospace, heavy equipment, and many other applications. The conventional method of steel production through continuous casting has evolved to achieve improved yield, quality, productivity and cost efficiency. After the final adjustments of composition and temperature at the furnace in order to ensure the mechanical properties for the desired grade of steel, molten steel is then transferred to the continuous caster. After that, the steel is passed through submerged entry nozzle (SEN) where it is partially solidified in a water cooled copper mould tube, before being totally solidified using water cooling spray nozzles lower down the strand. These products of continuous casting process are finally shaped into "semi-finished" products comprising billets, blooms, slabs, etc. for subsequent processing.

1.2 Continuous Casting Process and Tundish Metallurgy

About 92.8% of steel produced, worldwide, currently passes through the continuous casting process [1]. Continuous casting is the process of converting molten steel directly from a furnace into a solid ingot, on a continuous basis, for subsequent processing. These casting processes are currently the most advantageous, due to reduced energy costs, increased yield, improved quality and less pollution.

Figure 1 shows a schematic diagram of a single strand continuous casting system comprising of a ladle, a tundish, a mould, and system of water cooling nozzles. In this process, molten steel flows from the furnace into a teaming ladle, which then transfers it to the tundish. The tundish refers to an intermediate vessel placed between the ladle and the mould. It is used to supply and distribute molten steel to the moulds, at a near constant rate. In the moulds, molten steel solidifies against the water-cooled walls of a copper mold, so as to form a solidified shell. The molten steel flow rate is regulated by controlling the opening in the submerged entry nozzle (SEN) using a level sensor in the

mold. The steel flow is kept as steady as possible, since meniscus level fluctuations can create surface cracks. A mold slag layer or an oil layer, is used so as to prevent the steel from being exposed to air. It also offers thermal insulation and works as an "inclusion absorbers", plus its primary task of providing a lubricating layer of molten slag to prevent sticking of the steel strand to the copper mould. When the molten core is fully solid, the ingot is cut with oxyacetylene torches to the desired lengths. Later, these transfer bars are reheated to a homogeneous temperature and rolled into sheet, rods, rails, and other shapes. Now-a-days, the position of the rolling mills are set up closer to the caster so as to reduce energy consumed by the gas fired reheating furnace [2].

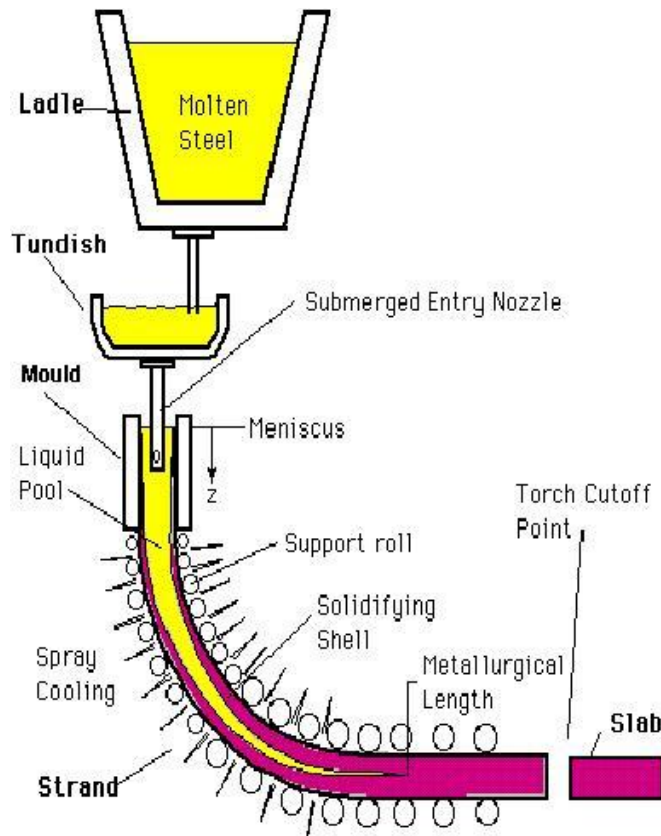


Fig.1.1. Schematic diagram of a continuous casting machine [2].

The tundish plays an important role in producing refined steel. If the inclusion particles exist in the ingot, then various surface defects such as “slivers” may occur during subsequent rolling operations. Similarly, internal inclusions can lead to local internal stress concentrations that might lower the fatigue life of the material. Presently, a tundish

is designed to provide the maximum opportunity for carrying out various metallurgical operations such as inclusion separation, flotation, alloy trimming. Similarly, a tundish as well as acting in its traditional role as a buffer or steel distribution vessel, can be used to avoid re-oxidation of molten steel, to control superheat, to prevent slag entrapment during ladle changing operations and to provide thermal and particulate homogenization. The general trends to obtain these metallurgical effects are to optimize steel flow patterns and to prolong the residence time of liquid steel in the tundish. This is accomplished by either increasing the volume of tundish and/or using flow control devices, such as impact pads, dams and weirs, within the interior of the tundish [2].

1.3 Motivation for the Present Work

Steelmakers have to face enormous challenges to improve liquid steel quality during continuous casting. Proper measures must be taken in order to achieve desired compositions and steel purity. Basically, inclusions contaminate the molten steel and later, they are entrained into the ingots where they can cause minor or major failures during rolling processes in the solid state. As we know, the tundish acts as a buffer and distributor of liquid steel between the ladle and the moulds of the continuous casting machines. As such, the tundish can play an important part in the removal and control of inclusions. To minimize the numbers and sizes of inclusions, one can modify the fluid flow patterns. Currently, this is accomplished by using different types of flow control devices (FCD), such as dams, weirs, baffles, impact pads, turbulence inhibitors, etc. and/or a combination of these. This “furniture” can provide sufficient time for the inclusions to float up and out, into a protective layer of slag, and by generating surface directed flows that can significantly reduce the amount of inclusions entraining the moulds. However, these melt flows can change significantly due to density differences during ladle change operations when, for instance, hot steel is poured into existing cooler steel within a tundish. This will enhance the effect of thermal buoyancy forces on the melt flow pattern. Another factor requiring consideration is the temperature drop of molten steel while held in the ladle. This can change fluid flow patterns appreciably due to heat losses from molten steel, through heat conduction and convection from the side walls and from the bottom, and from radiation from the top surface of bath. So, in an

actual tundish system, both incoming molten steel temperature variations and tundish heat losses to the ambient surrounding occur. Therefore, the effects of thermal buoyancy forces and mixed convection patterns need to be taken into account in any study of molten metal flows.

Slag entrainment in tundishes during ladle change operations has a very detrimental effect on steel quality. It has been reported by a few researchers that this should be considered very carefully in designing new flow modifiers for the industry. The literature is rather lacking on this aspect. Intensive research work is going on at the McGill Metals Processing Centre (MMPC) to minimize the amounts of entrained slag, particularly during ladle change operations. This could provide better consistency and quality of steel. Similarly, few researchers have studied thermal stratification of steel flows in a tundish, using different flow control arrangements. A non-isothermal water model has been used in this work to assess the practical conditions within a steel plant. There needs to be further analyses on these two aspects.

1.4 Objectives

In this research, physical modelling of a tundish (one third scale) was performed in order to investigate the fluid flow fields and inclusion removal efficiency, under 1) isothermal conditions within a tundish, i.e. approximately zero temperature difference between the incoming fluid passing through ladle shroud into the tundish and existing fluid within a tundish, and 2) non-isothermal conditions in a tundish with a step up temperature of $\Delta T = +10^{\circ}\text{C}$ and a step down temperature of $\Delta T = -10^{\circ}\text{C}$. The objective of the study was to identify suitable impact pads on the basis of tracer dispersion studies, residence time distribution (RTD) analyses, and slag entrainment experiments. We compared the performance of a recently proposed flow modifier, the McGill Improved Impact Pad (MIIP) with the conventional McGill Standard Impact Pad (MSIP) currently being used by the RTIT plant, and a bare tundish. Also, the effects of slag entrainment tests in tundishes during ladle change operations were carried out using increased bath heights in the tundish fitted with the McGill Improved Impact Pad (MIIP), for raising the volumetric flow of steel through the ladle-tundish-mould system .

CHAPTER-2

LITERATURE REVIEW

2.1 Introduction

Numerous operating conditions such as high temperatures, visual opacity, the relatively large size of industrial tundishes, etc. cause severe problems in direct experimental approaches. For this reason, reduced scales transparent models (e.g. a plexi glass model using water as a simulating fluid) have been used extensively in order to investigate the hydrodynamics, and associated transport phenomena, taking place within a continuous casting tundish. Beside water models, mathematical modeling has also become another reasonable alternative for investigating the fluid-dynamic characteristics and associated heat and mass transfer phenomena in tundishes [3].

2.2 Physical Modeling Principles

The physical model is created in accordance with a real unit of an industrial tundish, using the principle of geometrical similarity [4]. Water can be used for the physical simulation, because the kinematic viscosities of liquid steel (at 1600°C) and water (at 20°C) are equivalent. As such the flows of both fluids are similar from an inertial, or Reynolds Number, point of view. The properties are listed in Table 01.

Table 01: Properties of Water and Steel [3].

Property	Water (at 20°C)	Steel (at 1600°C)
Molecular Viscosity(μ), kg/m-s	0.001	0.0064
Density(ρ), kg/m ³	1000	7014
Kinematic Viscosity($\nu = \frac{\mu}{\rho}$), m ² /s	10×10^{-7}	6×10^{-7}
Surface Tension(σ), N/m	0.073	1.6

A comprehensive review of such investigations was first carried out by Mazumdar and Guthrie [3] in 1999, and lately by Chattopadhyay, Isac and Guthrie [5] in 2010. From these reviews, it can be observed that experimental measurements using water models are widely used, and considering the similarity laws, the results from water modelling can be transferred to the real process.

2.3 Similarity Factors and Modelling Criteria Study

For a reliable depiction of flow in the model tundish, there should be constant ratios between corresponding quantities in the model and the actual tundish. It is noted that the industrial vessel and laboratory-scale water-plexiglass tundish are known as the prototype and the model, respectively. Dyes or other tracer dispersion experiments in water models have proved to be very efficient in developing a qualitative understanding of various flows in real liquid steel systems. Furthermore, residence time distributions (RTD) in water model experiments have been measured by many researchers, as this is another important parameter in the analysis of flow within the whole volume of a tundish. Similarly, Particle Image Velocimetry (PIV), Laser Doppler Velocimetry (LDV) and hot wire anemometry techniques have all been used to obtain two dimensional, or even three dimensional vector fields and local velocities. For melt flows in tundishes, the necessary similarity criteria can be divided into several categories. These are geometric, kinematic, dynamic and thermal similarity [5].

Geometric Similarity implies that the actual tundish and its model should be geometrically similar. The scale factor, λ should be constant for all dimensions. All dimensions should satisfy the following relations.

$$Length_{model}, (L_m) = Scale\ factor, (\lambda) \times Length_{prototype}, (L_p)$$

Kinematic similarity deals with the similarity of motions. Each corresponding fluid element in the two systems should follow a geometrically similar path, and the time intervals between the corresponding events should bear a constant ratio which is known as the time scale factor.

Dynamic similarity means forces acting in the two systems which accelerate or retard the moving liquid element in the system at a corresponding time and corresponding location in a model tundish, should bear a constant ratio with the forces in an actual tundish. Inertial force (F_i), viscous force (F_μ), and gravitational force (F_g) are considered as governing forces for the flows in the tundish, and are described as follows[6] :

$$\frac{F_{i,m}}{F_{i,p}} = \frac{F_{g,m}}{F_{g,p}} = \frac{F_{\mu,m}}{F_{\mu,p}} = \text{Constant}$$

Where subscript m and p denote model and prototype (actual tundish), respectively.

However, there are some other similarity criteria like thermal and chemical similarity, which most often are not considered in the hydrodynamic studies of melt flows in the tundish. Geometric and dynamic similarities are used extensively to describe the hydrodynamic studies of melt flows in the model tundish and prototype [7].

2.4 Dimensional Analysis

Dimensional analysis or the principle of similitude, is an important method for the experimenter in thermo-fluid dynamics. From this analysis, a researcher can quantify certain information about the relations which hold between measurable quantities associated with various phenomena. It acts as a guideline towards efficient and correct experimental procedures and modeling criteria. The three most important approaches to modelling or the 'Differential Equation Approach', 'Rayleigh's Method of Indices' and ' Buckingham's π Theorem'. The 'Differential Equation Approach' is treated as the most precise one and hence is described briefly [8].

In this approach, some dimensionless groups are derived by non-dimensionalizing the differential equations that describe the fluid flow, heat and/or mass transfer. The non-dimensionalizing of the Navier-Stokes equation (Equation 1) that governs the fluid flow is shown in below [6].

In Cartesian coordinate system for isothermal flow the Navier-Stokes equation is written as:

$$\rho \frac{Dv}{Dt} = -\nabla P + \mu \nabla^2 v + \rho g \dots \dots \dots (2.1)$$

By defining different non-dimensional variables using scaling parameter, we get:

$$v^* = \frac{v}{V}, x^* = \frac{x}{L}, t^* = \frac{tV}{L}, p^* = \frac{P-P_0}{\rho V^2}, \nabla^* = L\nabla \text{ and } \nabla^{*2} = L^2\nabla^2$$

Substituting these values in equation (2.1) and simplifying, we can get the non-dimensional equation (2. 2).

$$\rho \frac{Dv^*}{Dt^*} = -\nabla^* P^* + \frac{\mu}{\rho VL} \nabla^{*2} v^* + \frac{gL}{V^2} \dots \dots \dots (2.2)$$

$$\Rightarrow \rho \frac{Dv^*}{Dt^*} = -\nabla^* P^* + \frac{1}{Re} \nabla^{*2} v^* + \frac{1}{Fr} \dots \dots \dots (2.3)$$

$$Re = \frac{\text{Inertial Force}}{\text{Viscous Force}} = \frac{\rho UL}{\mu} = \text{Reynolds Number}$$

$$Fr = \frac{\text{Inertial Force}}{\text{Gravity Force}} = \frac{U^2}{gL} = \text{Froude Number}$$

For modelling surface flow where surface tension value can be important. Govindarajan. et al. [9], and Lifeng Zhang et. al [10] have also used Weber number. This dimensionless number represents the ratio of the inertia and surface tension forces.

Froude similarity in water model and steel systems require:

$$Fr = \left(\frac{U^2}{gL}\right)_w = \left(\frac{U^2}{gL}\right)_s$$

$$\Rightarrow \frac{U_w}{U_s} = \sqrt{\lambda} \text{ [Replacing the geometry scale factor, } \lambda = L_w/L_s \text{] } \dots\dots\dots(2.4)$$

Where subscript *w* and *s* indicate water and steel, respectively.

Similarly, Weber similarity in water model and steel caster requires

$$Wb = \left(\frac{\rho U^2 L}{\sigma}\right)_w = \left(\frac{\rho U^2 L}{\sigma}\right)_s \dots\dots\dots(2.5)$$

Here, the density of liquid steel, ρ_s and water, ρ_w are 7020 kg/m³ at 1550°C and 998 kg/m³ at 20°C, respectively and the surface tension of liquid steel, σ_s and water, σ_w are 1.6 N/m at 1550°C and 0.073 N/m at 20°C, respectively [10].

By combining equation (2.4) and (2.5), we get:

$$\lambda = \left(\frac{\rho_s \sigma_w}{\rho_w \sigma_s}\right)^{0.5} = 0.5665 = 0.6 \text{ (Approx.)}$$

Therefore, a 0.6 scale water model can satisfy both Froude similarity and Weber similarity simultaneously, but not Re and Fr. For the latter, a full scale water model is needed.

Moreover, the scaled down water flow rate (Q_w) and molten steel throughput (Q_s) for small scale models are correlated according to [11] :

$$\frac{Q_w}{Q_s} = \frac{U_w L_w^2}{U_s L_s^2} = \sqrt{\lambda} \times \lambda^2 = \lambda^{5/2} \dots\dots\dots(2.6)$$

The important forces which govern liquid flow in tundish are inertial, viscous and gravitational forces. Thus, at corresponding points, and corresponding times, in the model and in an actual tundish, the Reynolds Number and Froude Number are constant. So full scale modeling tundish studies were done based on Reynolds and Froude criteria [10].

Reynolds similarity in water model and steel system are:

$$Re = \left(\frac{\rho UL}{\mu}\right)_w = \left(\frac{\rho UL}{\mu}\right)_s \dots\dots\dots(2.7)$$

Where molecular viscosity of liquid steel, μ_s and water, μ_w are 0.0064 kg/m-s at 1550°C and 0.001 kg/m-s at 20°C, respectively [3].

Combining (2.4) and (2.7), we obtain:

$$\lambda = \left(\frac{\rho_s \mu_w}{\rho_w \mu_s}\right)^{\frac{2}{3}} = 0.88 = 1(\text{approximately})$$

So full scale modeling tundish (Geometry scale factor, $\lambda=1$) studies were done based on Reynolds and Froude criteria.

However, Bond number (Bo) has also been used recently for modeling upper slag which is ratio of the body force to surface tension forces.

$$Bo = \frac{\text{Body force}}{\text{Surface tension force}} = \frac{\rho g l^2}{\sigma} \dots\dots\dots(2.8)$$

For a one third scale tundish, if d_{in} is the diameter of inclusion; ρ_{Inc} and ρ_p is the density of steel inclusion and stimulant particle, respectively then, based on Stokes rising velocity, diameter of the stimulant particle, d_p , are as follows [12] :

$$d_p = \lambda^{0.25} \left[\frac{1 - \rho_{Inc}/\rho_{Steel}}{1 - \rho_p/\rho_{water}} \right]^{0.5} d_{inc} \dots\dots\dots(2.9)$$

Furthermore, considering the effect of steel solidification on the density increase, the casting speed (measured for the solid strand) can be calculated in terms of liquid steel flow rate [10].

$$V_c = \frac{Q_s}{A} \times \frac{7020}{7800} \dots\dots\dots(2.10)$$

Where V_c is the casting speed, Q_s is liquid steel flow rate, 7020/7800 is the ratio of solid to liquid steel densities, and A is the cross-section area of the ingot (m^2). The stated above similarity criteria are correct provided there are no temperature changes and no effects of buoyancy forces.

To study water modeling of non-isothermal melt flows in continuous casting tundishes, Damle and Sahai [13] used a number. They called the Tundish Richardson number (Tu), also known as the buoyancy number (Bu) which represents the ratio of buoyancy forces to inertial forces.

$$Bu \text{ or } Tu = \frac{\text{Buoyancy Force}}{\text{Inertial Force}} = \frac{\Delta \rho g L^3 \times \left(\frac{\rho}{\mu^2}\right)}{\rho U^2 L^2 \times \left(\frac{\rho}{\mu^2}\right)} = \frac{\beta \Delta T g L^3 / \nu^2}{Re^2} = \frac{Gr}{Re^2} \dots\dots\dots(2.11)$$

Here Gr is the thermal Grashof number, which approximates the ratio of the buoyancy force to viscous force generated by lighter liquid, L is the characteristic length of the system (usually the bath height), U is the average water velocity through the cross section of the tundish and β is the thermal coefficient of volumetric expansion.

The buoyancy forces arise due to the non-uniform temperature distribution within the tundish. These forces cause the flow profiles within the tundish under non-isothermal conditions to be different from those under isothermal conditions. When $Tu \ll 1$, inertial forces dominate fluid flow, leading to forced convection patterns; When $Tu \gg 1$, buoyancy forces dominate the fluid flow, leading to natural convection patterns; When $Tu \cong 1$, both inertial and buoyancy force are equally dominant, resulting in a mixed convection pattern [14].

For the water model and the actual tundish prototype, the equivalence of temperature rises in two fluids can be defined as follows [15].

$$\left(\frac{Gr}{Re^2}\right)_{steel} = \left(\frac{Gr}{Re^2}\right)_{Water} \dots\dots\dots(2.12)$$

Where Gr and Re are the Grashof and Reynolds numbers, respectively.

By simplifying this expression we can finally obtain,

$$\Delta T_{Steel} = \frac{\beta_{Water}}{\beta_{Steel}} \Delta T_{Water} \dots\dots\dots(2.13)$$

Where the coefficient of thermal expansion of steel, β_{steel} and water, β_{water} are $1.27 \times 10^{-4} \text{ K}^{-1}$ and $2.95 \times 10^{-4} \text{ K}^{-1}$, respectively.

The density of water and steel in term of the function of temperature is calculated by the following co-relation [13]:

$$\rho_{Steel} = 7010.0 - 0.833(T-1808.0) \text{ [The temperature, T is in Kelvin]}$$

$$\rho_{water} = 654.619 + 2.5446T - 0.004683T^2 \text{ [Valid in the temperature range 273-323K]}$$

To study water modeling of non-isothermal melt flows in continuous casting tundishes, A. Aguilar-Corona et. al [16] used hotter water which was $+15^\circ\text{C}$ and $+9.5^\circ\text{C}$ higher than the initial water in the tundish. This was fed through the ladle shroud for both of the low and high flow rates of water, respectively.

2.5 Metallurgical Performance Studies of the Continuous Casting Tundish

Metallurgical performance of the continuous casting tundish is very important to know what's happening inside the tundish. All steels contain the non-metallic inclusions that are harmful to their qualities in most cases, and all possible means are used to minimize the amount of inclusions. One of the most important functions is to float out and separate inclusions from the liquid steel. In the last few decades, many physical and mathematical modelling studies have been performed to improve the quality of steel. But due to large differences in models and full scale systems and the complex physical chemistry reactions involved in practice, it is not possible to determine correctly the float out inclusions [3].

Two different experimental approaches have been widely applied by researchers to analyse metallurgical process performance i.e. the ability of a given tundish design to float-out and separate non-metallic inclusions. The two approaches are as follows:

1. The measurement of residence time distributions (RTD).
2. The direct measurement of inclusion separation through aqueous simulation.

2.5.1 Residence Time Distributions (RTD)

The residence time distribution (RTD) is a statistical representation of the time spent by an arbitrary volume of the fluid in the tundish. The RTD curve is used to analyse the different effective flow volumes, such as the plug flow volume, the dead volume and the well mixed volume, inside the tundish. In order to transfer molten steel to the mould of the CCM, molten steel remains in the tundish for a significant time. Examination of RTD curves shows that all the fluid elements do not have the same residence time but there is a distribution of residence times. With the availability of these residence times, tundish provides an excellent opportunity to perform metallurgical treatments like inclusion separation and flotation, alloy trimming of steel, calcium induced inclusion modification, etc. during the process of continuous casting [17].

The “Stimulus response technique” is a widely used experimental method for finding the desired distribution of residence times of fluid within the vessel. The stimulus or input is simply an addition of a tracer material (e.g. dye, salt, acid, etc.) into the fluid stream. An appropriate (instantaneous input or step input) tracer is injected into the liquid passing through ladle shroud at time $t = 0$. The step and pulse input methods are commonly used for tracer injection. Various online measurement techniques, like colorimetry, conductimetry, spectrophotometry etc. are used to measure experimentally the tracer concentration as a function of time. By plotting, the data vs. time gives a curve, known as ‘C’ curve for a pulse, or instantaneous addition and an ‘F’ curve for a step, or jump input, is produced generally in the non dimensional form of curve, e.g., non-dimensional time and concentration set on the ‘X’ and ‘Y’ axes. (i.e. $\frac{C_0 V}{Q}$ vs $\frac{t}{\bar{t}}$), respectively. The concentration is normalized on the basis of a uniform, well mixed concentration value (inlet concentration), and the residence time is normalized with respect to the theoretical or nominal residence time [6, 8].

The overall flow pattern of water in the tundish consists of a combination of *plug*, *mixed*, and without or with *short circuited flow*. There are also some areas where fluid elements stay much longer than the mean residence time which are known as *dead volume* of tundish [6].

In a Plug flow or piston flow system, all the fluid elements have an identical residence time (equal to the mean residence time) in the vessel. According to Levenspiel [18], fluid flow through a plug flow vessel is orderly, and no element of fluid overtakes or mixes with any other element to the front or to the back of it. Lateral mixing or diffusion along the flow path will not be observed. In the C-curve for plug flow, the injected tracer pulse exits after the dimensionless time, θ of 1, and in F-curve, in response to a step input has a similar shape to the input signal, except that it is also shifted by the mean residence time as shown in Fig. 2.01.

In a well mixed flow system, maximum possible mixing of the fluid particle in the tundish is predicted. As a result, the outlet concentration and the bulk concentration in the tundish are identical. For well mixed flows, the C-curve starts at a dimensionless concentration of

1 and the exit fluid concentration gradually drops as the amount of tracer in the vessel decreases. In case of F-curve, the output raises gradually from 0 to 1, as shown in Fig. 2.01.

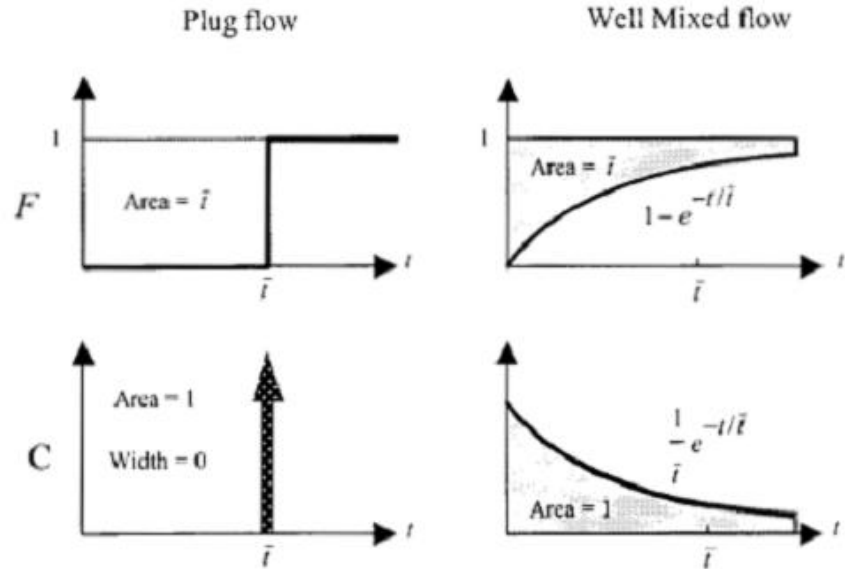


Fig. 2.01. C-curve and F-curve for plug flow and well mixed flow system [6].

Any combination of the plug flow and well-mixed flow volumes can be defined as an *active volume*. In short circuited flow system, the incoming steel from the ladle into the tundish immediately reports to the outlet of tundish, which is very detrimental with regard to steel purity and the thermal homogeneity of cast steel taking individual strands [19]. Basically, this faster moving melt may not spend sufficient time to separate and float out the non-metallic inclusions. As such, nonmetallic inclusions may not have an opportunity to float up and be entrapped in the surface slag [20].

Thus volume of real tundish in terms of flow, V can be expressed as [3]:

$$V = V_m + V_p + V_d \dots\dots\dots(2.14)$$

where V_m = Mixed volume, V_p = Plug volume and V_d = Dead volume.

The existence of a dead volume can significantly decrease the active volume of tundish, and reduce the residence times of steel within the tundish. In the area of dead volumes, there is a great danger of local solidification of steel. This is the reason for minimising the dead volume in tundish [19]. As such, any increase in the dead volume fraction proves detrimental for mixing.

Consider an active (Plug flows and well-mixed flows) and dead regions existing in a model tundish. Figure 2.02 represents a typical RTD curve with a dead region, V_d . Let the dimensionless mean time of the C-curve up to the interrupt point of dimensionless time, $\theta = 2$ be $\bar{\theta}_c$, then

$$\bar{\theta}_c = \frac{\text{Measured mean time upto } \theta=2}{\text{Nominal residence time}} = \frac{\text{measured } \bar{t}_c}{\bar{t}} = \frac{V_a/Q_a}{V/Q} = \frac{V_a}{V} \cdot \frac{Q}{Q_a} \dots\dots\dots(2.15)$$

$$\Rightarrow \frac{V_a}{V} = \frac{Q_a}{Q} \cdot \bar{\theta}_c \dots\dots\dots(2.16)$$

$$\text{Therefore, the dead volume fraction will be, } \frac{V_d}{V} = 1 - \frac{Q_a}{Q} \cdot \bar{\theta}_c \dots\dots\dots(2.17)$$

Here, V , V_a , V_d , Q , Q_d and Q_a respectively denote the total volume, active volume, dead volume, total volumetric flow rate, flow-through dead region and flow through active region of the tundish.

The term $\left(\frac{Q_a}{Q}\right)$ is the area under the C-curve from $\theta = 0$ to 2, and represents the fractional volumetric flow rate through the active region.

In the case of a fully stagnant dead volume, $Q_d = 0$, then $Q = Q_a$. Therefore, by using equation (2.17), the dead volume fraction will be

$$\frac{V_d}{V} = 1 - \bar{\theta}_c \dots\dots\dots(2.18)$$

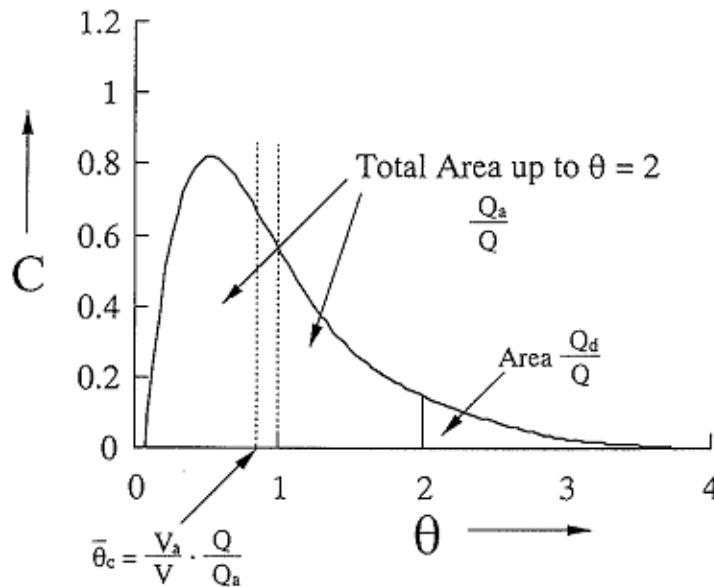


Fig. 2.02. A typical residence time distribution curve for flow in a tundish [21].

From a review of earlier literature [21], it is observed that most of the researchers used ‘C’ curve to analyse the ‘Residence time distribution’. It has a “minimum sharp break through time” with a rapid increase in concentration and subsequent near exponential decay. For a typical ‘C’ curve, the minimum “break through time” (t_{min}), or the corresponding dimensionless form (θ_{min}), the time to attain peak concentration (t_{peak}) or θ_{peak} , and the average residence time (t_{av}) or θ_{av} are the important RTD parameters that can easily be calculated, and used in an appropriate flow model to calculate dead volume (V_d), plug volume(V_p) or dispersed plug volume(V_{dp}), and well-mixed volume (V_m).

Mazumdar & Guthrie [3] reported various fractional volumes which are correlated with the RTD parameters is as follows:

$$V_d = 1 - \theta_{av}; V_p = \theta_{min} = \theta_{peak}; V_m = \frac{1}{C_{peak}}$$

Ahuja and Sahai [21] mentioned in their experimental observations and suggested that a mixed model is not truly relevant to tundish systems. They considered axial or longitudinal, diffusion is present in tundish system, so the minimum break through time and the time at which peak concentration is reached, are not equal i.e., $\theta_{min} \neq \theta_{peak}$. Instead of a plug volume, they proposed using the ‘dispersed plug volume’ (V_{dpv}) term, (shown in Fig. 2.03) and modified form as:

$$V_d = 1 - \theta_{av}; V_{dp} = \frac{(\theta_{min} + \theta_{peak})}{2}; V_m = 1 - V_{dp} - V_d$$

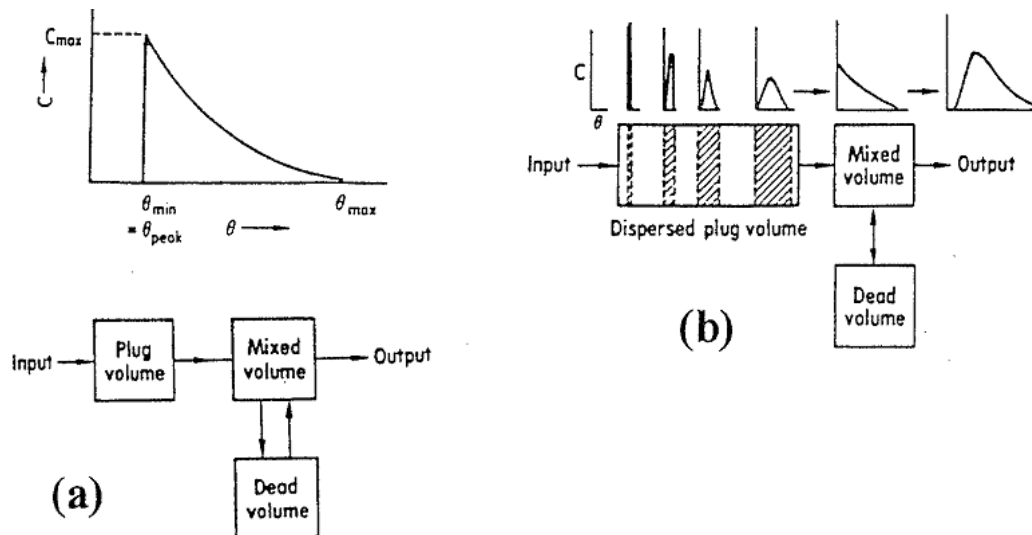


Fig. 2.03. Flow models and theoretical C-curves (a) Mixed model, and (b) Modified mixed model [21].

Mazumdar and Guthrie [3], and Sahai et. al [6] demonstrated that all possible flows should be considered to calculate the dead volume (V_d). So all other calculations of different volume fractions in a tundish will be more accurate. Sahai and Emi [20] reported that neglecting the flow through the dead volume can lead to significant errors in flows through the active volume. Furthermore, they mentioned that assuming the dead volume as the area under the C-curve after two times the nominal residence time is not the correct procedure. They calculated dead volumes from RTD curve which extend well beyond the dimensionless time of $\theta = 2$. They reported both the value of $\bar{\theta}_c$ and the Q_a/Q will change if there is any change in the tundish configuration. These include the use of different flow control devices, changes of total flow rate, depth of liquid in the tundish, etc.

Ahuja and Sahai [21] predicted surface directed fluid streamlines give a net upward velocity to the inclusions which facilitates the top slag layer to absorb the inclusion from the molten steel. The following criteria should be considered to achieve better performance of the tundish with respect to inclusion separation and float out and other metallurgical functions [3, 17] :

1. Minimum spread of residence time.
2. Minimum dead volume.
3. Large ratio of plug to dead volume and relatively large ratio of plug to mixed volume.
4. Surface directed flow.
5. Quiescent slag layer.
6. Maximum average residence time.
7. Contained regions of mixing.

Singh and Koria [17] studied a wide range of tundish designs and operating parameters in a water model to make a summary on steel melt flows in tundishes. They used different widths of tundish, bath heights, inlet volumetric flow rates, inlet-exit distances, slag cover, submerged depth of the ladle shroud, exit flow control devices (stopper rod or nozzle), tundish wall inclination, etc. By analysing the RTD curves it was found that there were two peak values of concentration for wider tundishes and only single peak

values of concentration for narrower tundishes (Figure 2.04). In a wide tundish, the RTD curve consists of two peaks; one due to the straight movement of certain amount of tracer with the portion of the liquid (short-circuiting) and the other due to the movement of the remaining tracer with the rest of the liquid. In the case of a narrow tundish, width-side walls impede straight movement of the fluid and at a critical width, the sidewalls force the portion of the liquid towards the middle of the tundish, where it mixes with rest of the fluid. Thus, the tracer contained in the portion of the liquid are eliminated as a consequence of which RTD curve shows a single peak.

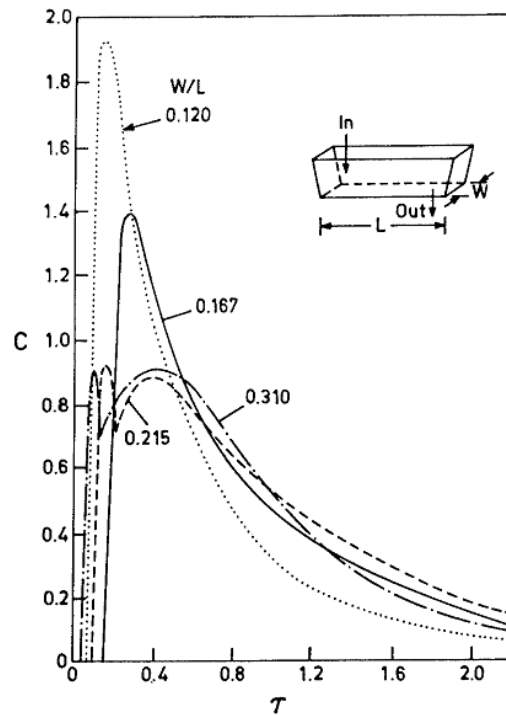


Fig. 2.04. Typical RTD curves for different widths of the tundish (Inlet Froude number 0.74, bath height 260mm and inlet exit distance of 780mm) [17] .

Singh & Koria [22] reported in case of all tundish widths, weirs of all sizes were found to produce short circuiting in the tundish fluid flow system. Besides, they also noticed that the use of a dam alone, or in combination with weir, or with a slotted dam eliminates short circuited flow completely and the dam produces surface directed flow. It also reduces the turbulence of the inlet stream, which leads to uniformity of the flow field in the rest of the tundish. Moreover, they added the minimum and the peak residence times were affected by the size, position and number of flow modifiers, inlet-exit distance and

tundish width. Similarly, employing a dam in the tundish, or a weir along with a dam combination increases minimum residence time in a wider tundish much more than that in a narrow tundish.

S. Garcia-Hernandez et al. [23] carried out experiments in a 1/3 scale model of 20 ton, 30 ton, 35 ton and 40 ton slab tundishes. By varying the height of the tundish liquid level, they analyzed the effect of vortex formation and short circuit flows on the steel cleanliness within a tundish for steel production. It can be observed that increasing the tundish capacity resulted in an increase of the mean residence time (Fig. 2.05), resulting in more inclusions floating out to the upper layer, and enhancing the quality of steel. However, the dead volume fraction also increased, and this must be avoided, since it negatively affects the flow patterns and the active volume.

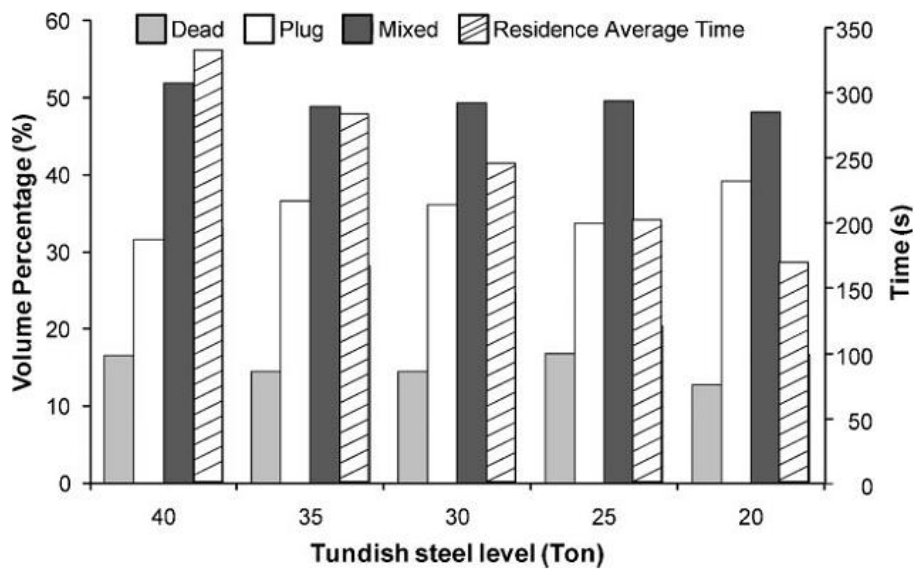


Fig. 2.05. Simulated average residence time, dead volume, plug volume and mixed volume for different equivalent water levels in a tundish [23].

Besides, Lopez-Ramirez et al. [24] also predicted that the higher the height of the tundish, the shorter will be the vortex (Fig. 2.06) and more short circuited flow in a high capacity tundish. These should be considered seriously during operation.

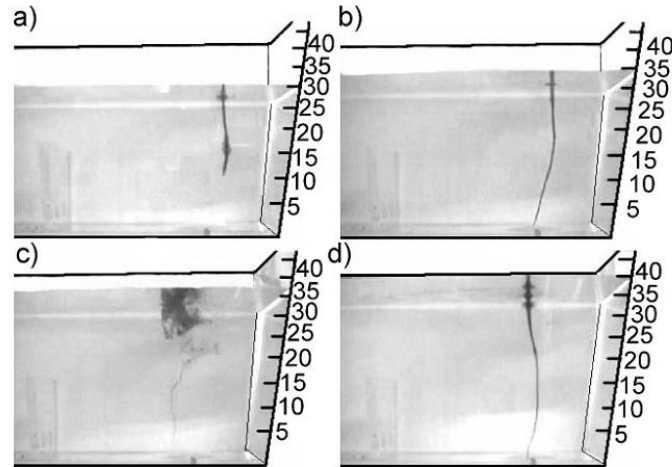


Fig. 2.06. Vortex formation in a water model for different tundish equivalent steel levels in tundish, a) 30 ton, b) 35 ton, c) 37 ton and d) 40 ton[24].

Mazumdar d., Yamanoglu G., Guthrie R. I. L [25] also demonstrated the optimum design of baffles with various combination of furniture (dam, dam along with weir, baffles with holes, etc.) which were found to modify the RTD characteristics and provide superior metallurgical performances, and the slotted baffles with inclined holes (inclined to the horizontal in upwards direction) could give similar, or better results than the result as weir/dam arrangement.

K. Sinha et al. [26] carried out experiment using a submerged entry nozzle (SEN), open entry nozzle (OEN) and T-shaped SEN, in a model tundish of a mini-steel plant. They plotted the tracer response profiles as a function of time so as to simulate the flow behaviour in the slag layer in an actual tundish. It has been found that there is a critical immersion depth of nozzle that produces the optimal level of mixed flow in the tundish. Similarly for a T-shaped entry nozzle at higher depth, mixing and plug flow increase and dead volume decreases, and an OEN configuration did not show any major differences in response of tracer.

Recently, a turbulence inhibiting tundish pouring pad is used to minimize splash on start-up for a safer work environment and reduced turbulence in the tundish. Aguilar-Corona A et al. [16] carried out experiments by using a pair of baffles (arrangement B), and a turbulence inhibitor and a pair of dams (arrangement TI-D). They found that the TI-D

arrangement enhances the flotation of inclusions, and gives a higher fraction of plug flow regime, which is also independent of the ladle shroud position. K. Chattopadhyay, M. Isac, and R.I.L. Guthrie [27] employed 12 different combinations of flow modifiers in order to demonstrate the effect of flow modifiers on liquid metal cleanliness, each of which consisted of the standard impact pad (SIP) of QIT and two dams located in between the inner and outer strands. Dams were found to be reduced inclusion if these could set at proper height and position. However, they also noticed from their mathematical modeling predictions that increasing the height of the SIP from its current height of 0.152 m to 0.30 m, provides better results in terms of inclusion removal, and can be used alone, without placing extra dams within the tundish.

Recently, J. Li et al. [28] experimentally studied the effect of bath depth, H and tundish length, L , for improved inclusion removal in an oval shaped tundish. They predicted that L/H ratio should be in between 2.0~2.7 for better flow field patterns of liquid steel and inclusion flotation.

Many researchers studied the role of gas injection in tundishes in addition to flow modifiers. Mazumder and Guthrie [3] summarised that both water models and plant trials have indicated inert gas bubbling can substantially reduce the dead volumes within tundishes. But appropriate location of gas bubblers must be determined by trial and error, for each individual tundish geometry and baffle configurations. Vargas-Zamora A et al. [15] also suggested that under thermal stratification conditions, gas injection at small flow rates can increase plug flow volume.

Jin-Ho Zong et al. [29] analyzed the residence time distribution for obtaining design concepts for a continuous refining vessel with a submerged gas injection. They also studied the effects of various design parameters, such as the gas blowing position, the gas flow rate, divided blowing with multiple lances, supplementary bottom blowing, and the installation of dams. They found the plug flow fraction could be increased by increasing gas flow rate, the nozzle diameter of lance, and the height of lance from the bath surface. Dead zone could be minimized by appropriate positioning the dams in between the lances.

Many researchers have studied RTD curve numerically using commercial software or in house codes and compared their computational results with the results of physical modeling experiments. By selecting proper geometry, subsequent meshing, grid independency, nodal configurations, boundary conditions, turbulence models to account for the effects of turbulence etc. and physical parameters (e.g., size, number of strands, inlet mass flow rates etc.), different parameters can be analysed. Anil Kumar et al. [30] used a FLUENT-based mathematical model, integrating k- ϵ turbulence model and Reynolds stress model (RSM) to predict time-averaged, fluctuating velocity components and tracer dispersion profile for tundish operations without and with a dam, plus turbulence inhibitor devices (TID). They compared the results with experimental data on RTD parameters collected from water model tundishes. They also used PIV to visualize instantaneous flows. They reported that the mathematical models are reliable and robust to estimates of RTD parameters close to experimental values in a tundish with and without flow modifiers

K. J. Craig et al. [31] employed two separate tundish configurations (dam-weir, and baffle with angled holes and an impact pad) to optimize the design variables, such as position, height and thickness of dam and weir. They used the commercial software FLUENT platform along with integrating k- ϵ turbulence model incorporating DYNAMIC-Q algorithm of Snyman, and found that minimum residence time (MRT) can be increased by 34% using a baffle with angled holes and an impact pad tundish configuration.

Anurag Tripathi & Satish Kumar Ajmani [32] analyzed the RTD curve produced by injecting the tracer at the inlet and measuring its concentration at the outlet with the help of conventional boundary conditions, again using a finite volume based commercial CFD package (FLUENT). They noticed the curved shaped tundish (Fig. 2.07) has the higher minimum as well as mean residence time for all the strands. They predicted that shapes of pouring chamber (flow control devices) or difference in the distance between two outlets lead to better fluid flow characteristics for the curved shaped tundish.

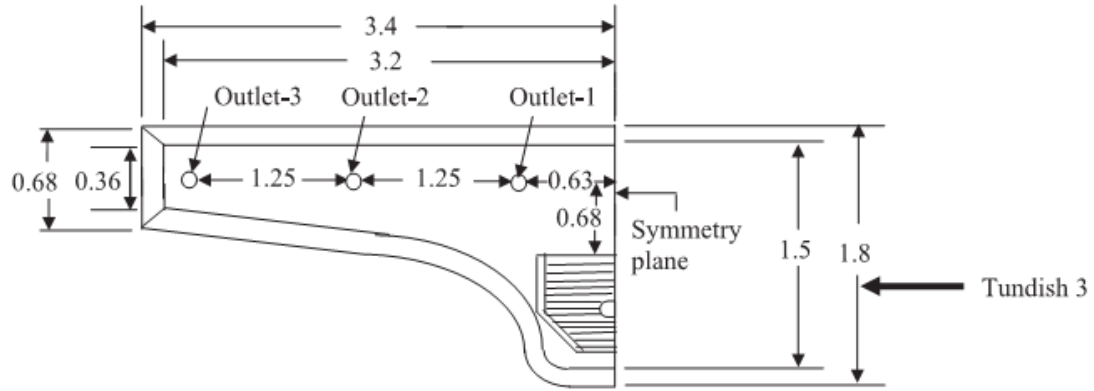


Fig 2.07. Schematic top view of curved tundish (symmetrical half) with flow control devices (pouring chamber) [32]

Moumtez Bensouici et al. [33] carried out mathematical model of residence time distribution (RTD) curve with three configuration (bare tundish, tundish with weir, tundish with weir and dam) again using the commercial CFD code FLUENT 6.0. They found the tundish with weir and dam arrangement (Fig. 2.08) provides the high residence time and plug volume, and reduced the dead volume compared to the tundish fitted with weir configuration.

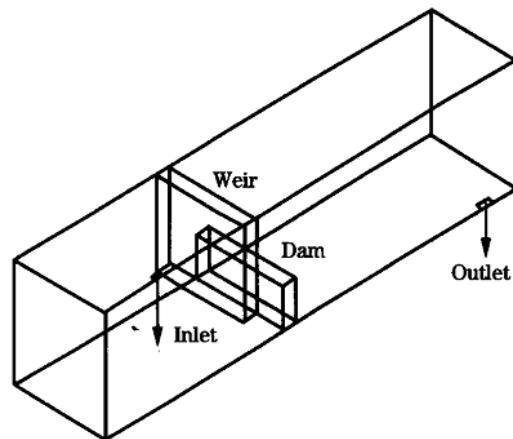


Fig 2.08. Tundish geometry with weir and dam arrangement [33]

Furthermore, D. J. de Kock et al. [34] developed RTD model by coupling the FLUENT solver with the DYNAMIC-Q optimisation algorithm of 'Snyman and Hay' and the LS-OPT design optimisation code to maximise the minimum residence time (MRT) at particular position and configuration, i.e. size, and angles of holes of a baffles and the

inlet region (pouring box) of a tundish. They noticed that increasing the operating level maximises the MRT as well as plug flow volume.

2.5.2 Inclusion Separation

Inclusions have an adverse effect on steel quality. So the principal objective of steelmaking is to remove as many of the inclusions as possible from liquid steel. Inclusion removal in a tundish is governed by many criteria, including the fluid flow pattern, inclusion agglomeration and flotation, and top surface condition, where inclusions may be either removed or generated. Similarly, it depends on the slag composition and re-oxidation conditions [35]. Many approaches have been developed to remove inclusions from liquid steel. Researchers are still trying to remove inclusions. Many researchers had studied on water modeling experiment using hollow glass spheres (simulating non-metallic inclusions in steel melt). In order to detect the numbers and sizes of inclusions in the inlet and outlet nozzles of the tundish, the Electric Sensing Zone (ESZ) technique was employed. When small, non-conducting particles pass through an orifice on which an electric current also passes, there is a change in electrical resistance within the ESZ, or orifice region and cause a voltage pulse. The change in voltage, ΔV through the Electric Sensing Zone is given by DeBlois et al. [36]:

$$\Delta V = \frac{4I\rho d^3}{\pi D^4} \frac{1}{\left\{1 - 0.8\left(\frac{d}{D}\right)^3\right\}}$$

Where d is the inclusion diameter, D is the orifice diameter, I is the imposed DC current, ρ is the electrical resistivity of fluid.

SK Ray, M. Isac and R.I.L. Guthrie [7] used the ESZ PAS instrument Inclusion Counter of Heraeus Electronite (Inclusion Counter) to measure the size of inclusions in a four strand delta shaped QIT tundish, either in a bare tundish and in a tundish fitted with impact pad. He analysed four size ranges of micro spheres, such as 50–60, 61–70, 71–80 and 81–90 microns which are injected at inlet, and found that tundish fitted with an impact pad has less inclusions reporting to exit nozzles, as compared to a bare tundish. The Aqueous Particle Sensor (APS) basically uses the same basic monitoring principle as the Liquid Metal Cleanliness Analyzer (LiMCA), which is an on-line liquid metal

cleanliness analyzing system first developed in the early 1980s at McGill University in collaboration with ALCAN. Both techniques use the software, Metal Windows for inclusion detection. Note that the LiMCA system can be applied for detection of inclusions in liquid metals as well as in aqueous system. However, off-line detection of inclusions was conducted on samples collected at various times following the continuous addition of inclusions from each of nozzles [37].

Various methods have been employed for analysing the number and sizes of inclusion particles in water leaving the model tundish and entering the moulds. Methods such as weighing the particles, or observing them under a microscope after filtration, or using of an online electric sensing zone technique (e.g. a Coulter counter, or equivalent) for determining the size and number density of the particles. Sahai et al. [6] assumed that the various sizes of inclusions that exist in the tundishes rise at their Stokes velocity. By balancing the drag force and the net buoyancy force acting on the inclusion, the Stokes rise velocity can be derived, i.e.

$$U_s = \frac{(\rho_s - \rho_{in})d^2 g}{18\mu}$$

where U_s is the terminal rising velocity, ρ_s and ρ_{in} are the density of the liquid steel and inclusion, respectively, d is the inclusion diameter, μ is the viscosity of steel and g is the acceleration due to gravity.

The graphical presentation of change in Stokes rise velocity with the size range of inclusions is shown in Fig. 2.09. It is observed that calcium oxide inclusions in steel trends matches to the water model (glass/water) results. As seen from the Fig. 2.09, the rest of the inclusions (silica, alumina, etc.) deviate little from the water model. Besides, in plant condition inclusion consists of two or more than two types of oxides. So it is very tough to visualize exact trend. However, Inclusions try to flow through the SEN rather than rise up to the slag layer. In other words, inclusion float out rate depends greatly on the size of the tundish, i.e. the residence time of the tundish. So it is observed that Stokes rise velocity similarity criterion does not predicts accurately the tundish performance based on inclusion removal.

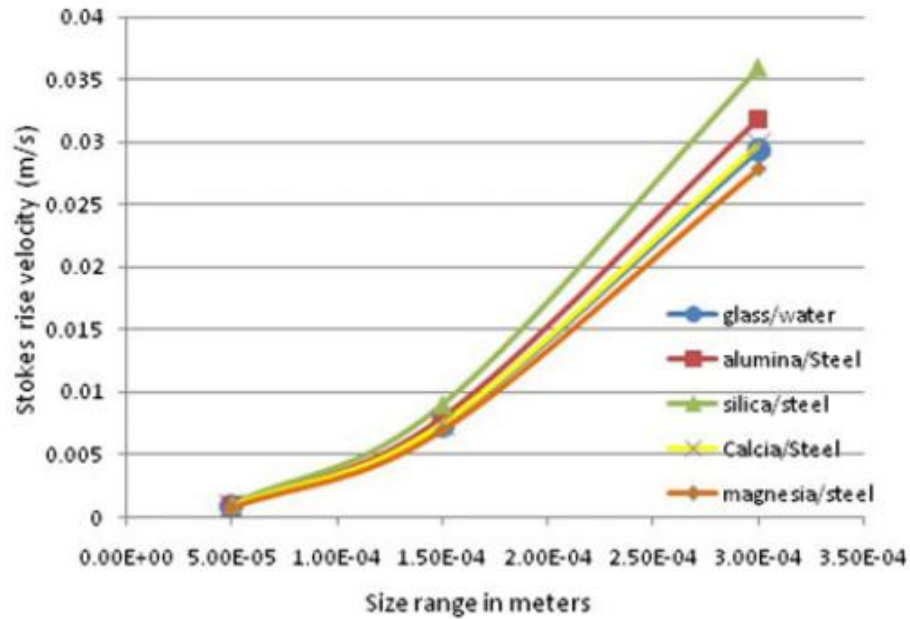


Fig. 2.09. Change in Stokes Rise Velocity with inclusion size [38].

Most recently K. Chattopadhyay, M. Isac [38] developed a dimensionless number for modelling inclusion removal known as the Guthrie number, Gu , which is the ratio of the residence time in the tundish to the inclusion float out time.

$$\text{Guthrie number, } Gu = \frac{\text{Residence time, } \tau_{\text{Residence}}}{\text{Inclusion float out time, } \tau_{\text{Float Time}}}$$

At higher residence time of the fluid, more inclusions will float out to the top layer of tundish. Gu can be analysed in terms of RRI (Residual ratio of inclusions) which is one of most important parameter to study the inclusion of tundish, and can be defined as follows,

$$\text{RRI \%} = \frac{\text{No. of particles leaving to SEN's}}{\text{Total no. of particles entering in the inlet}} \times 100 = \frac{N_{\text{Inlet}} - N_{\text{Outlet}}}{N_{\text{Inlet}}}$$

Where, N_{inlet} and N_{outlet} are the number of inclusion at the inlet and outlet, respectively. The lower the RRI, the lower is the inclusion content in the output steel. A high value of Gu implies a lower RRI (Residual ratio of inclusions). Here, RRI refers to the total number of inclusions passing through the outlet nozzles.

Apart from the electric sensing zone (ESZ) technique for determining RRI parameters, many researchers have performed RRI's and inclusion trajectory analyses

computationally, using commercial software or in-house codes. Finally, they compared with experimental result. S. Joo and R.I.L. Guthrie [39] used their METFLO 3D computer code to analyse 3-D fluid flows, heat transfer, inclusion behaviour, and their population distributions within steelmaking tundishes. They compared the numerically computed RRI (Residual ratio of inclusion), and experimentally obtained RRI by using the electric sensing zone (ESZ) technique and introducing many inclusions (hollow glass microspheres) into the full-scale water models. They observed higher values of RRI for small size inclusions (20 μm) and lower value of RRI for large size inclusions (120-140 μm). This is logical, since small particles have minimal Stokes rising velocities and need more time to float to the top surface, while the higher Stokes rising velocities of larger size inclusions improve their separation. Furthermore, S. Joo and R.I.L. Guthrie [40] carried out a numerical model on different types of tundish (conventional trough-type tundish; one-way flow, twin-strand tundish, trough-type tundish; and one-way flow, twin-strand, wedge-shaped tundish) using their METFLO 3D computer code. They demonstrated that conventional trough-type tundish with double dam arrangement showed the greatest potential for improvement in residual ratios of inclusion. They further mentioned that increased metal throughputs has a detrimental effect on metal quality due to reducing the inclusions float out times.

K Takalani et al. [41] developed a three-dimensional mathematical model using semi-implicit finite-difference procedure according to the SOLA method to represent the fluid flow, heat transfer and inclusion removal taking into account the effects of gas bubbles and thermal buoyancy and compared the numerical results to experimental measurements of particle (hollow glass sphere) separation in the water model. They reported the dam is effective for large inclusions and large plug flow region, and a tundish with a dam show better inclusion removal efficiency, and different pouring methods (e.g., pouring tube and long nozzle type) of the molten steel don't lead significant amount of inclusions.

S. K. Ray, M. Isac and Guthrie [42] carried out a numerical model of a four-strand delta shaped 12 ton billet casting tundish with three different flow modifying dam arrangements. These were i) a tundish attached with two dams upwardly angled 45°

height of 0.38 m with rectangular slots, ii) a tundish attached with two dams upwardly angled 45° height of 0.38 m with rectangular slots at top and iii) a tundish attached with two dams upwardly angled 45° height of 0.38 m using commercial software FLUENT 6.3.26 and compared the RRI with bare tundish. They reported that the 1st arrangement gave minimum RRI values, i.e. the least number of inclusions in the mould.

Recently most researchers have focused on an ‘Eulerian-Lagrangian’ approach to simulate inclusion trajectories, and predict inclusion separations ratios. A. Vargas-Zamora et al. [43] used the Lagrangian particle tracking approach, to solve a transport equation for each inclusion as it travels through the previously calculated flow field of water, so as to calculate inclusion trajectories. By balancing the drag force, buoyancy force and added mass force for accelerated flows using Newton’s second law of motion, transport equation of Lagrangian frame is obtained which is as follows [44]:

$$\frac{du_p}{dt} = \frac{18\mu C_D Re}{24\rho_p d_p^2} u_{rel} + \frac{g(\rho_p - \rho)}{\rho_p} + \frac{1}{2} \frac{\rho}{\rho_p} \frac{d(u - u_p)}{dt}$$

Where u is the velocity of fluid, u_p is the velocity of particle, C_D is the drag coefficient, d_p is the particle diameter, and ρ and ρ_p are the density of the fluid and particle, respectively. They observed inclusion trajectories of many particles of size ranges 1 to 10 μm suffer toward the outlet which are unable to float out. In non-isothermal conditions, these small inclusions flow closer to the bath surface due to the effects of buoyancy. In case of larger inclusions (10 to 50 μm) under isothermal conditions trajectories of inclusions seem to be irregular ‘S’ shaped shown in Fig. 2.10c and under the influence of buoyancy forces, their trajectories are straightly directed downstream (Fig. 2.10d). They concluded that the buoyancy forces originated by temperature differences are insufficient to enhance the flotation of small inclusions and the influence of flow control devices such as the inhibitor play a more important role to eliminate them.

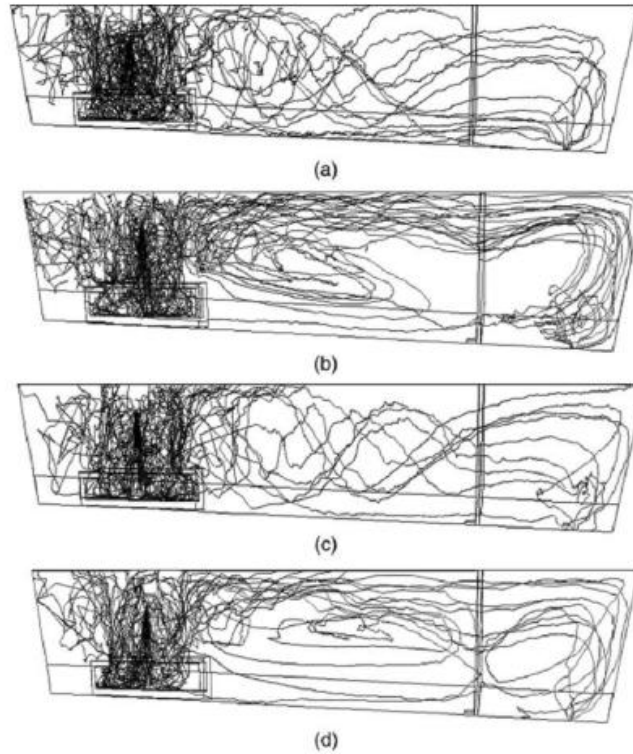


Fig. 2.10. Trajectories of inclusions in the water flow: (a) isothermal conditions and particle sizes from 1 to 10 μm , (b) non-isothermal and particles sizes from 1 to 10 μm , (c) isothermal conditions and particle sizes from 10 to 50 μm , (d) non-isothermal conditions and particles sizes from 10 to 50 μm [43].

Yuji Miki et al. [45] used FLUENT incorporating the $k-\varepsilon$ turbulence model to track the trajectories of inclusion particles through the 3-D flow distribution, and included thermal buoyancy forces based on the coupled temperature distribution. They also examined the effect of tundish geometry, specifically the length of the second chamber (Fig. 2.11) which was reduced from 3.1 to 2.1 m and the steel depth in the tundish was increased from 1.05 to 1.25 m without changing the throughput rate. They observed longer residence time with almost the same flow patterns and a fairly improved inclusion removal scenario. They further demonstrated that over 30% of inclusions smaller than 10 μm are predicted to be removed if there is a protective slag cover (no reoxidation), and with no collisions. Almost 100% of the inclusion clusters larger than 80 μm are assumed to be removed. Besides, due to reoxidation and collisions, the inclusion removal rates drop down to 0% and 75 % (approximately), respectively.

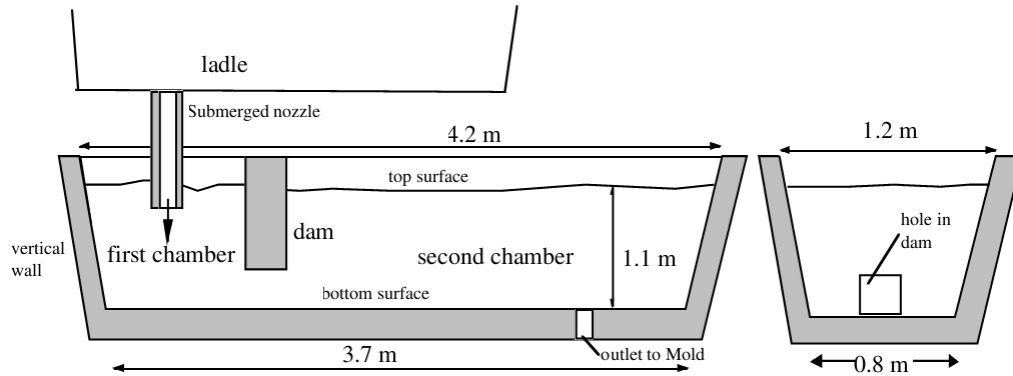


Fig. 2.11. Tundish geometry with first chamber and second chamber [45]

Lifeng Zhang et al. [46] introduced a mathematical model using the PHOENICS commercial computer code linked with the $k-\epsilon$ turbulence model of flows in a tundish with flow control devices: two dams and one weir. They discussed briefly the Brownian collision, Stokes collision, and turbulent collisions. Apart from inclusion removal by flotation to slag at the surface, they reported that collision of inclusions and adhesion to the solid surfaces are all important factors for inclusions removal. Flotation of inclusions to the free surface has a great effect in removing inclusion from a tundish that has been noticed both through experiments and simulations. Similarly, higher rates of inclusion float up in tundishes fitted with flow control devices compared to a bare tundish have been observed. Large size inclusions are considered to float out owing to their high rising velocities. They concluded that flow control devices also facilitate some inclusions to adhere and improve an inclusions adhesion to the walls and bottoms.

S. Lopez-Ramirez et al. [47] studied four different flow-control arrangements i) a bare tundish (BT), ii) a turbulence inhibitor (TI), iii) a turbulence inhibitor and low dams (TI & LD), and iv) turbulence inhibitor and high dams (TI & HD). From the mathematical simulation and the water-model results, they found that the turbulence inhibitor together with low dams provided the best flow characteristics, i.e., high plug flows with low dead volumes. They mentioned that turbulence inhibitors reduce the turbulence at the surface, and in the case of small particles, it traps them towards the wall of inhibitor and for large sizes particle, it pushes the particles straight up to the top free surface, and the dams reduce turbulence near the outlet nozzle during the filling of tundishes.

Anil Kumar et al. [35] also carried out both the physical and numerical simulations using FLUENT incorporating the $k-\varepsilon$ turbulence model in a tundish for three cases: i) a bare tundish, ii) in the presence of a dam, and iii) with the application of turbulence inhibiting device with side hole and dam (TID + Dam). They found two peak values of concentration in bare tundish which is due to short-circuiting phenomena in the tundish and other characterized by single peak value of concentration (TID + dam). They reported that use of a dam eliminates short-circuiting phenomena in the tundish and creates recirculatory loops which accelerate the inclusion float up. They observed high plug volume with minimum dead region which shows better inclusion removal in tundish with TID and dam configuration.

Pradeep K. Jha et al. [48] carried out a numerical investigation of the inclusion removal process using FLUENT 6.1.22 with the standard $k-\varepsilon$ model in order to study the effects of height and position of dams in a six-strand delta shape tundish. They found that inclusion removal tendency increases at critical height of dam and distance of these dams from the inlet. Besides, Solorio-Diaz et al. [49, 50] studied experimentally and mathematically in a tundish with Turbulence Inhibitor + Dam (TI + Dam), Conventional Ladle Shroud (CLS), Swirling Ladle Shroud (SLS) to the design of optimum steel flows in a tundish. From mathematical model, they observed that at low flow rate (3.8 ton/min), TI + Dam arrangement with SLS shows the best efficiency to control the turbulence and to remove inclusions, and at a high mass flow rate (7.6 ton/min), SLS dissipates the entry jet turbulence energy before it impacts the tundish bottom diminishing the fluid velocities that makes suitable to operate tundish at different flow rate.

K. Chattopadhyay, M. Isac and Guthrie [51] performed physical and mathematical modelling in a four strand delta shaped 12 ton tundish to study the effect of slight misalignments of the ladle shroud on liquid steel quality, and observed that more slag is entrained in the SEN in the direction of the bias, and that dye mixes rapidly in the direction of the bias during tracer dispersion experiments in lieu of symmetrical mixing patterns. By analysing a mathematical model incorporating DPM, they further observed that inclusions spread much more to one half of the tundish in the direction of the bias. Furthermore, B. Bul'ko et al. [52] also carried out experiment to predict the influence of

misalignment ladle shroud on tundish residence time. They adjusted the misalignment of ladle shroud by using laser builder's level which was 3° tilted in the direction to right casting stream and rear side of tundish. Measurements were carried out by using KMnO_4 indicator and also by water conductivity measuring at tundish inlets and outlets. It was found that significant reduction in residence times compared to the correct set ladle shroud due to stream of influent water reflected obliquely to the slag.

K. Chattopadhyay, M. Isac and Guthrie [53] did physical and mathematical modelling in a tundish to analyze the effect of the submergence depth of the ladle shroud on melts flow and liquid metal quality. They performed slag entrainment tests in a full-scale four strand water model tundish fitted with impact pad, and noticed that a higher depth of submergence of the shroud leads to very little slag entrainment during ladle change, even for the bare tundish. Besides, by performing mathematical modelling using FLUENT and incorporating the standard $k-\varepsilon$ turbulence model, they observed that turbulence is a maximum for non-submerged condition, and that the higher the submergence depth, the lower is the turbulence.

Singh et al. [54] reported that increasing the capacity of tundish from 40 to 65 tonne, that Nippon Steel Corporation obtained an increase in zero surface defect index of slab from 57% to 92% during ladle change. So they attempted a project to increase the capacity of tundish for a single slab caster from 17 tonne to 25 tonne. They applied 3-D steady-state mathematical simulation using standard $k-\varepsilon$ turbulence model of FLUENT with second-order upwind discretization scheme under assumptions of both isothermal and non-isothermal conditions. They predicted the residence time distribution (RTD) curves for analysis of flow behaviour inside the tundish. They proposed four different tundish configurations without re-locating the metal feeding and discharge points, changing the top and bottom widths, and the height of the liquid level. One of the configurations, which they selected for further development, was based on a higher mean residence time. Furthermore, they improved the performance of the proposed larger tundish by inserting a dam between inlet stream and the single outlet nozzle.

Guang-hua Wen et al. [55] carried out water modeling experiments (Fig. 2.12) on a 1/4 scale of 65 ton round tundish for three flow arrangements, i) a bare tundish, ii) a tundish with weir and dam, and iii) an oval shaped tundish with a weir and a dam containing a hole. It was found that the minimum residence time and the average residence time of the improved oval tundish was much longer with higher plug volume fraction, less dead volume fraction, a better fluid flow pattern while the removal effect of inclusions is much better compared to other arrangements. These are beneficial for inclusions to float up as well as improving the quality of heavy steel ingots.

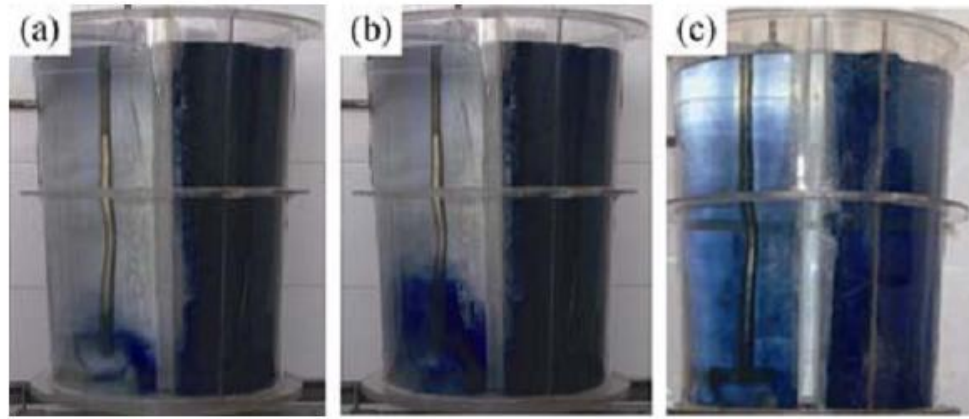


Fig. 2.12. Fluid flow in a round tundish with flow control devices after injecting blue ink: (a) 20s; (b) 30s; (c) 50s;

Yue Qiang et al. [12, 56] compared the performance of a tundish fitted with baffle and with turbulence inhibitor, and with a baffle and swirling chamber aimed at better flow control and enhanced flotation of inclusions. By analyzing RTD curves experimentally, they reported that the plug volume fraction to the dead volume, active volume fraction to dead volume, and minimum residence time to average residence time, all improved significantly for the tundish equipped with a swirling chamber as compared to a tundish with a standard turbulence inhibitor. Later, they analyzed the mechanism of inclusion aggregation in liquid steel in a 2/5 scale swirling flow tundish experimentally using polypropylene particles (0.912 g/cm^3) of sizes range of 51- 64 μm and 64 - 86 μm , and weight of 40 g and 2 g to simulate Al_2O_3 inclusions in liquid steel. It was realized that the flotation rate with 40 g inclusion particles addition is higher than that with 2 g addition. They concluded that the inclusion removal in a swirling chamber is characterized by centripetal forces, collisions and inclusion aggregation. Larger size inclusions are

particularly influenced by centripetal effects, while smaller size inclusions are influenced by collision and aggregation.

S.F. Yang et al. [57] carried out water modeling experiment in a 2/3 scale of a 15 ton tundish for a horizontal caster to analyse the fluid field patterns, residence times, and the location and size of the dead zone. They added KCl solution, with black ink through the shroud as a tracer into: i) the bare tundish, ii) the tundish with a turbulence inhibitor, and iii) tundish with an inlet launder and an inclined dam. They reported that the tundish combination of a launder with a low dam was the best of the three designs in terms of longer minimum residence time and peak concentration time, and smaller dead zone and diminished short circuit flows. Furthermore, Dong Heon Kam et al. [58] studied the effects of LSN (ladle submerged nozzle) and dams on the flow patterns in a horizontal caster by injecting KOH 5M solution with colored dye of KMnO_4 3M solution. They reported that the dead volume fraction was decreased with an increase in dam height, that overall flow patterns remained almost the same with changes in casting speeds, and that the major flow in the bare tundish with LSN was observed to be moving down toward the bottom of the tundish. They believed that this would be harmful and increase the chance of non-metallic inclusions goes through mould.

Tomasz Merder et al. [59] studied four different types of turbulence inhibitor (TI) in a T-type two-strand 7.5 capacity of tundish using physical and numerical modeling. They reported that employing a flange in the geometry of TI's enhances the good level of liquid steel mixing, and increases well-mixed volume flow and decreases the dead volume flow.

Antje Ruckert et al. [60] simulated inclusion removal in a 1:3 scale water model of a single-strand tundish, using a particle counter that consists of a photo-electric barrier with a laser diode as light source and a CCD sensor as receiver. They compared the experimented results against numerically prediction based on the ANSYS FLUENT code using the realizable k- ϵ turbulence model in Lagrangian model. They observed that the relative number of particles of all sizes (1 - 250 μm) in the SEN significantly decreases when using an impact pad and higher volume flow rate, and that the relative particle

number is highest in the top part of the tundish, and smallest in the bottom part of the tundish.

Some researchers have studied non-isothermal tundish melt flows by considering the heat losses through the top surfaces, bath surfaces and walls of the tundish, and the temperature difference between the incoming molten steel from the ladle and the liquid steel that is initially present in the tundish. For example, Damle and Sahai [13] predicted nature of the fluid flow phenomena taking place in an actual tundish, and obtained RTD curves under different flow conditions simulating the non-isothermal flows in a caster, for which the ratio of the buoyancy force to the inertial force is the same between the model and the prototype. Furthermore, Aguilar-Corona A et al. [16] concluded that thermal stratification due to changes in density is stronger in a tundish with a pair of baffles (B) than in a tundish fitted with a turbulence inhibitor plus a pair of dams (TI-D). Therefore the TI-D arrangement provided lower thermal gradients of liquid inside the vessel, and higher plugs flow volumes, at any position of the ladle shroud and casting rate.

S. Joo and R.I.L. Guthrie [61] carried out mathematical modeling to study transport phenomena when hotter steel from a new ladle is poured into existing cooler liquid steel in a tundish. They noticed that thermal natural convection due to buoyancy forces generate secondary recirculating flows and increased fluid motion near SEN of the tundish, even in the presence of flow control devices. A. Vargas-Zamora et al. [43] predicted that buoyancy forces caused by thermal gradients are not sufficient to enhance the flotation of small inclusions, and that the flotation of large inclusions are slightly enhanced by buoyancy forces and that the influence of flow control devices such as the inhibitor plays a more vital role to eliminate them.

Dong-Yuan Shen et al. [14, 62] observed the liquid flow moved upwards due to action of a dam when equal temperature of liquid were discharged and "dead zone" located at the upper-corner of side wall. Later, when high temperature liquid discharged compared to an existing cooler bath, the main stream flows upward more extensively and "dead zone" moves to near the central bottom of the tundish, and when the cooler liquid discharged, incoming liquid flows downward very rapidly, and forms a stratified flow and higher

"dead zone" was depicted. So inertia forced along with thermal buoyancy force should be considered in melt flow. After that, they explained counter gradient diffusion phenomenon caused by the thermal buoyancy force by using the two-fluid (inlet hot stream and original bulk cold liquid) with k- ϵ model incorporating IPSA algorithm, and found reasonable agreement with water modeling experiment.

R. D. Morales et al. [63] reported that flow behaviour changes significantly when a four strand tundish employing a pair of weirs and dams, or a turbulence inhibitor (TI), or a pair of dam, or only TI arrangement. Turbulence inhibiting device reduces the turbulence intensity in the pouring zone and suppress the harmful effect thermal stratification. Step temperature inputs or varying ladle stream temperatures affect melt flow fields just few minutes of pouring liquid steel. Since buoyancy numbers decrease as time goes and eventually its dominant role has been reduced. However, the effect thermal disturbance enhances at low melt flow rate. Mehdi Alizadeh et al.[64] analysed RTD curves and observed that warmer fluid floats to the free surface in non-isothermal conditions, and RTD curve for non-isothermal conditions has two maximum concentration peaks that indicates the mixed convection phenomena (Figure 2.13) in the non-isothermal tundish. He concluded that the degree of mixing in the tundish in non-isothermal conditions is lower than that of isothermal conditions.

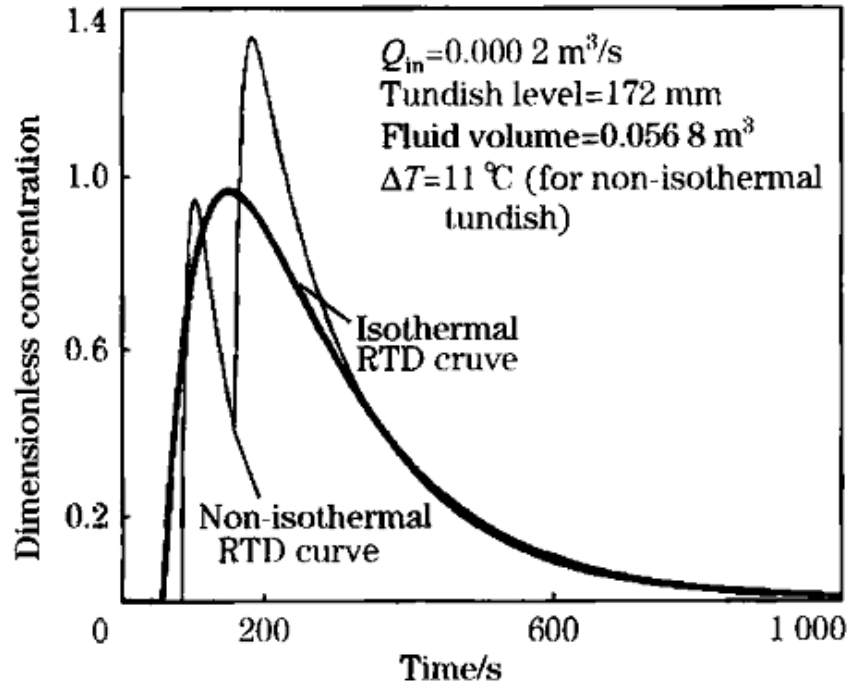


Fig. 2.13. Comparison of RTD curve for isothermal and non-isothermal tundish [64].

S. Lopez-Ramírez et al. [65] predicted that inertial forces dominate the flow in the bare tundish, and that buoyancy forces are dominant in a tundish fitted with a turbulence inhibitor and low dams (TI & D) during a step up change in inlet temperature. They reported that TI & D arrangement showed the best flow characteristics in terms of plug, mixed, and dead volume flow fractions. The analyzing of RTD curves for the non-isothermal case obtained from mathematical and physical models.

2.5.3 Slag Entrainment during Ladle Changing Operations

Slag entrainment during ladle changing is a major problem for the steel making operations. Basically slag entrainment can occur in a tundish during initial filling of tundish, during ladle changing times, and during last stages of casting, when the height of molten metal in tundish is very low [7]. S. K. Ray, M. Isac & Guthrie [42] carried out the slag entrainment experiments in a full scale plexi glass model of a tundish fitted with different flow modifiers. They used polyethylene beads with a density of 935 kg/m^3 to simulate the slag. When the steady state condition was reached, for a 50 cm water height, a layer of beads was spread evenly (approx. thickness of the layer of beads is 2.5–3.0 cm) on top of the water. Then, the inflow to the tundish was completely closed and the water

was drained for 3 min to simulate an actual ladle change in the steel plant. Basically, when the new ladle was opened, high flow rate was introduced so that liquid steel refill the steady state height of tundish. After that, slag was entrained in the bucket fitted with wire mesh bottoms at the tundish outlets were counted. This represents a quantitative value of the degree of potential slag entrainment which can happen in the real system. They found smaller numbers amount of beads in the tundish attached with two dam's upwardly angled 45° height of 0.38 m with rectangular slots arrangement compared to other configuration & slag entrained mostly in the outer SEN. In reduced (1/3) scale model, was used oil (corn) was used to simulate slag directly.

Although slag entrainment has a detrimental effect on steel quality, very few researchers have been able to use slag entrainment phenomenon for predictive purposes. Recently, Henrik Solhed and Lage Jonsson [66] developed a model of steel phase considering refractory, slag and flux, using commercial the program PHOENICS incorporating the grid as a Multi-Block-Fine Grid Embedded (MBFGE) grid. They assumed the typical slag composition (50% CaO, 12.5% Al₂O₃, 7.5% MgO and 30% SiO₂) for the thermodynamic calculations. They verified the model with velocity and temperature measurements in steel and refractory, and the flow field was re-designed with weirs, adding a vertical component to Stokes equation. They observed slag concentration in the upper-most steel layer.

2.6 Final Remarks

From this review it is observed that the main objective of researchers is to increase mean residence time, and increase minimum residence times by decreasing the dead volume, and to limit the mixed zone and increase the plug volume for producing better quality steel. To attain this objective, water modeling experiment are used extensively to analyze the effect of flow control devices, residence time distribution (RTD) curves to study short circuiting flows and compute fractional flows through “plug volume”, “dead volume” and “mixed volume” inside the tundish, as well as inclusion removal. Plant trials are also used to realize the possible complexity and ways of solution. Furthermore, mathematical modeling is also employed to understand the transport phenomena taking place within the

tundish. Many researchers around the world have tried tundishes with different flow modifiers, such as weirs, dams, baffles, and impact pads, to enhance steel cleanliness, especially for the intermediate (50 μm) to larger (120 μm) inclusions. Recently, the impact pad has been proven to be an effective flow control device which reduces turbulence in the pouring zone and act like a redirecting flow device so as to distribute molten steel uniformly to each strand. Increasing the height of the impact pad could result in better steel cleanliness and be an efficient way for inclusion removal. This could be used to replace the use of extra dams which is highly position and height dependent.

A common trend that has been observed in the literature is to improve inclusion flotation efficiency of a tundish by modifying the size, design and optimal position of flow modifiers. So increasing the capacity of the tundish facilitates inclusion separation by allowing an increase of residence time of the melt that provides longer times for non-metallic inclusions to float by buoyancy effect and to be captured by the slag. The review also depicts the study of buoyancy forces developed by the fluid density changes during ladle change operations when the new and hotter steel is poured into the tundish. This contributes to the modification of the steel flow patterns. Similarly, molten steel in the tundish also loses heat through the walls and the free surface. So steel flow in tundish is controlled by both buoyancy forces and inertial force.

CHAPTER-3

EXPERIMENTAL SET UP AND PROCEDURES

3.1.1 Introduction

In our study, a one third scale (Model: Prototype, $\lambda = 1/3$) plexiglass model of the industrial tundish was used. Figure 3.01 and 3.02 show the three dimensional schematic illustration of the tundish fitted with an impact pad and an orthographic projection of a 4 strand delta shaped tundish fitted with impact pad, respectively. The two central outlets are known as the inner SEN's (submerged entry nozzle) and the two outer most outlets which are located far from ladle shroud plane are denoted by the terms, outer SEN's. The ladle shroud was placed at a distance of 150 mm from the apex on the base of the tundish, and then submerged to a depth of 20 mm under the free surface of the fluid. It is noted that the exact dimensions could not be provided here for reasons of confidentiality, since our set up is a one third scale model of the running plant at Rio Tinto Iron and Titanium (RTIT) Inc., Sorel, Québec.

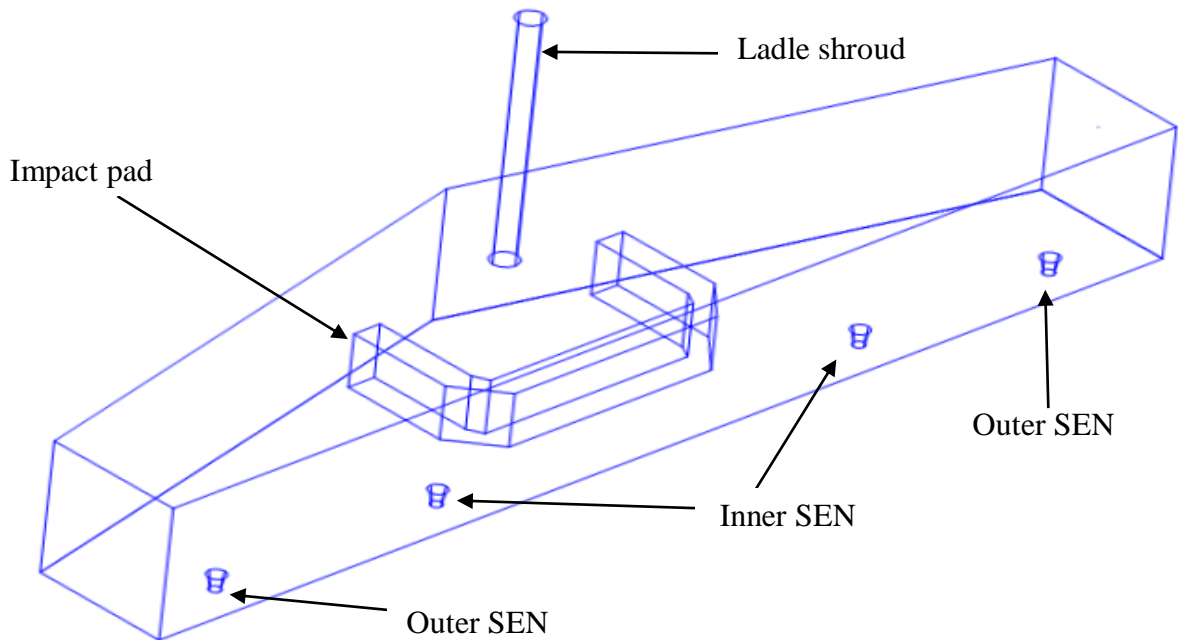


Fig. 3.01 Three dimensional schematic illustration of tundish fitted with impact pad

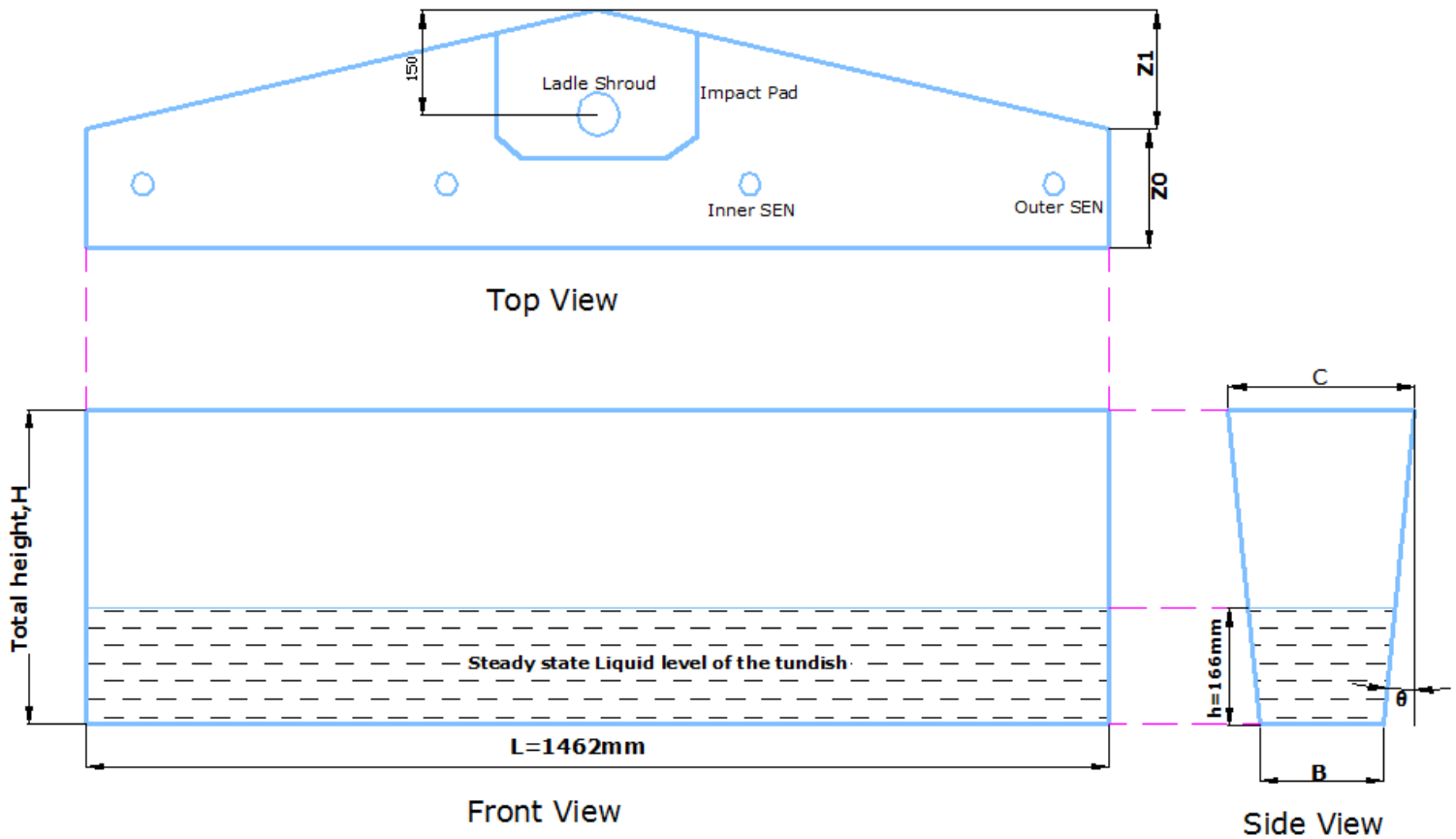


Fig. 3.02 Orthographic projection of a 4 strand delta shaped tundish fitted with an impact pad

The volume of liquid steel as a function of the liquid level within the tundish from the bottom of the inside tundish can be calculated according to [37] :

$$V = L \left(Z_0 + \frac{Z_1}{2} \right) h + Lh^2 \tan \theta \dots\dots\dots(3.1)$$

Where, L is the length of tundish bottom

Z_1 is the width difference between the rectangular and triangular apex on the bottom surface of the tundish

Z_0 is the width of rectangular apex on the tundish bottom

θ is the sidewall angle

h is the liquid level in the tundish.

When height of liquid level is 50 cm (16.67 cm in 1/3 scale), then according to the equation (3.1), the volume of the tundish is 12 tonne. Furthermore, if the liquid level within the tundish is maintained at 66 cm (22 cm in 1/3 scale) and 70.5 cm (23.5 cm in

1/3 scale), the corresponding capacity of tundish goes up to 18 tonne and 20 tonne, respectively.

The experiments were carried out for the following three cases:

1. Tundish without any flow modifiers (Bare tundish)
2. Tundish fitted with the McGill Standard Impact Pad (MSIP)
3. Tundish fitted with the proposed McGill Improved Impact Pad (MIIP)

The geometry of the conventional McGill standard impact pad (MSIP) is depicted in Figure 3.03. It was fitted within the pouring zone of the tundish to suppress the turbulence and optimize the fluid flow so as to enhance inclusion flotation towards the top free surface.

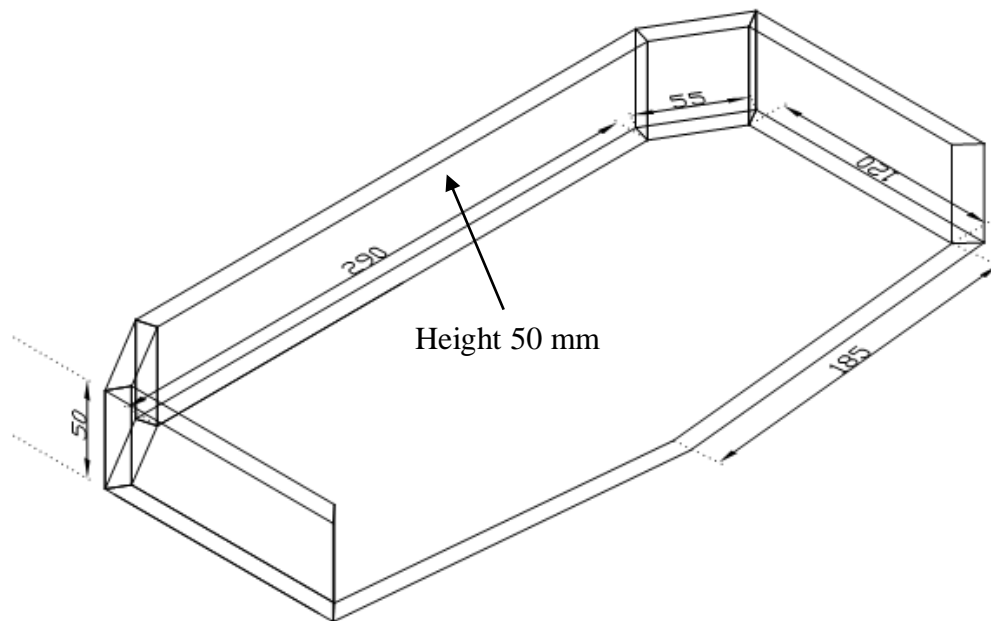


Fig. 3.03 Schematic view of McGill standard impact pad (MSIP)

The outline of the McGill Improved Impact Pad (MIIP) configuration used is given in Figure 3.04. This is our proposed optimized impact pad in terms of inclusion removal efficiency and, was based on a CFD optimisation analysis done by Chattopadhyay, M. Isac and R.I.L. Guthrie [27]. We considered the height of the MIIP impact pad 100 mm (one third scale) to conduct our physical experiments.

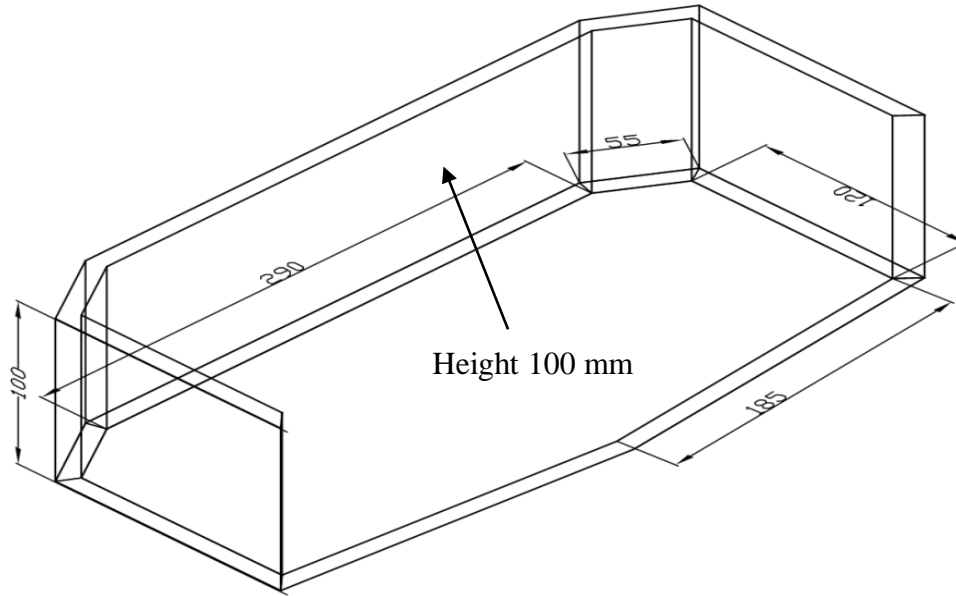


Fig. 3.04 Schematic view of McGill improved impact pad (MIIP)

Water was used in the tundish to simulate molten steel. This is because the kinematic viscosity of liquid steel at 1600°C and water at 20°C are equivalent (i.e. within a 10% variation). In this study of fluid flow modeling of a four strand delta shaped tundish, geometric and dynamic similarities were satisfied based on considering Froude based modeling criteria. As such in this one third scale model of a 12 tonne tundish, the liquid flow rate was 10.90 litre/minute, in accordance with the formula, $Q_W = \lambda^{\frac{5}{2}} Q_S$ [10], while the flow rate in the prototype tundish was 170 litre/minute.

3.1.2 Slag Entrainment Experiments

The experimental set up for slag entrainment tests is shown in Figure 3.05. Corn oil (density, 923.7 kg/m³; viscosity, 0.061 pa-s) was used to simulate slag. To visualize the oil clearly, Sudan IV (Molecular formula: C₂₄H₂₀N₄O) dye was used. This dye is very soluble in oil but is insoluble in water, thereby visually distinguishing the “slag” layer on the top of water, the interfacial level representing the slag interface in the steel plant. A low flow rate, fine porosity Watman 5 filter paper (particle retention 2.5 µm) was used to collect the entrained slag particles (droplets) passing into the SEN's during a ladle change simulation. Under steady state flow conditions, a layer of oil-dye mixture (thickness

roughly 10 mm) was distributed uniformly on top of the water. The ladle changing operation in the actual plant was simulated by closing the inflow shroud valve for 104s. As a result, the tundish liquid level dropped to around 35 mm. Then the inflow valve was fully re-opened to regain the constant height of 166.7 mm as soon as possible, similar to events in the steel plant when a new ladle is opened up for casting. Finally, the ladle shroud valve was again closed, the tundish drained and the filter paper removed and carefully dried, in order to measure the weight of entrained “slag”(oil) during a ladle change.

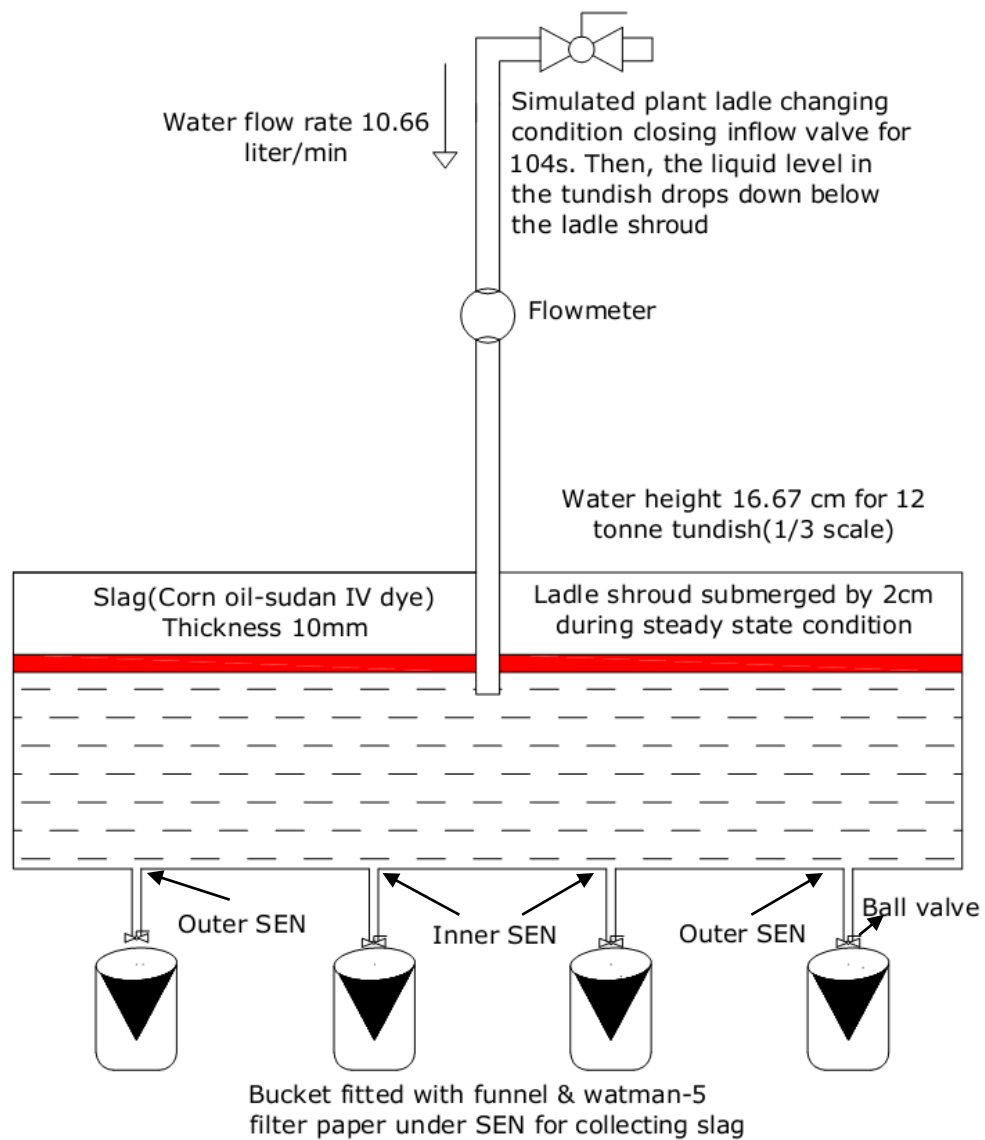


Figure 3.05. Schematic representation of tundish during slag entrainment test

3.1.3 Tracer Dispersion Studies

Tracer dispersion experiments were carried out in order to determine mixing patterns within the tundish. This was accomplished by adding 30 gm of red dye (food coloring pigment) into 700 ml of water. A 50 ml syringe was placed in the upper part of ladle shroud to inject the tracer solution. The schematic representation of the tundish during a tracer dispersion test is shown in Figure 3.06. A high definition movie camera, *SONY HDR CX-100*, was used to record the change in the color of the water with respect to its residence time within the tundish. From the video recording, the character of the flows, including path lines and speeds of flow, dead volumes, and areas with short-circuiting flows, were evaluated. For the non-isothermal cases, hot/cool water was introduced to provide the necessary positive/negative temperature differences with the existing water contained within the tundish.

In the case of the non-isothermal step-up temperature condition of $+10^{\circ}\text{C}$, the temperature of incoming fluid was maintained at 10°C higher than that of the existing fluid contained within the tundish. Furthermore, for the non-isothermal step-down temperature condition of -10°C , relatively cool water (10°C lower) was introduced through ladle shroud compared to existing fluid within tundish. It is noted that, at step input of 10°C in water model refers to the step input of approximately 23.2°C in molten steel based on equation (2.13). A K-type thermocouple was used to control precisely the required temperature variation in between the inlet fluid and existing fluid within the tundish. The temperature of the water coming out through the SEN's was also measured with the help of a conductivity meter, so as to determine the extent of mixed convection prevailing with the tundish in the non-isothermal cases. Finally, tracer solutions were injected from the upper part of ladle shroud in the same way as for the isothermal cases.

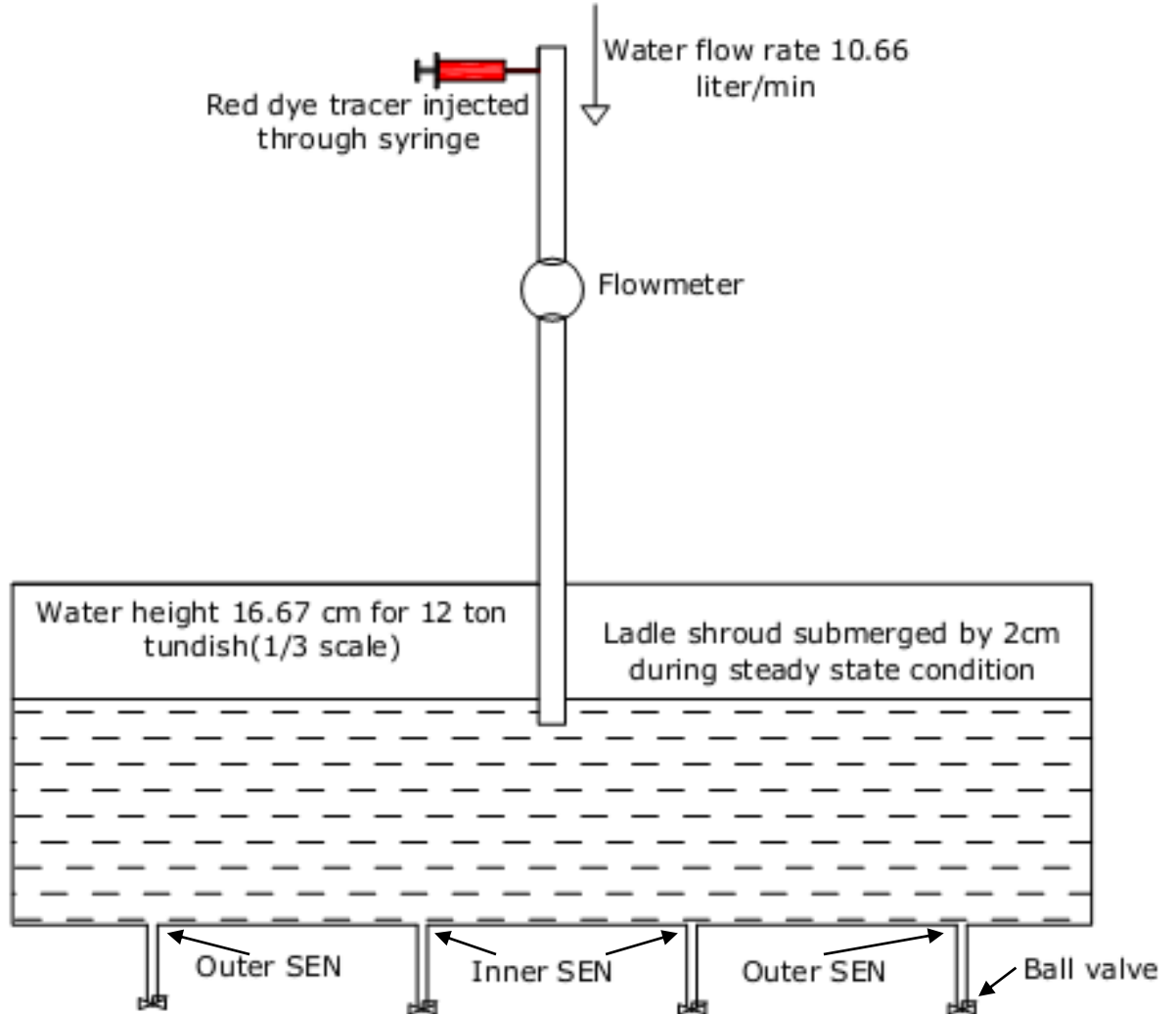


Figure 3.06. Schematic representation of tundish during tracer dispersion test

3.1.4 Residence Time Distribution (RTD) Analysis

To investigate the fluid flow characteristics such as the extent of mixing, short circuiting flows and dead zone volumes in the tundish, residence time distribution (RTD) curves have proved to be an important tool in studying of metallurgical performance of continuous casting tundishes. We used an online conductivity meter to measure, experimentally, the tracer concentration as a function of time. The experimental procedure was very similar as the tracer dispersion experiment. In our residence time

distribution (RTD) analysis experiment, we injected salt (sodium chloride) water solution of concentration 200 gram/liter as a pulse input through the ladle shroud, with the help of 50 ml syringe, under steady state conditions in the tundish. Furthermore, red dye was also added into the solution, in order to be able to visualize the fluid flow clearly within the tundish. To measure the water conductivity after injecting the tracer solution, we installed electric conductivity probes at the inner and outer SEN's. Later, we interfaced the reading of conductivity meter with the laptop computer through the RS-232 communication port cable and data acquisition software, WinWedge[®]. The schematic illustration of the residence time distribution (RTD) experiment is depicted in Figure 3.07.

The four strand delta shaped tundish has an attribute of a symmetrical shape which exhibits exactly similar dimensions on opposite sides of a dividing plane. So we considered half of the tundish for our experiments that contain one inner outlet and one outer outlet. Later, during experiments, we have seen that the flow is symmetrical and the change of the conductivity in outer SEN's and inner SEN's follow the same trend on the both symmetrical side. Finally, we took the reading of water conductivity up to two times of nominal residence time of the tundish and plotted the curve of change of conductivity against residence time of the tundish. One should note that this is only true, provided the ladle shroud is exactly vertically aligned to the center of longitudinal and transverse similarity [51].

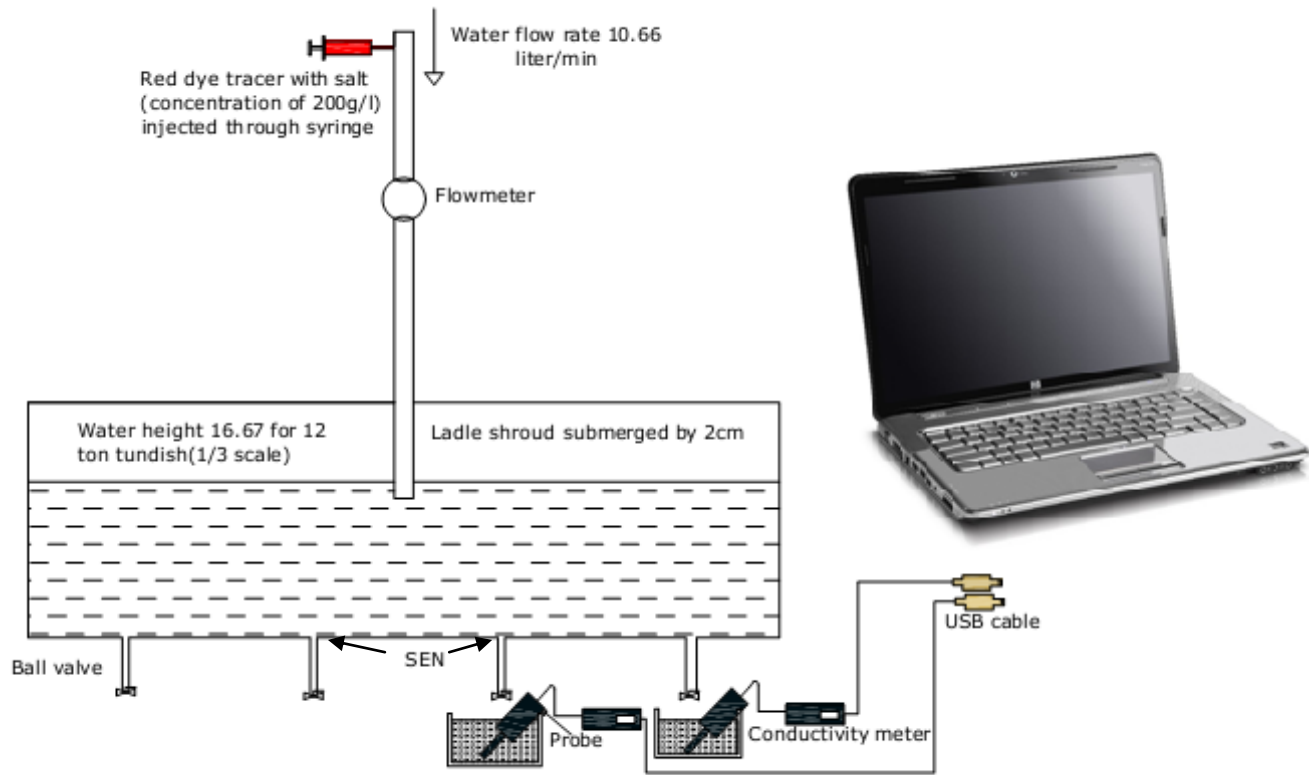


Figure 3.07. Schematic view of tundish during residence time distribution (RTD) analysis

Chapter 4.

RESULTS AND DISCUSSION

Our physical modeling experiments are discussed in details in this section. We carried out all the experiments in the one-third scale model of a four strand delta shaped tundish, first with bare tundish (tundish without flow modifier), secondly using McGill standard impact pad (MSIP) and finally McGill Improved Impact Pad (MIIP). We also elaborately analyzed possible non-isothermal conditions of tundish, as well as those for isothermal conditions, in order to assess practical conditions within a steel plant.

4.1 Slag Entrainment Experiments

The experimental set up for slag entrainment tests is shown in Figure 4.01. Corn oil (Density, 923.7 kg/m³; Viscosity, 0.061 pa-s) was used to simulate metallurgical slag. To visualize the oil clearly, Sudan IV (Molecular formula: C₂₄H₂₀N₄O) dye was employed. This dye is very soluble in oil but insoluble in water, thereby distinguishing the “slag” layer on the top of water, the interfacial level representing the slag interface in the steel plant. The simulated slag layer on the top of the fluid layer is shown in Figure 4.02. A very low flow rate and fine porosity Whatman[®] filter paper (Grade no. 5, Particle retention 2.5µm) was used to collect the entrained slag passing into the SEN's during a ladle change simulation. Under steady state flow conditions, a layer of oil-dye mixture (thickness roughly 10 mm) was distributed uniformly on top of the water. The ladle changing operation in the actual plant was simulated by closing the inflow shroud valve for 104s. As a result, the tundish liquid level dropped to around 35 mm. Then the inflow valve was fully opened to regain the constant height of 166.7 mm as soon as possible, similar to events in the steel plant when a new ladle is opened up for casting. Later, we have seen that slag was entrapped in the fine porosity filter as shown in Figure 4.03 after exiting from SEN. Finally, the ladle shroud valve was again closed, stopping the flow and allowing the filter papers to be removed and carefully dried, in order to measure the weight of entrained “slag”(oil) during the ladle changing operation.

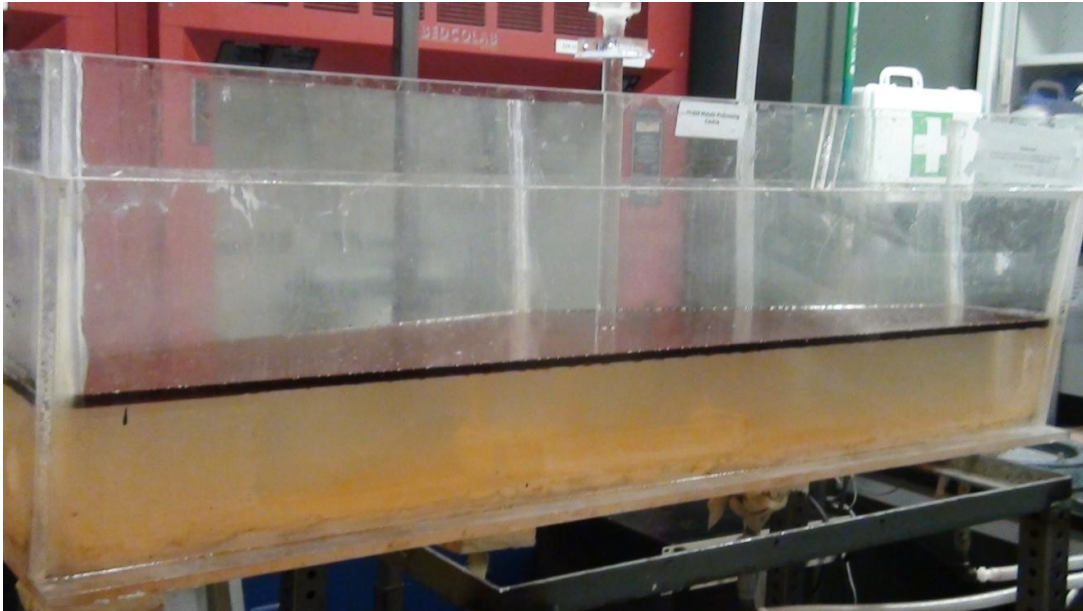


Figure 4.01. Schematic diagram of tundish during slag entrainment experiments

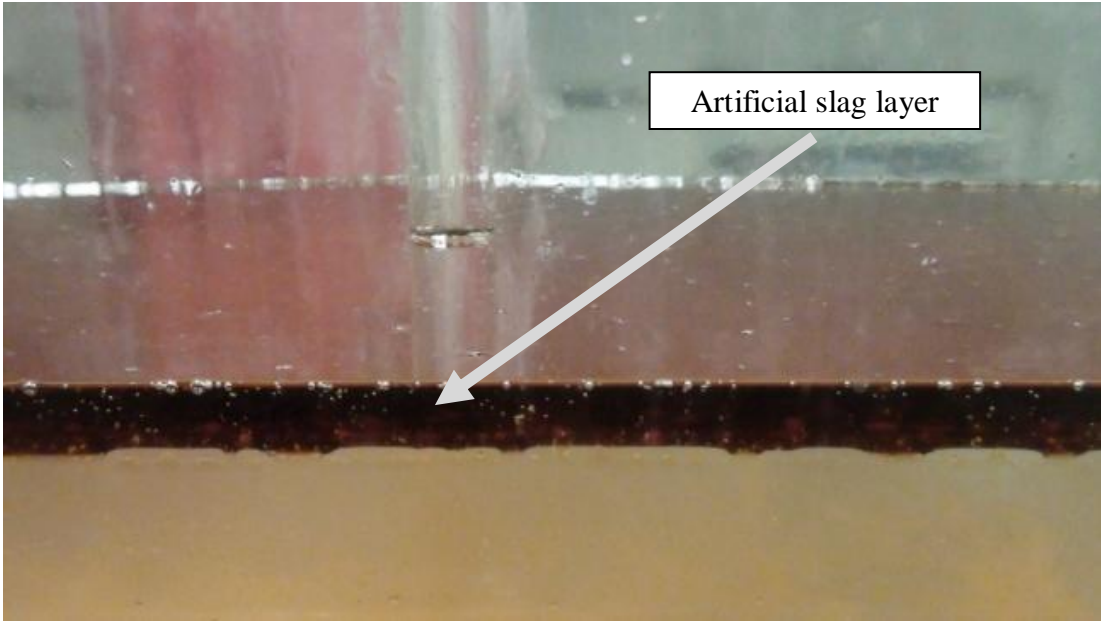


Figure 4.02. Simulated slag layer (Oil-Sudan IV dye) on the top surface of tundish at steady state water level



Figure 4.03. Attached Watman-5 filter paper in the SEN in order to collect entrained slag

4.1.1. Slag entrainment analysis in a bare tundish and tundish fitted with different flow modifiers

In order to study the effects of flow modifying devices on slag entrainment, the model tundish was fitted with the different types studied, including the McGill Standard Impact Pad (MSIP) and the newly proposed optimized flow modifier namely McGill Improved Impact Pad (MIIP) in a four strand delta shaped 12 tonne capacity tundish. Similarly, the bare tundish and changes in the ratio of tundish length and bath height (increasing the capacity of tundish by increasing the height) were evaluated. It was observed from Table 4.01 that the tundish, fitted with an McGill Improved Impact Pad (MIIP), entrained less slag compared to a tundish with a McGill Standard Impact Pad (MSIP) and much less versus a bare tundish during a ladle change simulation. For the bare tundish, more inclusions were entrained in the inner strand (~5734 mg) as compared to the outer strand (~719 mg), since flows were not interrupted by any turbulence inhibiting devices. The high value of the standard deviation in the bare tundish case indicates the uneven distribution of slag, as well. When the tundish was fitted with the MSIP, the weight of simulated slag (Oil-Sudan IV dye layer) reporting to the inner strand (~2630 mg) was

reduced considerably, since the impact pad redirected flows upwards towards the surface, completely changing the velocity field as shown in Figure 4.04.

However, even smaller amounts of slag were entrained in the tundish fitted with the optimized impact pad, MIIP, as shown in the bar chart shown in Figure 4.06 for both inner nozzles (~435 mg) and outer nozzles (~350 mg). Similarly, a more homogeneous distribution of slag was observed in this case compared to other arrangements. This is because the fluid delivered by ladle shroud hits the bottom of the tundish at a high momentum and distribute the turbulent energy more uniformly compared to the tundish equipped with MSIP cases and bare tundish cases. As a result, strong upwelling flows were generated in the MIIP zone towards the free surface as demonstrated in Figure 4.05. These flows emanate from the corners of the impact pad and gradually proceed towards the outer SEN region, front wall and back wall of tundish, which allow it to maintain a uniform distribution of non-metallic particles into each mould. So it is evident from the slag entrainment tests that the tundish furnished with MIIP performed the best among the configurations studied, in terms of optimized fluid flow, which is beneficial for inclusion flotation.

Table 4.01: Slag entrainment in tundish with different flow modifiers

Arrangement	Governing parameters for two experiment	Weight of collected oil (mg)	
		Inner Strand	Outer Strand
Bare Tundish (Tundish without flow modifiers)	Exp. 1	6319.00	563.00
	Exp. 2	5149.00	876.00
	Average	5734.00	719.50
Tundish fitted with standard impact pad (MSIP)	Exp. 1	2480.00	590.00
	Exp. 2	2780.00	890.00
	Average	2630.00	740.00
Tundish with improved impact pad (MIIP)	Exp. 1	470.00	340.00
	Exp. 2	400.00	360.00
	Average	435.00	350.00



Figure 4.04. Slag movements in a tundish fitted with as MSIP during ladle change operation



Figure 4.05. Slag movements in a tundish fitted with a MIIP during a ladle change operation

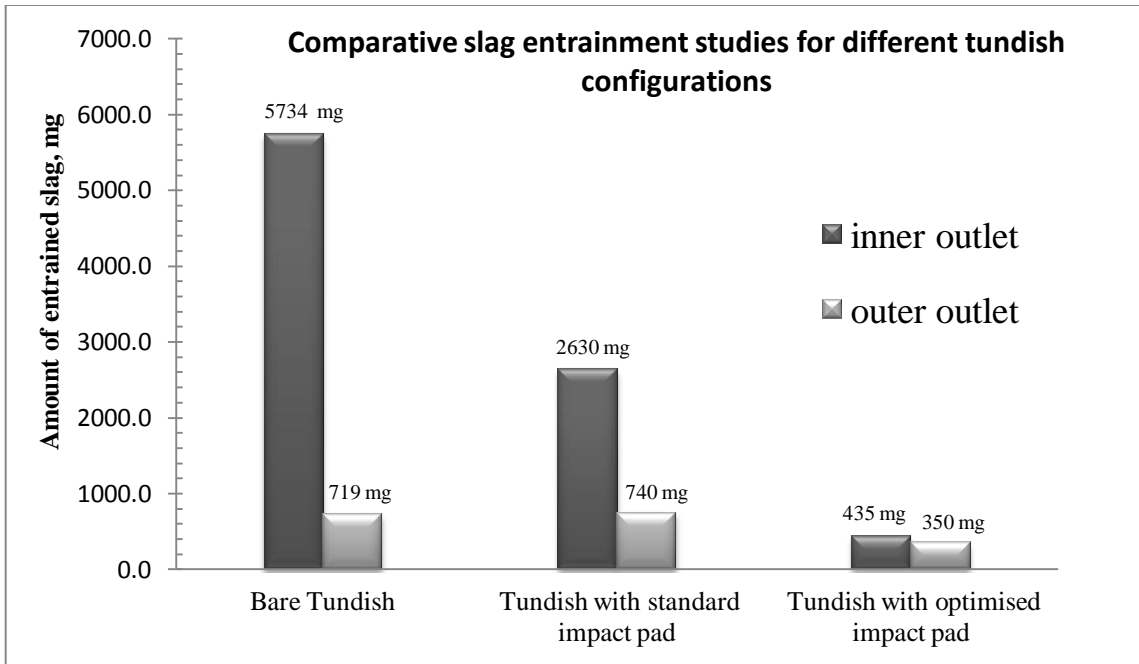


Figure 4.06: Comparative chart of weight of “slag” entrained during a ladle change simulation, for different FCD’s.

4.1.2 Slag Entrainment Studies on Increased Capacity Tundish

The molten steel capacity of a tundish can be further increased by increasing the height of the tundish. When there is an increased volume of molten metal within the tundish, this will prolong the residence time of liquid steel within it. As such, this could enhance inclusion flotation. It has been observed in the comparative bar chart shown in Figure 4.07 that reduced amounts of slag were entrained during ladle changing operations at both the inner and outer SEN’s when increasing the capacity of the tundish from 12 tonne to 20 tonne fitted with MIIP. This was accomplished by increasing the height of the liquid level from 166.7 mm to 235 mm. To maintain the steady state height, we considered the inflow rate of 16.365 liter/minutes and 18.183 liter/minutes for 18 tonne and 20 tonne capacity tundish, respectively whereas for 12 tonne capacity tundish, we maintained incoming flow rate of 10.67 liter/minutes through the ladle shroud. For the experiments involving the 12 tonne capacity tundish fitted with the MIIP, significantly more oil reported to the inner nozzle (~435 mg) than the outer nozzle (~350 mg), compared to the 18 tonne capacity tundish followed by weight of entrained slag during ladle changing period in the inner nozzle 368 mg and outer nozzle 206 mg, respectively

and for the 20t tundish followed by weight of entrained slag in the inner nozzle 320 mg and outer nozzle 190 mg, respectively.

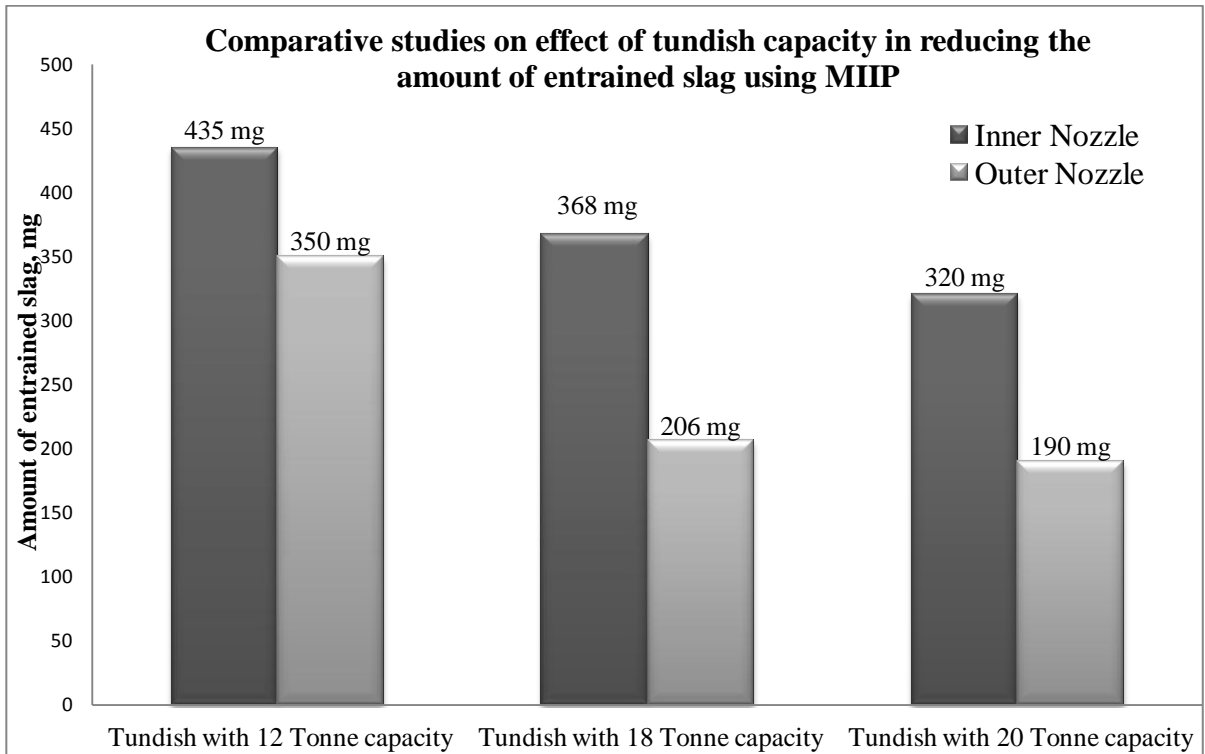


Figure 4.07: Comparative bar chart of weight of “slag” entrained during a ladle change simulation, with varying capacity of the tundish

It was predicted that more inclusions were floated on the top free surface of a higher capacity tundish of 18 tonne and 20 tonne in comparison with 12 tonne tundish fitted with the MIIP. This is because higher residence time of fluid promotes the flotation of inclusions in a better way by enabling the inclusion particles to move towards the top slag layer. In addition, in a higher capacity tundish, a lesser amount of inclusions were attached in the both of inner SEN's and outer SEN's. In these cases, the overall fluid level was higher in 18 tonne and 20 tonne capacity tundish after the drop in level during a ladle change operation when there was no incoming steel passing through the ladle shroud. This created a strong surface directed flow originating from the center of the impact pad towards the surrounding area of the tundish and reduced the amounts of inclusions significantly.

The trend of slag entrainment test during ladle changing operations can also be analysed qualitatively by knowing the amount of entrained simulated slag in each strand as depicted in Figure 4.08. For the case of 18 tonne and 20 tonne tundishes, owing to the higher bath levels, the strong, inflowing jet of water through the ladle shroud, after impinging near the base of tundish, spreads outwards towards the location of the outer nozzle (SEN) and gradually proceeds towards the front wall and back wall of tundish. However, in the case of 12t tundish, the high velocity inflowing jet of water impacts directly on to the base of tundish, and increases the tendency to re-direct flows into the SEN's. This leads to higher amounts of slag reporting to the inner and outer nozzles. For the outer SEN's, the fluid particles move towards the location of the outer nozzle after intercepting the inner nozzle or following a different path across the length of the tundish and therefore, contained smaller amount of slag being collected at the outer nozzles. Because outer SENS's being located at a distant position from shroud axes, facilitate enough time for the simulated oil (slag) to float out during ladle change operations.

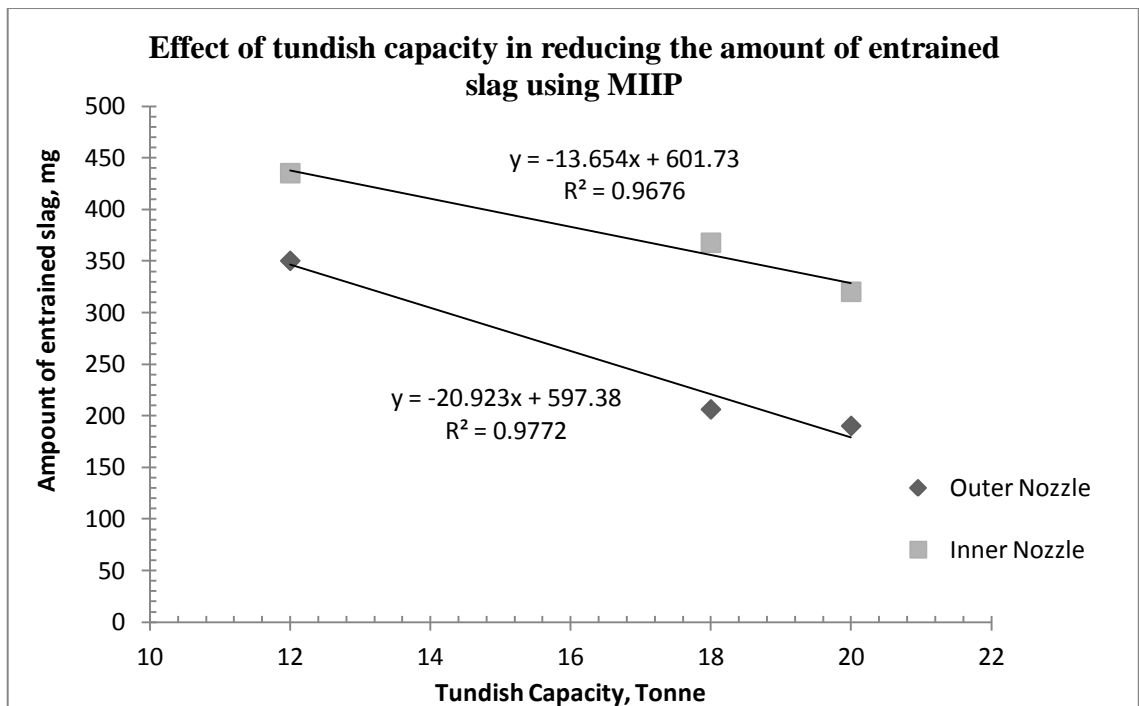


Figure 4.08. Effect of tundish capacity in reducing the amount of entrained slag

4.2 Tracer Dispersion Studies

We investigated two conditions during tracer dispersion studies, namely isothermal and non-isothermal. In the isothermal case, the temperature of the molten steel through ladle shroud is equivalent to the temperature of molten steel within the tundish. Non-isothermal melt flow conditions can happen in the plant due to heat losses in the tundish or in the ladle transfer station.

4.2.1 Isothermal conditions of Tundish with Different Flow modifiers

A visual observation of red dye tracer mixing phenomena in the model tundish after a few seconds of injection is shown in Figures 4.09, 4.10, 4.11, 4.12, 4.13 and 4.14 for a bare tundish, a tundish fitted with a McGill standard impact pad (MSIP) and a tundish, fitted with the McGill improved impact pad (MIIP) in isothermal conditions.

For a bare tundish, the tracer fans out across the bottom surface of the impact pad, proceeding quickly to the front wall, followed by the back wall, (or the delta shaped wall) and later towards the side walls of the tundish. In the bare tundish, the incoming tracer from the ladle into the tundish immediately enters the SEN outlets of the tundish, representing a “short circuiting” flow. The inner SEN's show higher “short circuiting” flows, whereas in outer SEN's, the “short circuiting” flows are reduced tremendously, as those are located far from ladle shroud position. These flows are very detrimental with regards to steel quality and thermal homogeneity among steels cast through the individual strands. This type of flow also creates the non-uniform residence times between the inner and outer strands, illustrated in Figures 4.09a, 4.10a and 4.11a. In the upper corners of the tundish, the fluid moves very slowly, denoting “dead” regions. It was observed that bare tundish experienced large dead volumes, substantial short circuiting flow and strong turbulence, that worsen the steel quality significantly. When the tundish is fitted with the standard impact pad shown in Figures 4.09b, 4.10b and 4.11b, less short circuit flows and dead volume were observed. The use of the improved impact pad (Figure 4.09c, 4.10c and 4.11c) changed the flow patterns significantly, largely eliminating the short circuiting phenomena and dead volumes. So the tundish fitted with this type of flow furniture shows that the tracer initially impinges on the bottom surface of the tundish and then disperse laterally in an upward direction, and later on, at the front and back walls. For tundishes fitted with the MSIP and MIIP, the tracer solution moved upwards because a

strong recirculation flow is generated in the impact pad zone. Therefore, the tracer moves towards the free surface due to this recirculation force, causing larger size inclusions to be directed straight up towards the top slag layer.

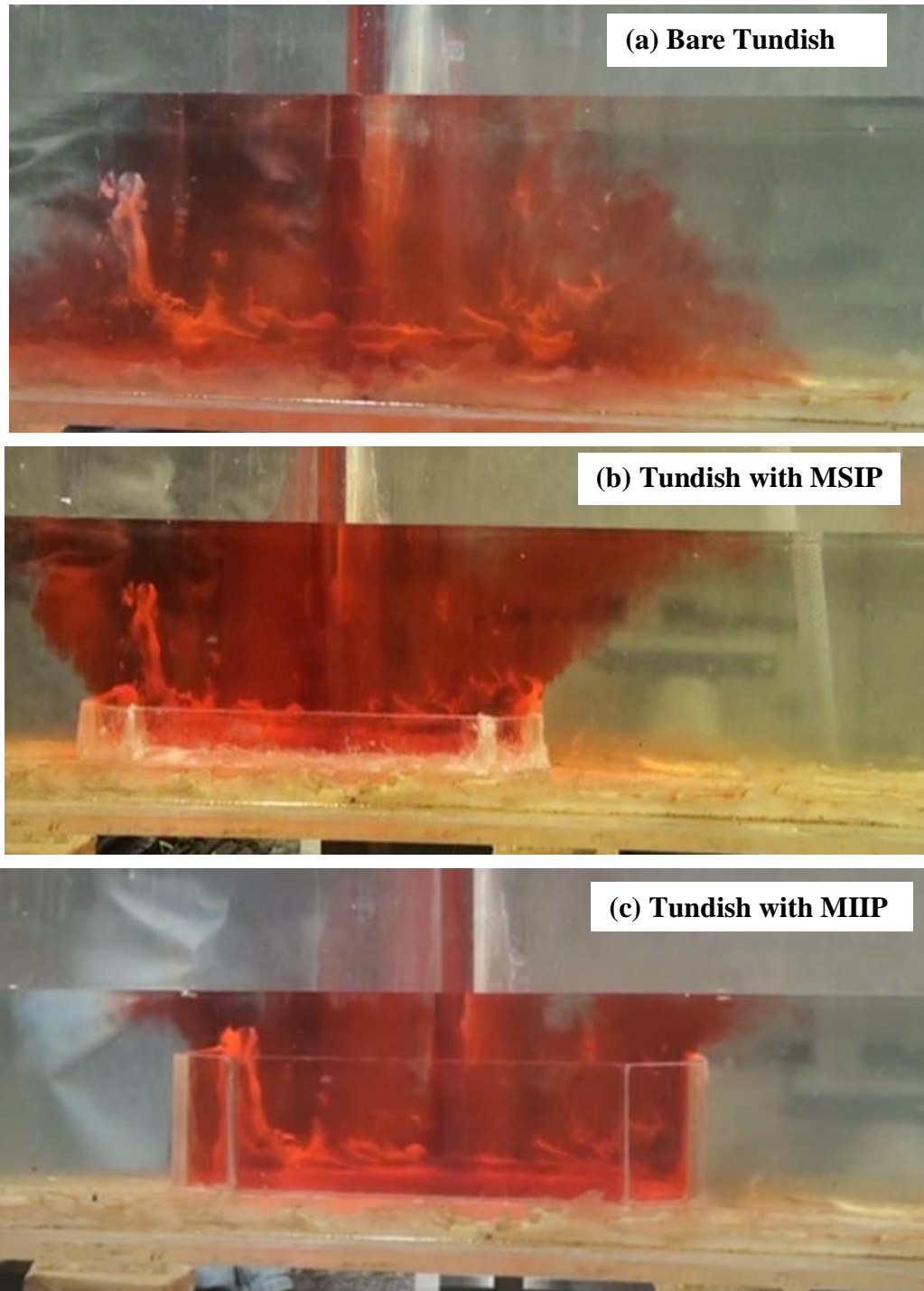


Figure 4.09. Tracer distribution within the tundish under isothermal conditions, $\Delta t = 5s$, using different flow arrangements

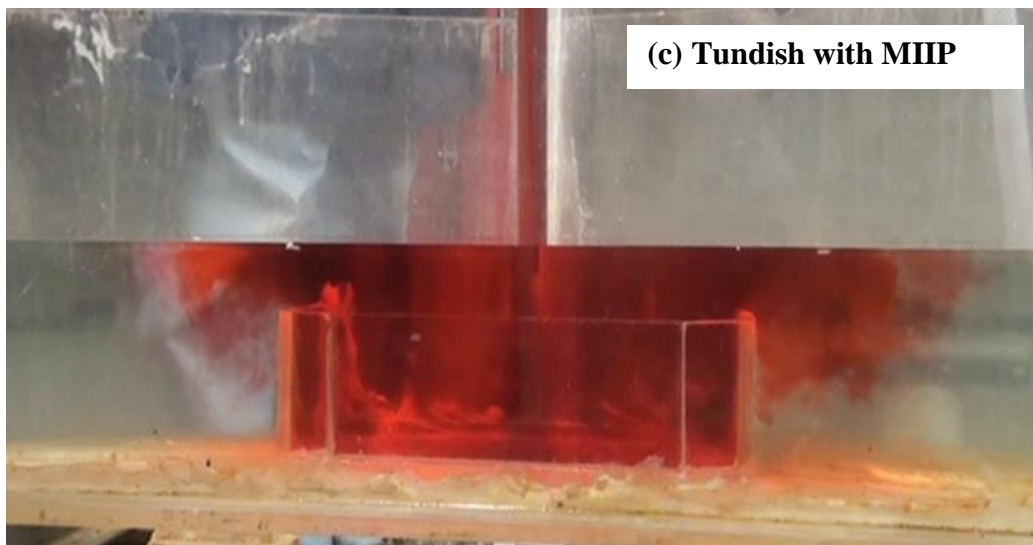
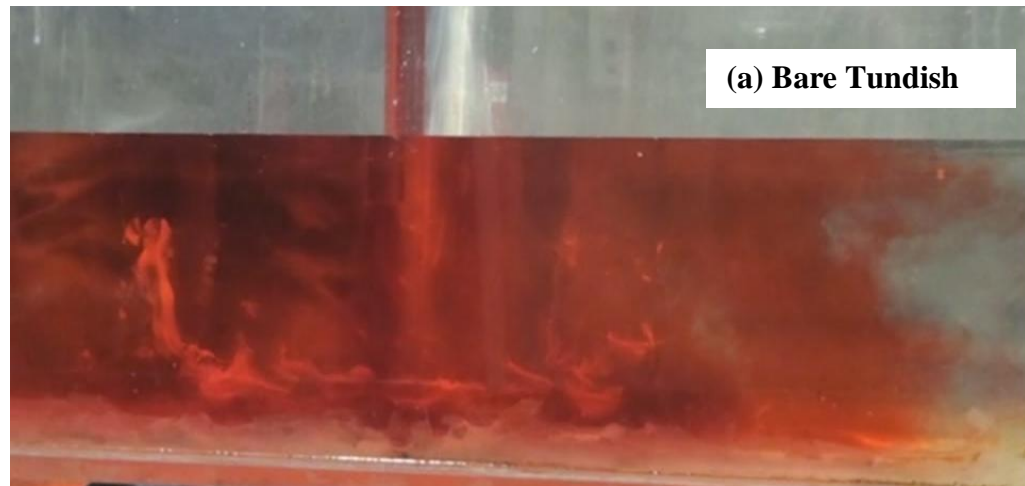


Figure 4.10. Tracer distribution within the tundish under isothermal conditions, $\Delta t = 8s$, using different flow arrangements

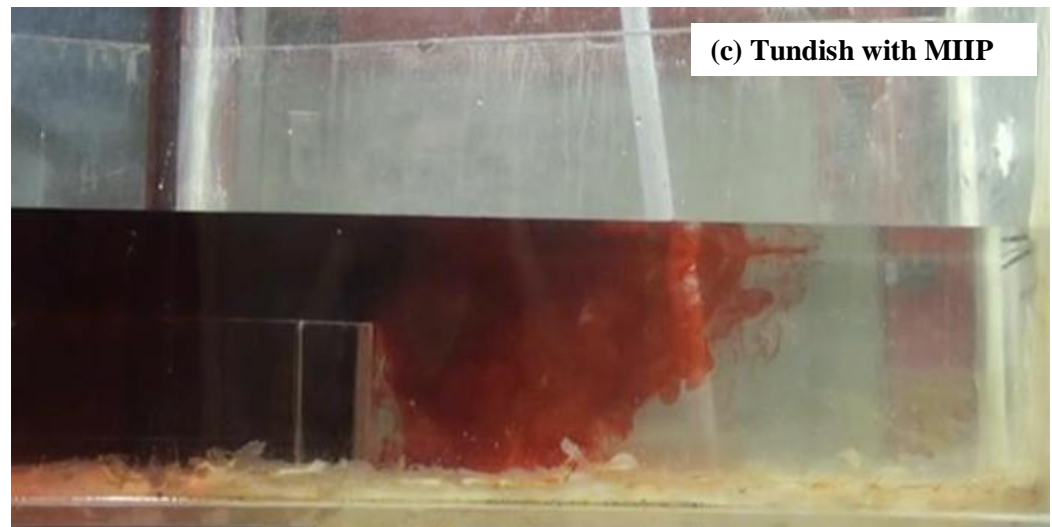
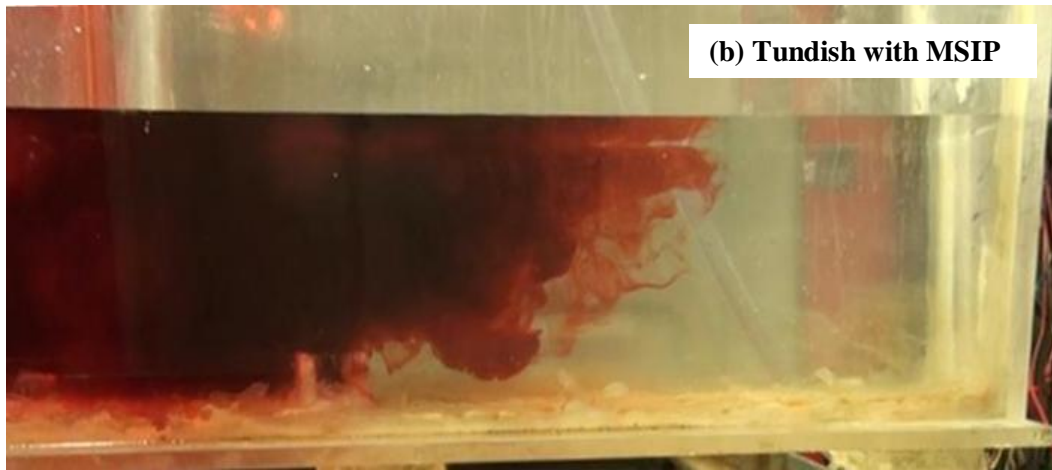
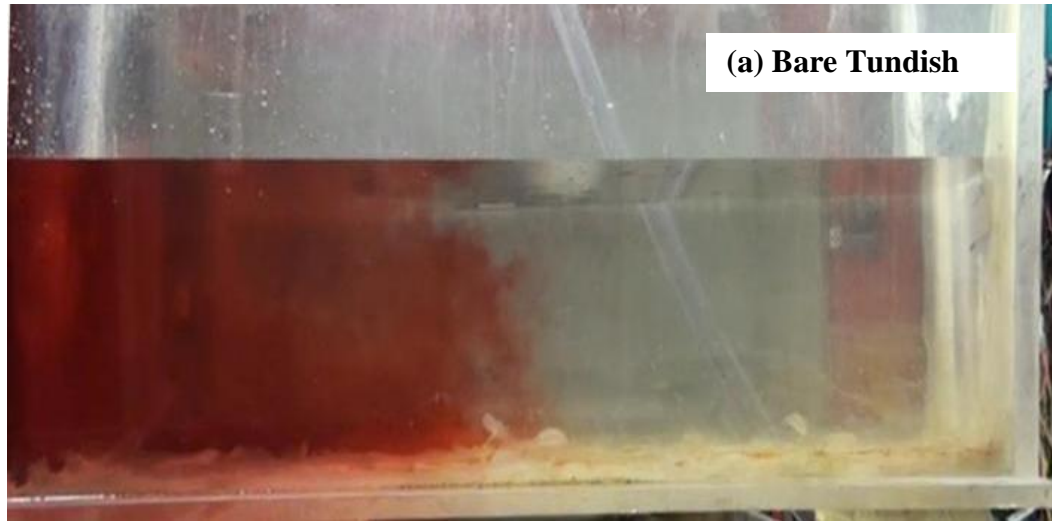


Figure 4.11. Tracer distribution within the tundish under isothermal conditions, $\Delta t = 15s$, using different flow arrangements

After 32s of tracer dispersion (Figure 4.12), it has been observed that the fluid moves towards the outer SEN's without changing the flow direction. For a tundish fitted with the MSIP, fluid flow has been changed due to the recirculation flow as shown in Figure 4.12b. The most beneficial flow in terms of steel cleanliness was observed when the tundish was furnished with the MIIP (Figure 4.12c). The MIIP generates more recirculatory upward flows compared to the MSIP. This impedes the fluid particles from proceeding towards the SEN's instead of filtering the non-metallic particle from the melt fluid by changing the direction to the upward surface as well as towards the front and the back wall of the tundish. For the MIIP-tundish, the tracer is distributed more evenly within the tundish, and finally proceeds towards the inner strand and outer strand in a trend, same as fluid flow satisfies the plug flow characteristics. Basically, an improved impact pad works as a resistive wall to fluid flow, and diminishes the turbulence and velocities in the jet pouring zone. Therefore, lining wear near the tundish wall could also be reduced. After 58s, we have seen that there is slow moving region called the dead volume zone in the corner of bare tundish (Figure 4.13a) which is not desired during casting, as it could be liable to result in local solidification within the tundish. Similarly, it could create problems in maintaining accurate strength and ductility in the water cooled mould due to subsequent heat loss in the dead volume zone. For a tundish fitted with MSIP, a small amount of dead volume was observed, as shown in Figure 4.13b. The interesting phenomenon, we noticed that the dead volume zone is predominately eliminated when the tundish was equipped with the MIIP, as shown in figure 4.13c. However, the incoming tracer was fully mixed within the tundish after 120s for all tundish configurations, as portrayed in Figure 4.14.

The improved impact pad seems to disperse the fluid motion along the transverse and longitudinal axes of tundish in a better way, as compared to the MSIP and certainly the bare tundish. This could ensure the homogeneity of melt mixing within the bath. Furthermore, these types of impact pads can also be useful in reducing the smaller size inclusions by pushing them towards the nearest tundish wall that acts as a barrier. So, the inclusions could not go towards the SEN's. Finally, a higher quality "steel" could be obtained.

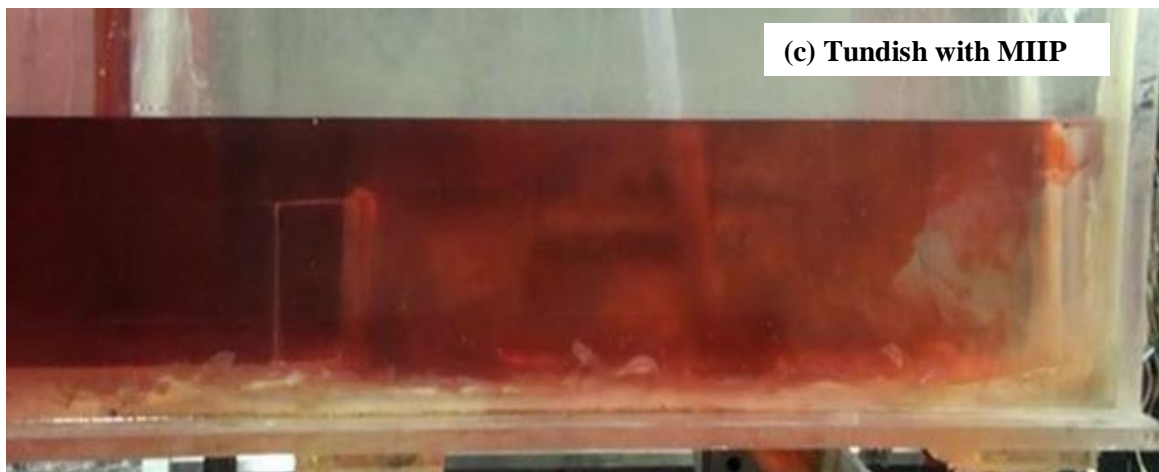
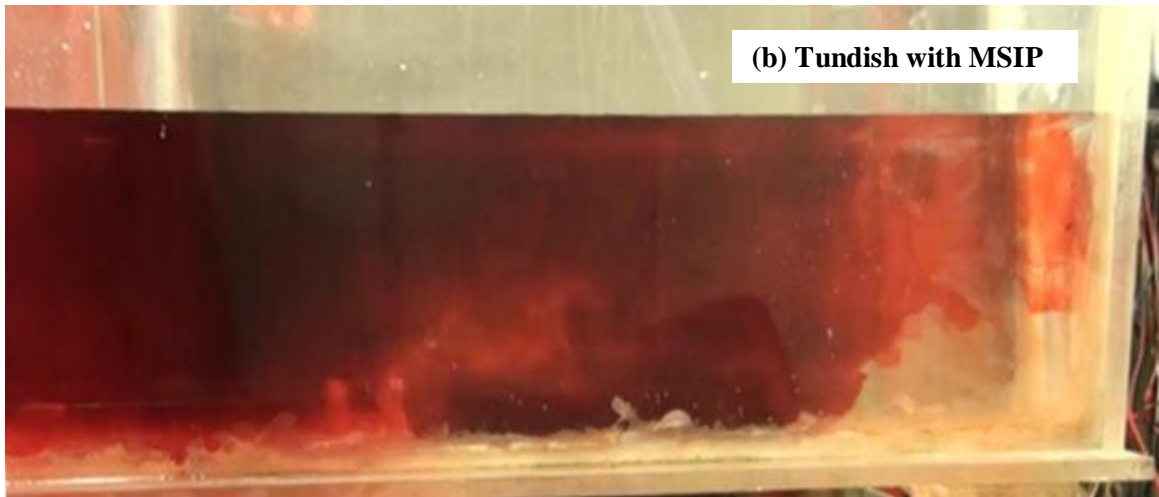
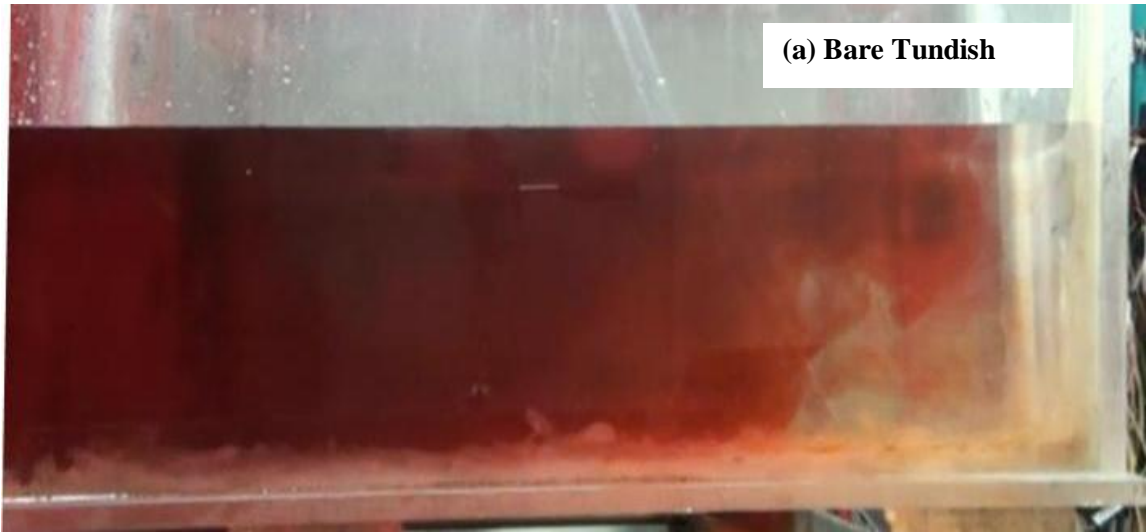


Figure 4.12. Tracer distribution within the tundish under isothermal conditions, $\Delta t = 32s$, using different flow arrangements

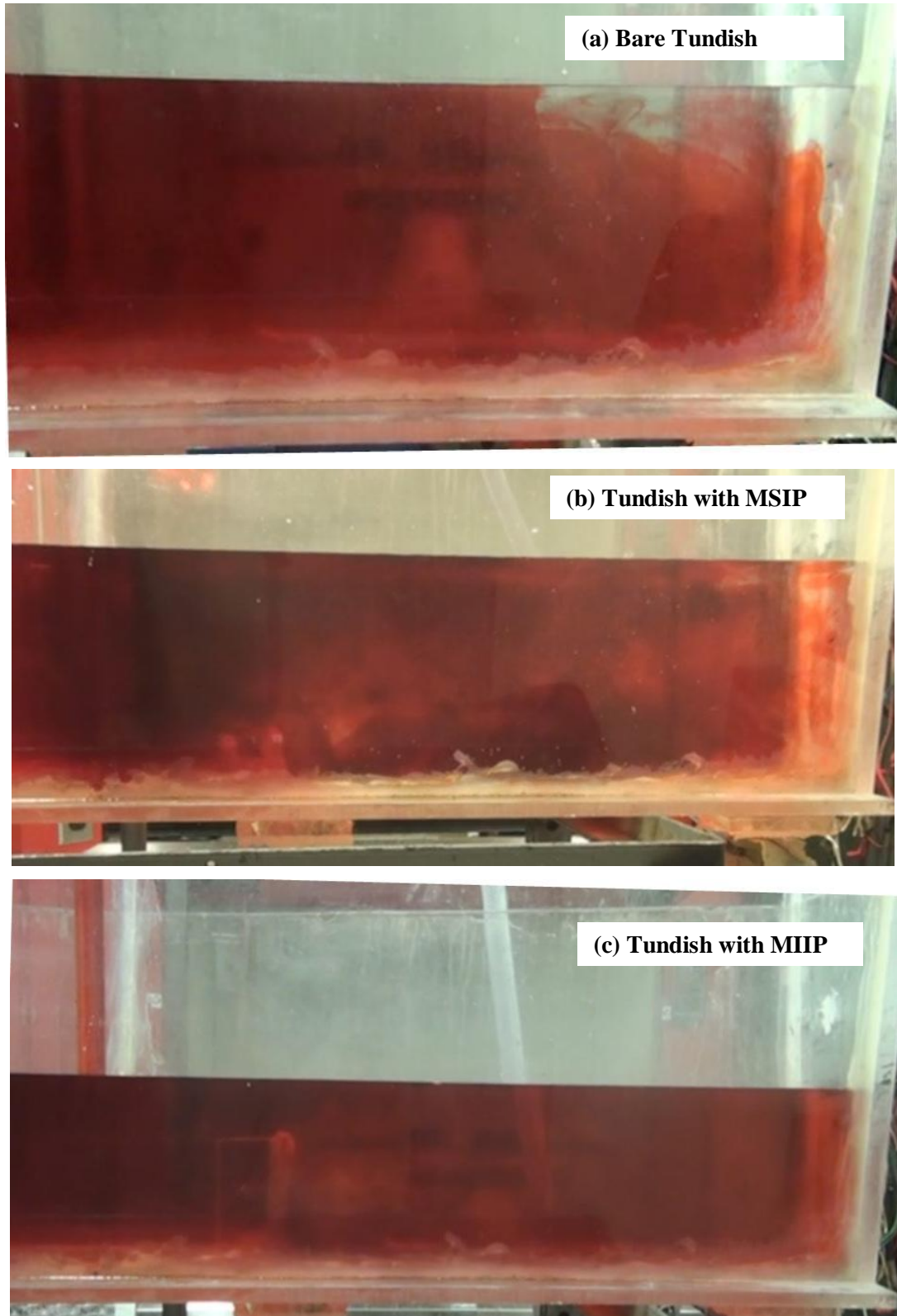


Figure 4.13. Tracer distribution within the tundish under isothermal conditions, $\Delta t = 58s$, using different flow arrangements

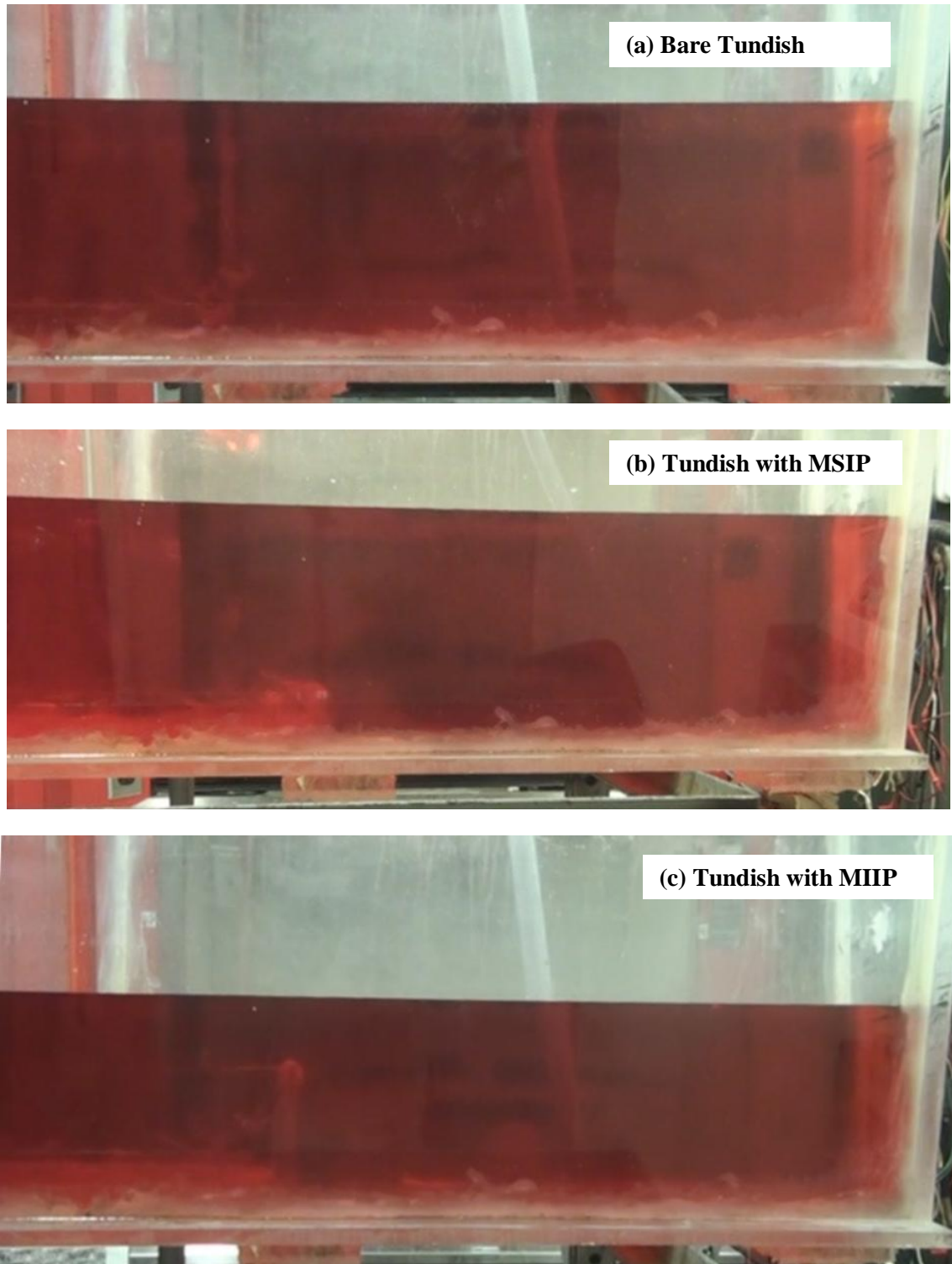


Figure 4.14. Tracer distribution within the tundish under isothermal conditions, $\Delta t = 120s$, using different flow arrangements

4.2.2 Non-isothermal conditions of Tundish with Different Flow modifiers

Isothermal conditions in a tundish is a pretty rare condition within an industrial plant due to temperature variations of incoming liquid steel and existing steel within the tundish, which is also losing heat. So, most often, non-isothermal conditions of tundish are exhibited in the plant. In non-isothermal cases, there are two sub-classes consisting of a step-up and step-down condition. The non-isothermal step up condition happen in the plant when the temperature of the incoming steel entering the shroud is higher than the temperature of molten steel in the tundish. This is due to the heat losses through the conduction and convection from the side walls and bottom of the tundish, and radiation from the top surface of tundish. The non-isothermal step down condition can occur in the plant when the temperature of the incoming steel is lower than the temperature of the existing molten steel within the tundish. This can happen when molten steel has taken a longer time to reach the turret and has been losing heat in the ladle during transfer between the steelmaking furnace and ladle turret, or equivalent pouring station.

These variable melt temperatures can affect the overall quality of steel. Usually a higher incoming melt temperature is liable for surface defects in the subsequent rolling process of the ingot and a lower incoming temperature tends to cause local solidification of molten metal in the slow moving (cooler area) zone of tundish [67]. So the effect of buoyancy forces on molten steel flow must be analyzed broadly to predict the optimized fluid flow that helps to obtain more refined steel.

4.2.2.1 Step-up in temperature of 10°C (+10°C)

The non-isothermal step-up temperature conditions in the tundish will likely occur in any plant. To analyse the effect of a non-isothermal step-up temperature condition, we introduced the " hot " water of 19°C through the ladle shroud, whereas the temperature of the existing water within the tundish was maintained at around 9°C. The interesting phenomena in the step up delta temperature increments reveal that the tracer dye mixes in the same path for the first 10s, equivalent to the isothermal case (Fig. 4.15). This is because at the beginning of the tracer dispersion, turbulence is very high in the pouring zone and flows are dominated by only inertial forces. Later, the fluid flow characteristics

change dramatically. After 20~25s, buoyancy forces begin to dominate, and the tracer is pushed towards the top surface and gradually proceeds towards the bottom of the tundish as depicted in Figure 4.15a. In the case of a tundish without flow modifiers (Bare Tundish), for a step up of 10°C, the tracer first moves to the bottom of the tundish. Basically, two way fluid flows were observed of which in one way fluid disperse towards inner outlet (SEN) and other way fluid flow directs towards top surface owing to density difference (Fig. 4.15a and Fig. 4.16a). When the tundish was fitted with the MSIP, the improved fluid flow behavior was observed in terms of non-metallic particle entrapment in the SEN. The MSIP redirects the flow towards the top surface, rather than dispersing the fluid directly into the inner SEN's (Fig. 4.15b and Fig. 4.16b). However, the optimised fluid flow was observed when the tundish was fitted with the MIIP. In this case, the tracer first hits the wall of impact pad and the back wall of the tundish, then proceeds laterally (Fig. 4.15c and Fig. 4.16ac). A strong upward flow was generated in the impact pad zone. So the tracer moves towards the top surface due to this force.

Over the subsequent residence time, the dominant role of buoyant force asserts itself and redirects the fluid flow towards the upper free surface. After 32s, it was evident that the hot incoming fluid, being lighter, had moved towards the top surface (Fig. 4.17). The trends in this fluid flow phenomena are practically same for all tundish configurations. However, lower upward flows were generated in the bare tundish due to absence of the turbulence inhibiting device and re-directing the flows in the pouring zone. Furthermore, a tundish furnished with a MSIP or a MIIP, produce more upwind force due to presence of impact pad. So, the placement of an impact pad in the pouring zone for the step-up temperature conditions helps to obtain better quality steel. After 60s, it was observed that the tracer solution mixes homogeneously all over the tundish for all configurations (Fig. 4.18). The interesting characteristics of non-isothermal step-up conditions is that the fast uniform mixing of incoming fluid within the tundish and the higher upward force were generated force due to density differences.

The buoyancy force could be higher when the liquid within the tundish experienced a step-up temperature of 15-20°C. The upward force facilitates inclusion removal since it drives some inclusions to the free surface and these can be captured in the slag layer.

Therefore, a non-isothermal " step-up " condition can be beneficial, within specific melt temperature variations in the plant in terms of molten steel cleanliness.

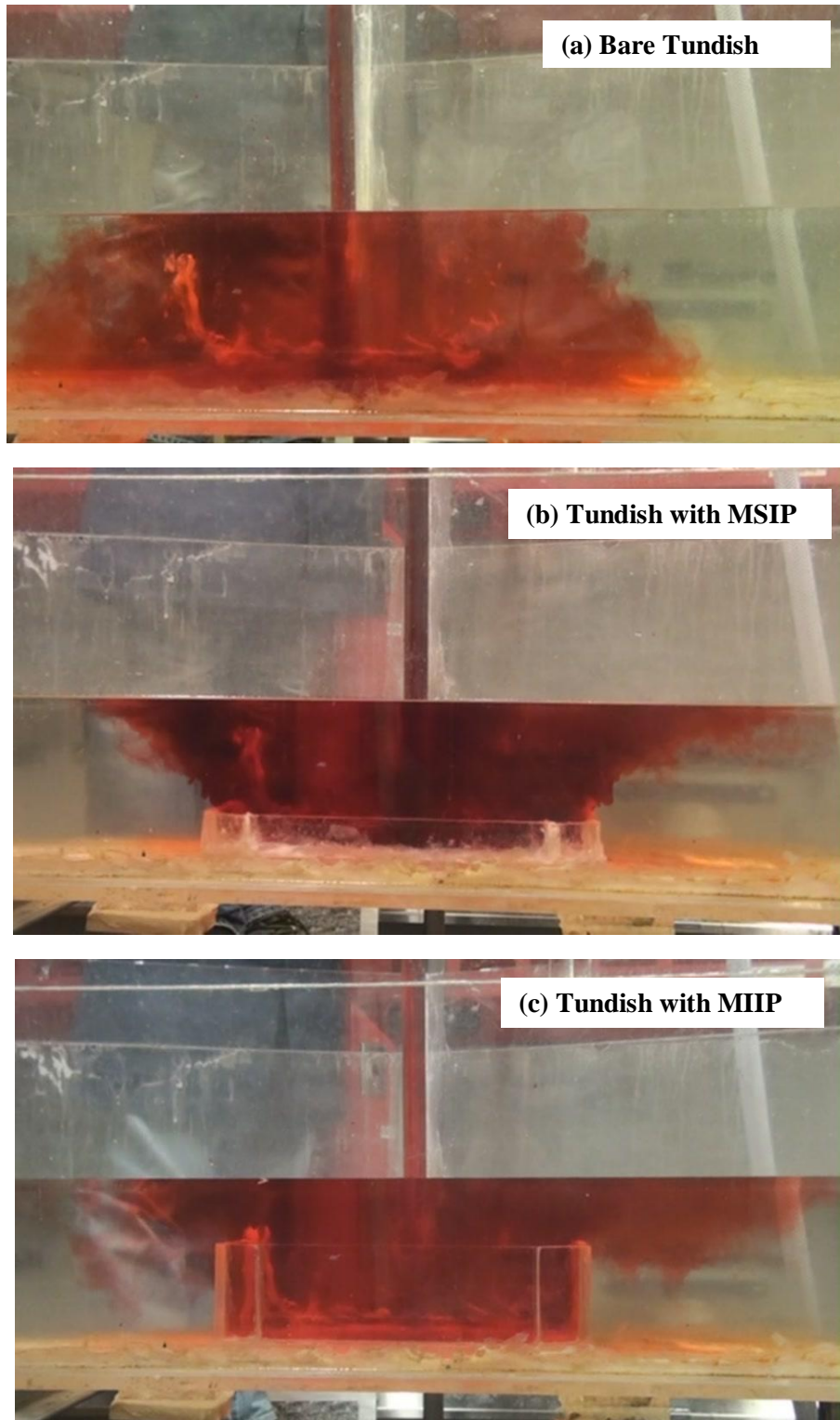


Figure 4.15. Tracer distribution within the tundish under non-isothermal conditions after 10s, for different flow arrangements for a step up of $\Delta T = +10^{\circ}\text{C}$

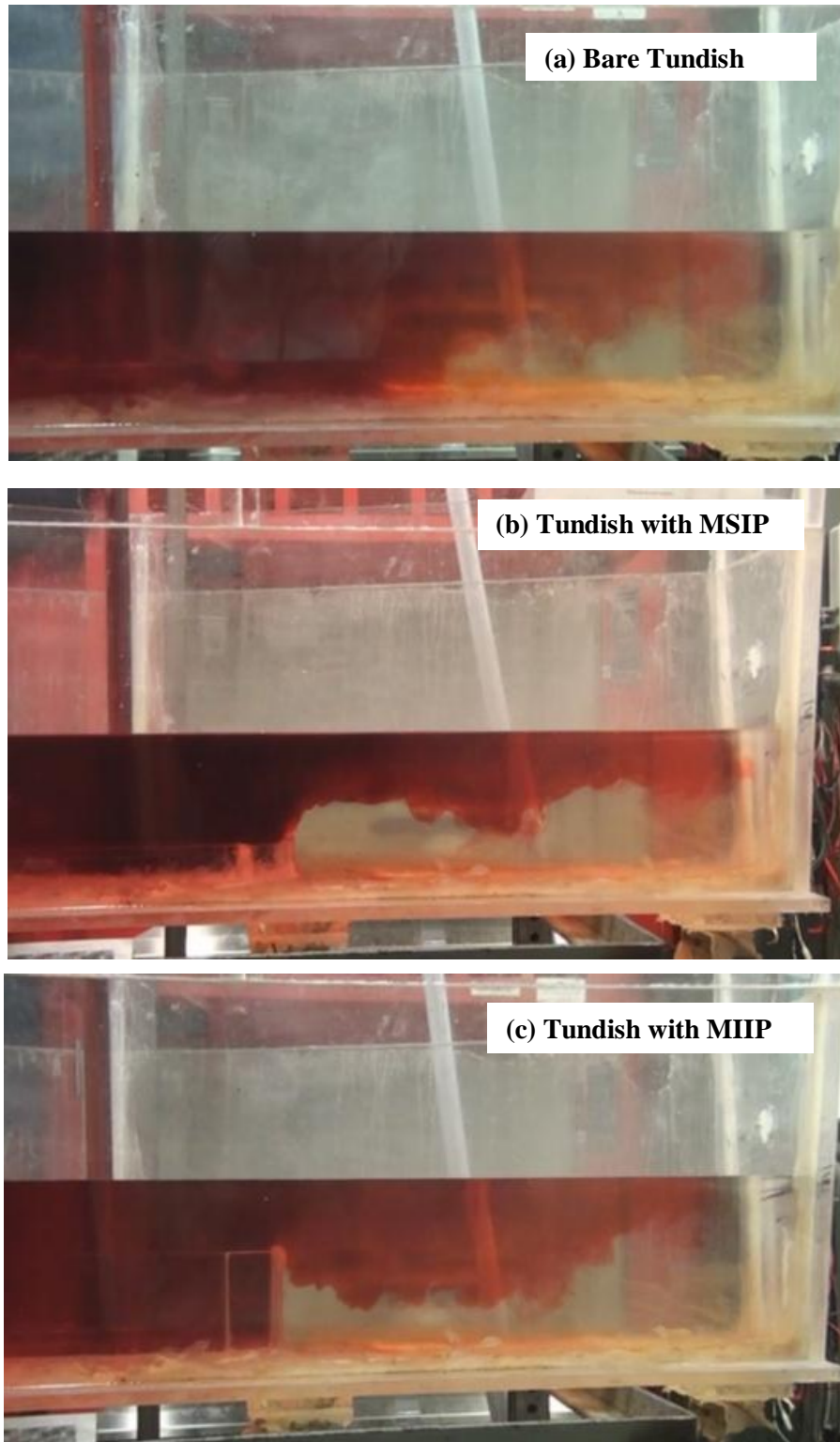


Figure 4.16. Tracer distribution within the tundish under non-isothermal conditions after 20s, for different flow arrangements for a step up of $\Delta T = +10^{\circ}\text{C}$

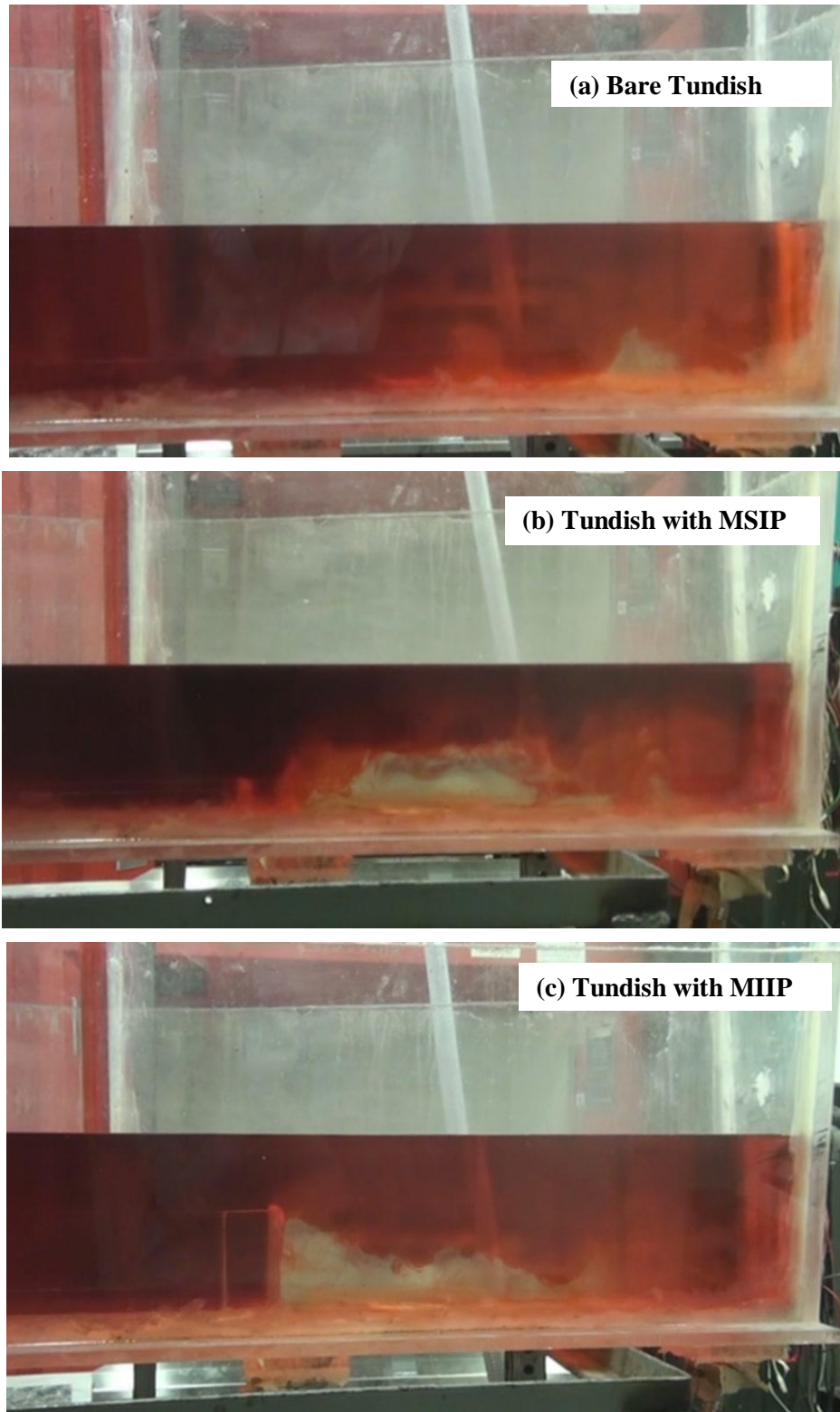


Figure 4.17. Tracer distribution within the tundish under non-isothermal conditions after 32s, for different flow arrangements for a step up of $\Delta T = +10^{\circ}\text{C}$

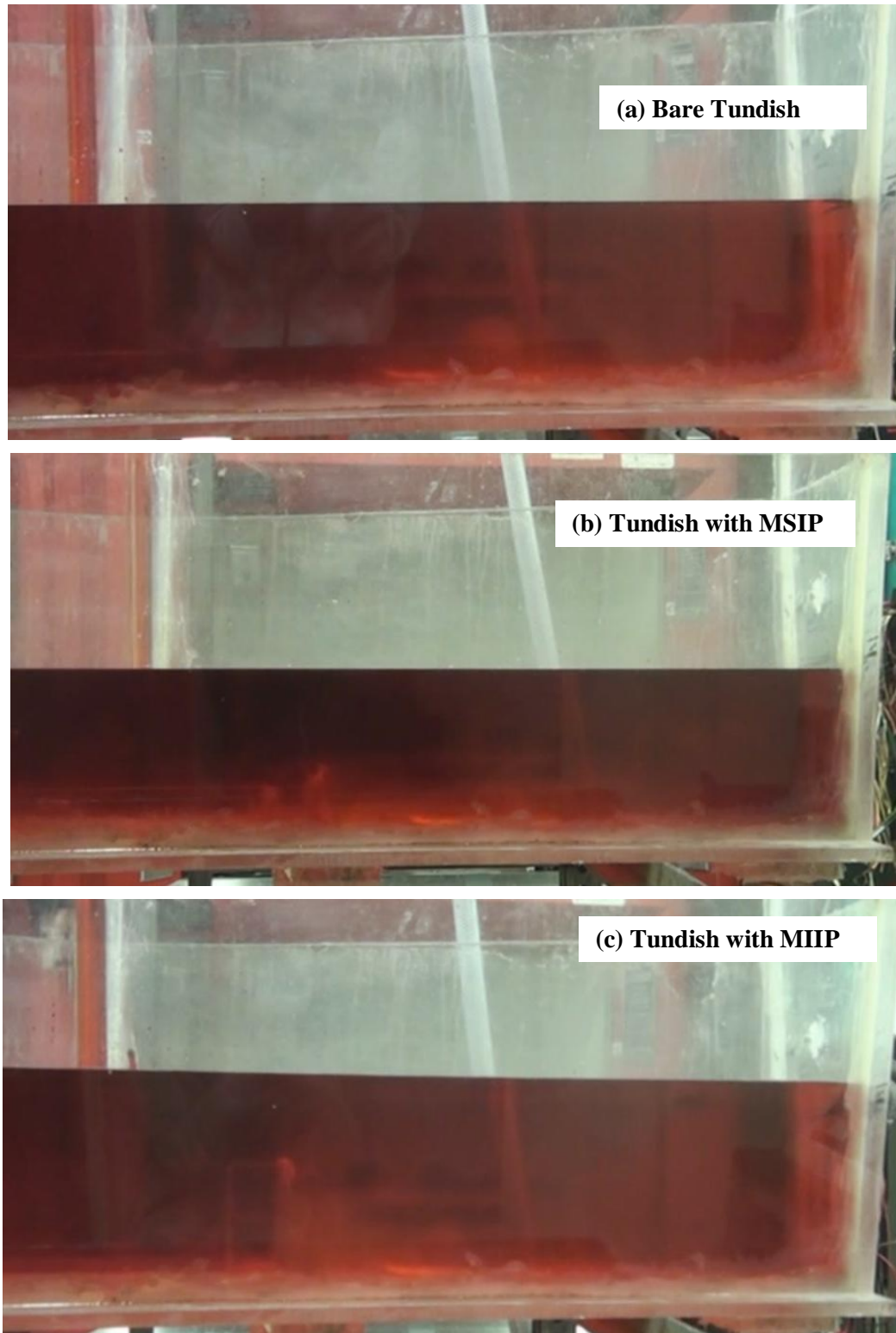


Figure 4.18. Tracer distribution within the tundish under non-isothermal conditions after 60s, for different flow arrangements for a step up of $\Delta T = +10^{\circ}\text{C}$

4.2.2.1 Step-down in temperature of 10°C (-10°C)

In some operational cases within an industrial plant, the temperature of the incoming molten steel can be lower than the temperature of the existing steel within the tundish. To examine the effect of steel quality for this condition, we kept the temperature of water at 25°C within the tundish by adding hot water through ladle shroud. After that, cold water of 15°C was added to make the temperature difference. The interesting observation is that tracer mixing phenomena up to 10-12s in this non-isothermal step down temperature system was again quite identical to the isothermal conditions in all configurations of tundish (Fig. 4.19). This same trend, we also observed in the non-isothermal step up temperature system of tundish with different flow furnitures and bare tundish, as well. So after introducing cooler incoming fluid, it was analysed that the downward flow due to density difference did not abruptly come into effect in the overall fluid flow behavior within the tundish. After elapsing certain time, the difference in the movement of tracer due to incoming heavier liquid, were figured out. The general trends demonstrated in this case is noted that the tracer proceeds from the back side of the tundish to the front side of the tundish and an inward force is predicted to be dominant due to heavier incoming fluid.

When the bare tundish was considered, after approximately 20-25s, the heavier (colder) incoming tracer went down directly towards the SEN without any impediment, (Fig.4.20a). This will deteriorate steel quality greatly leading to many more non-metallic particles reporting to the ingot. But a little upward flow was generated in the pouring zone when the tundish was fitted with a MSIP as shown in Figure 4.20b. This carries the incoming fluid towards the free surface and promotes inclusion flotation. Furthermore, when tundish was fitted with an MIIP, higher upward flows were produced inside the impact pad region (Fig. 4.20c), as compared to the MSIP case. This would also promote inclusion flotation towards the top free surface. However, it was observed that all the incoming colder fluid proceeds towards the inner and outer SEN's entraining more inclusions. After 42s of tracer dispersion (Fig. 4.21), strong downward flow are seen. This will raise the tendency of tracer being pushed down directly into the SEN's. The buoyancy forces become stronger with time in all cases of tundish studied i.e. bare

tundish, tundish fitted with MSIP and MIIP. After 120s following the pulse injection of tracer, it was observed that the tracer mixing pattern did not cover the whole projected area of the tundish (Fig. 4.22). So the extent of mixing in the tundish in the non-isothermal step down conditions is lower than the non-isothermal step up conditions due to heavier incoming fluid going down directly to the bottom of the tundish. The slow moving region, known as the dead volume zone, was observed in the top right corner of all the tundish configurations. So in the non-isothermal step down case, there could be a higher tendency for local solidification in the top corner of tundish. This could worsen the ingot quality severely through uneven solidification in the water cooled mould tube. So a step-down condition in a tundish is believed to be more detrimental to steel quality as compared to a step up condition, since during this condition most of the inclusions are directly entrained into the SEN's being worsening steel purity in the plant. Therefore, adequate measures must be put in place to eradicate this problem.

It is predicted that the buoyancy effect could be even more dominant when the temperature difference between incoming fluid and existing fluid of tundish is higher than 10°C. This could deteriorate the quality of steel badly, directing significant amounts of inclusions directly towards the SEN's where they are subsequently entrained into the solidified ingot.

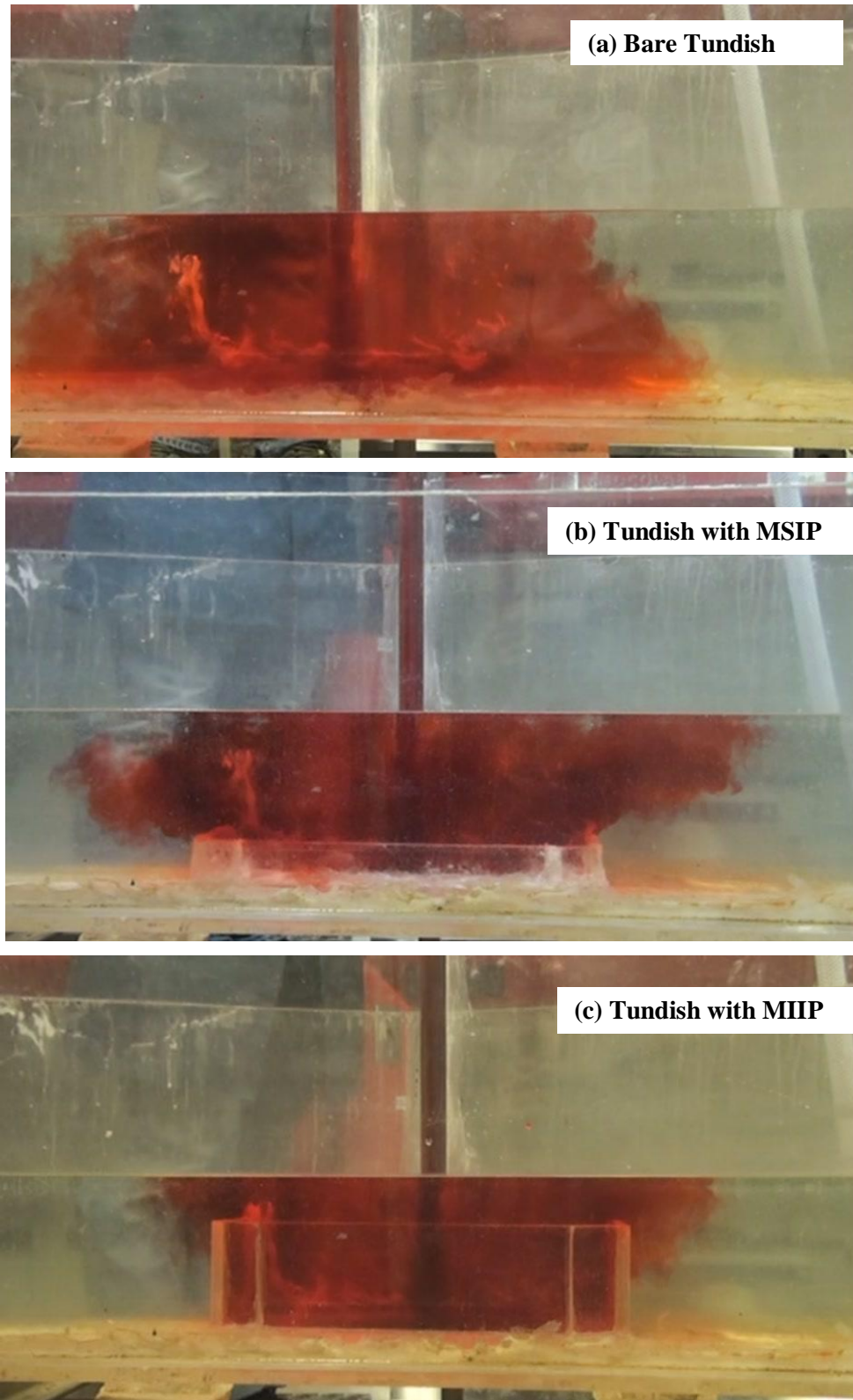


Figure 4.19. Tracer distribution within the tundish under non-isothermal conditions after 10s, for different flow arrangements for a step down of $\Delta T = -10^{\circ}\text{C}$

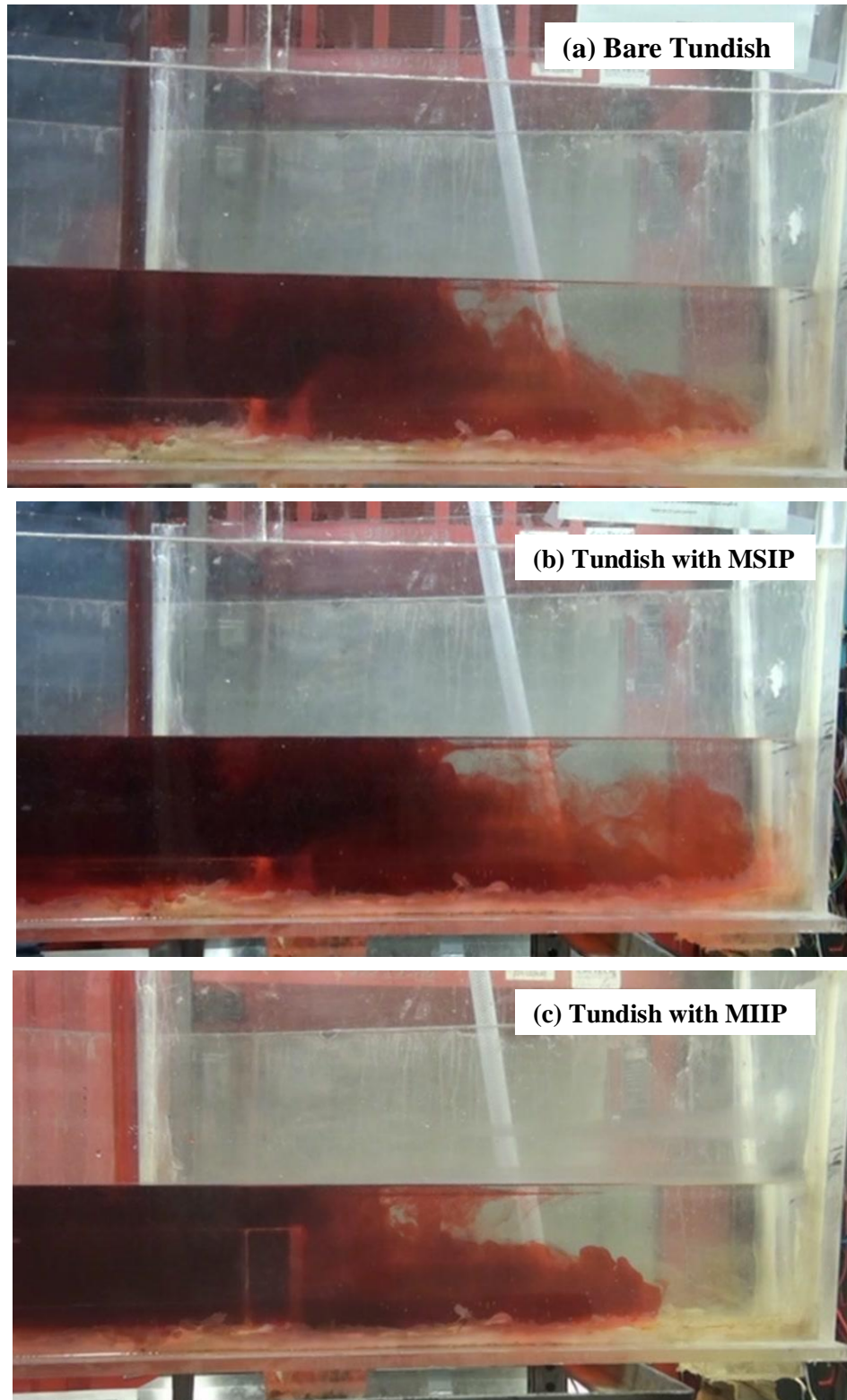


Figure 4.20. Tracer distribution within the tundish under non-isothermal conditions after 25s, for different flow arrangements for a step down of $\Delta T = -10^{\circ}\text{C}$

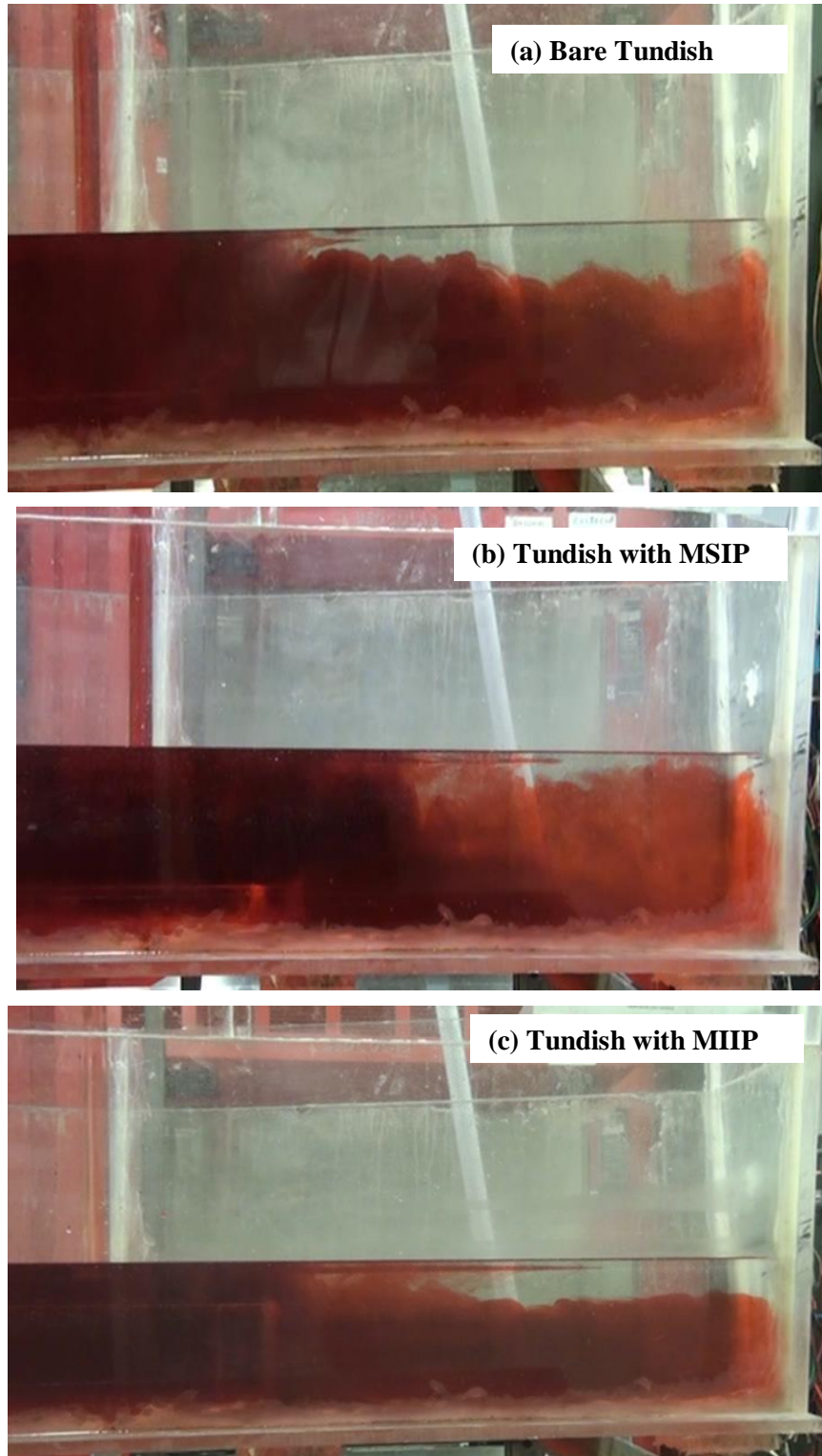


Figure 4.21. Tracer distribution within the tundish under non-isothermal conditions after 42s, for different flow arrangements for a step down of $\Delta T = -10^{\circ}\text{C}$

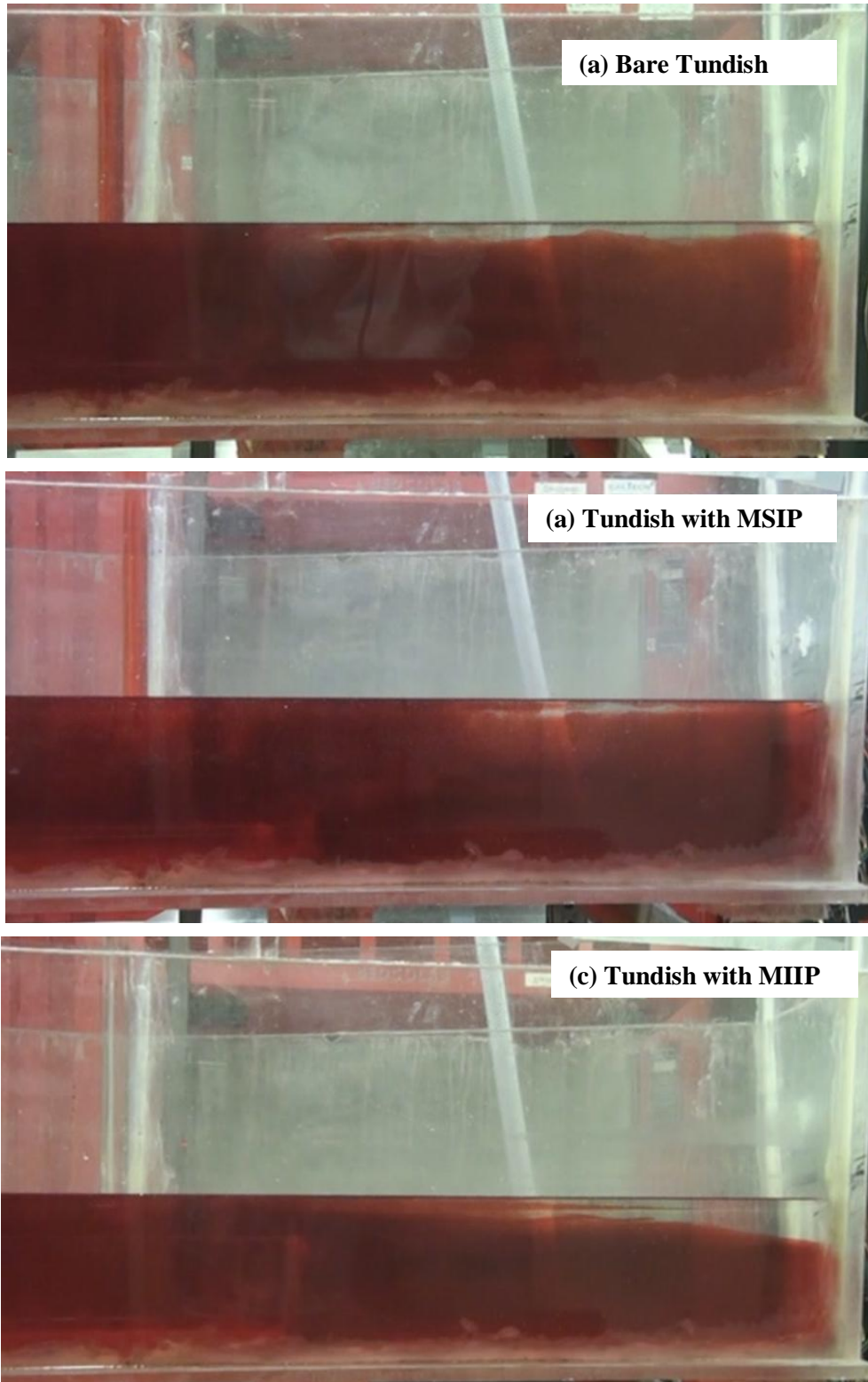


Figure 4.22. Tracer distribution within the tundish under non-isothermal conditions after 120s, for different flow arrangements for a step down of $\Delta T = -10^{\circ}\text{C}$

4.2.3. Non-isothermal conditions of tundish : Effect of buoyancy number

Non-isothermal tundish phenomena can be further quantified using the Buoyancy Number, Bu which represents the ratio of inertial forces to buoyancy driven forces. For the water model and the actual tundish prototype, the equivalence of temperature rises in two fluids can be defined as follows :

$$Bu = \frac{\text{Buoyancy Force}}{\text{Inertial Force}} = \frac{\beta \Delta T g L^3 / \nu^2}{Re^2} = \frac{Gr}{Re^2}$$

$$\left(\frac{Gr}{Re^2} \right)_{\text{Steel}} = \left(\frac{Gr}{Re^2} \right)_{\text{water}}$$

By simplifying this expression we can finally obtain,

$$\Delta T_{\text{Steel}} \approx \frac{\beta_{\text{water}}}{\beta_{\text{Steel}}} \Delta T_{\text{Water}}$$

Hence, the average stokes rising velocity of a particle through a cross section of tundish can be calculated using the formula [39], $u_{\text{particle}} = \frac{\Delta \rho g d^2}{18\mu}$. For industrial plant conditions, we predicted density of the molten steel and inclusion (alumina) are 7000 kg/m³ and 3100 kg/m³, respectively. Furthermore, for simulating actual inclusions in water modeling, hollow glass microspheres (Density 300 kg/m³) were considered. Hollow glass microspheres in water and alumina inclusions in liquid steel were assumed to be in the size range of 50-300 μm. For 1/3 scale tundish, we found the diameter of glass microspheres 214.92 μm using equation (2.9).

Bu predicts the intensity of buoyancy force in comparison with the inertial forces. We evaluated the $Bu(U_o^2/u_p^2)$, where U_o is the inlet fluid velocity and u_p is the inclusion particles velocity within the tundish. When the temperature increments of the incoming fluid and existing fluid within the tundish are between 1~3°C, all the flow arrangements, including the increased capacity tundish, exhibit practically equivalent results, as observed in Figure 4.23 and 4.24. However, for temperature difference of 5°C, the 20 tonne capacity tundish evaluated to be higher $Bu(U_o^2/u_p^2)$, in comparison with 12 tonne capacity tundish. This is because, higher turbulence flow leading to higher level of fluid in the 20 tonne capacity tundish in the vertical plane near the ladle shroud which could accelerate the degree of mixing within the tundish. When a tundish with a capacity of 12t

was considered with a temperature difference of 20°C in the liquid steel tundish and the water model tundish, $Bu(U_o^2/u_p^2)$, ranges from 3.4E+06 ~ 6.7E+07 (shown in Table 4.03 and 4.04). Further increasing the volume of fluid in the tundish raises the $Bu(U_o^2/u_p^2)$, considerably, and this enhances the recirculating upwind flow. Figure 4.23 shows that when the height of bath 50cm (12t capacity full scale tundish), $Bu(U_o^2/u_p^2)$, increases very slowly. But for the temperature difference of 20°C, the buoyancy forces are stronger. When the height of the bath increases to enhance the volume of liquid metal in tundish, the $Bu(U_o^2/u_p^2)$, increases very fast.

Table 4.02. Calculation of average particle rise velocity through a cross section of Tundish

Simulated criteria	Density of fluid, kg/m ³	Density of particle, kg/m ³	g m/s ²	Particle diameter, μm	Viscosity of fluid Kg/m-s	Average rise velocity m/s
Steel-alumina	7000	3100	9.81	300	0.0067	0.029
Water- glass microsphere	1000	295	9.81	300	0.00114	0.030

Table 4.03. $Bu(U_o^2/u_p^2)$ calculation in liquid steel tundish varying the size of tundish(full scale)

β_s	g	H _s for 12 Ton capacity tundish, L cm	H _s for 20 Ton capacity tundish, L cm	u _p m/s	U ₀ m/s	Δ T K	Bu(U _o ² /u _p ²) for 12 Ton tundish	U ₀ m/s	Bu(U _o ² /u _p ²) for 20 Ton tundish
1.27 E-04	9.81	50	70.5	0.029	60.83	1	3.4E+06	100.25	1.3E+07
						5	1.7E+07		6.4E+07
						10	3.4E+07		1.3E+08
						15	5.0E+07		1.9E+08
						20	6.7E+07		2.6E+08

Table 4.04. $Bu(U_o^2/u_p^2)$ calculation in water model tundish varying the size of tundish (full scale)

β_w	g	H _w for 12 Ton capacity tundish, L cm	H _w for 20 Ton capacity tundish, L cm	u _p m/s	U ₀ m/s	ΔT K	Bu for 12 Ton tundish	U ₀ m/s	Bu for 20 Ton tundish
2.95 E-04	9.81	50	70.5	0.030	60.83	1	6.5E+06	100.25	2.5E+07
						5	3.2E+07		1.2E+08
						10	6.5E+07		1.2E+08
						15	9.7E+07		3.7E+08
						20	1.3E+08		5.0E+08

Table 4.05. $Bu(U_o^2/u_p^2)$ calculation in water model tundish varying the size of tundish (1/3 scale)

β_w	g	H _w for 12 Ton	H _w for 20 Ton	$u_{inclusion}$	u_o	ΔT	Bu for 12 Ton	U_o	Bu for 20 Ton
k^{-1}	m/s^2	capacity tundish, L cm	capacity tundish, L cm	m/s	m/s	K	tundish	m/s	tundish
						1	8.9E+06		3.7E+07
						5	4.5E+07		1.8E+08
2.95	9.81	16.67	23.5	0.0156	33.93	10	8.9E+07	57.88	3.7E+08
E-04						15	1.3E+08		5.5E+08
						20	1.8E+08		7.3E+08

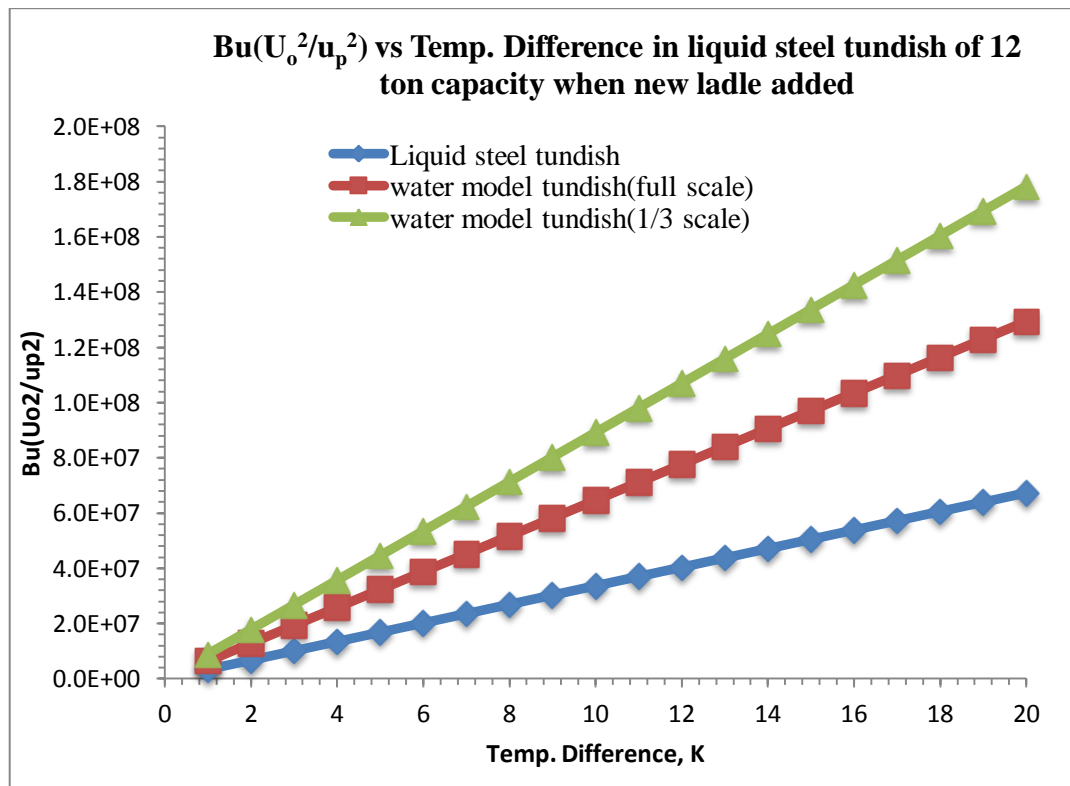


Figure 4.23: $Bu(U_o^2/u_p^2)$ vs. temperature difference in a liquid steel tundish steel, for a 12 tonne capacity when a new ladle containing fresh liquid steel is employed

Figure 4.24 shows that the buoyancy forces are stronger in a tundish with a capacity of 20t versus a 12t capacity reported in Fig. 4.23. So the buoyancy force plays a more dominant role in deeper, higher capacity tundishes. This will enhance recirculating flows as well as residence time of the fluid particles. Tundishes with large volumes of liquid

metal might contain less inclusions if the higher upward recirculating flows generate higher rates of inclusion flotation.

The interesting observation in every case is that at low bulk temperature differences, the buoyancy forces become closer to inertial forces for both systems (liquid steel tundish and water model tundish). So at low temperature increment of melt between incoming fluid coming through ladle and existing fluid within tundish, overall fluid flow is dominated by only inertial forces and high turbulence is generated by the high velocity of the entering stream in the pouring zone. This turbulence is diminished in the impact pad zone and then observed the mixed convection patterns in the rest of the tundish system.

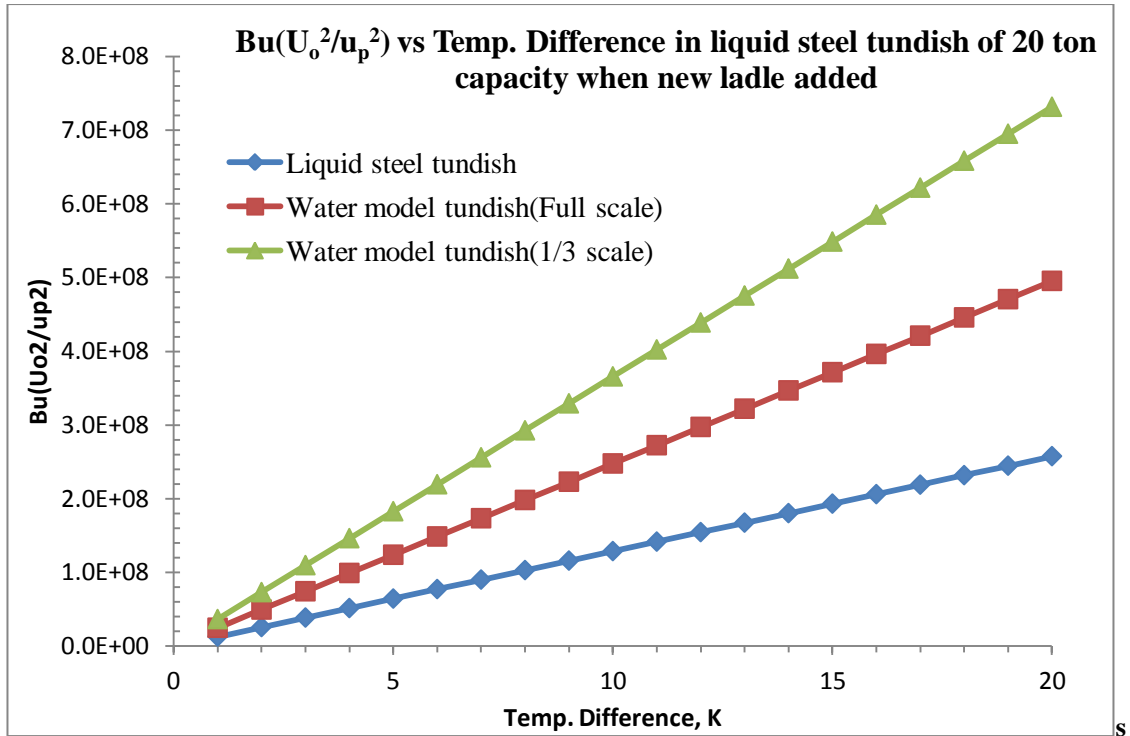


Figure 4.24. $Bu(U_o^2/u_p^2)$ vs. temperature difference in a liquid steel tundish steel, for a 20 tonne capacity when a new ladle containing fresh liquid steel is employed

4.3 Residence Time Distribution (RTD) Analysis

We obtained the residence time distribution (RTD) for various tundish configurations under isothermal and non-isothermal conditions. Residence time distribution is done by making an artificial fluid disturbance at the ladle shroud and evaluating the system response at the outlet (submerged entry nozzle) with time.

We predicted RTD curves for different tundish configurations with isothermal and non-isothermal conditions. Basically, it is a technique obtained by creating an artificial pulse in the inlet and evaluating the system's response at the exit of a SEN with respect to instantaneous time. The RTD curve, commonly known as the 'C' curve, is generally produced in a non-dimensional form of curve, e.g., dimensionless time and concentration set on the 'X' and 'Y' axes, respectively. The non-dimensional time can be measured by the ratio of instantaneous time and the mean residence time. In our case, the mean residence time was 355s. The non-dimensional concentration can be obtained by the ratio of instantaneous tracer concentration evaluated from conductivity meter and nominal concentration calculated by the mass of tracer dye added.

The theoretical or nominal residence time can be expressed as

$$\bar{t} = \frac{V}{Q}$$

where V is the volume of liquid in the tundish and Q is the volumetric flow of liquid. The non-dimensional mean residence time up to $\theta=2$ can be calculated as

$$\theta_c = \frac{\sum_{\theta=0}^2 C_i \theta_i}{\sum_{\theta=0}^2 C_i}$$

The mean residence time up to $\theta=2$ can be defined as: $t_m = \theta_c \times \bar{t}$

From the plotted RTD curves, we can also evaluate the percentage of plug, dead flow and mixed volume for each SEN. In our works, the percentage of plug, dead flow and mixed volume were calculated according to model suggested by Sahai and Emi [20].

$$\frac{Q_a}{Q} = \sum_{\theta=0}^2 C_i \Delta \theta$$

$$\frac{V_d}{V} = 1 - \frac{Q_a}{Q} \bar{\theta}_c$$

$$V_{dp} = \frac{\theta_{min} + \theta_{max}}{2}$$

$$V_m = 1 - V_{dp} - V_d$$

4.3.1 Isothermal Conditions of Tundish with different Flow modifiers

The isothermal experience of RTD test were performed in different tundish configurations, namely bare tundish, tundish fitted with MSIP and tundish fitted with MIIP. Each RTD curve is characterized by few peak values of concentration, known as "blips" that could be observed soon after the injection of tracer or after some time. After visualizing the few peaks, tracer concentration drop down with respect to time. The appearance of two peak values in the concentration-times curve is a clear indication of short circuiting in the tundish fluid flow system, as the incoming tracer with high concentration did not mix evenly within the tundish. That is recorded as a the higher concentration at the nozzle, leading to the very short residence times of some fluid particles. This phenomenon was observed largely when the tundish was being studied without any flow modifiers, i.e., a bare tundish.

During the RTD test, a high concentration of fluid was recorded at the inner strand (Fig.4.25) of a bare tundish soon after the injection of tracer, as a consequence of uneven mixing of fluid particles within the tundish. This phenomenon certainly harms the quality of steel, leading to more inclusions in the ingot. Since a bare tundish condition can be attributed to the highest peaks and the shortest residence times, representing uneven fluid mixing within the tundish. Furthermore, sharp peaks were observed up to half of the residence time that confirm the longer short circuiting flow, leading to higher amount of inclusions into the SEN's. This phenomena was verified in the tracer dispersion analysis discussed in the previous sections. Tundishes furnished with MSIP shown much less short circuiting flow. A comparatively reduced number of peak with moderate height were analyzed for this configuration (Fig. 4.26). However, it was observed that a tundish fitted with the MIIP facilitated a more balance concentration of tracer and longer mean residence time in the inner and outer strands of the RTD curves (Fig. 4.27). This is because, MIIP generates strong upward flows in the vicinity of the ladle shroud, retards any significant motions towards the bottom of tundish, as is normally observed in the bare tundish. These anticipated characteristics of fluid flow within the tundish could largely diminish the short circuiting effect, leading to better inclusion separation and removal in the size ranges from 50 μ m to higher sizes. To this end, it has been confirmed

through RTD experiments that, the mixing behavior in the tundish, especially the MIIP-tundish under isothermal conditions, might enhance the rate of inclusion flotation and could provide more clean steel.

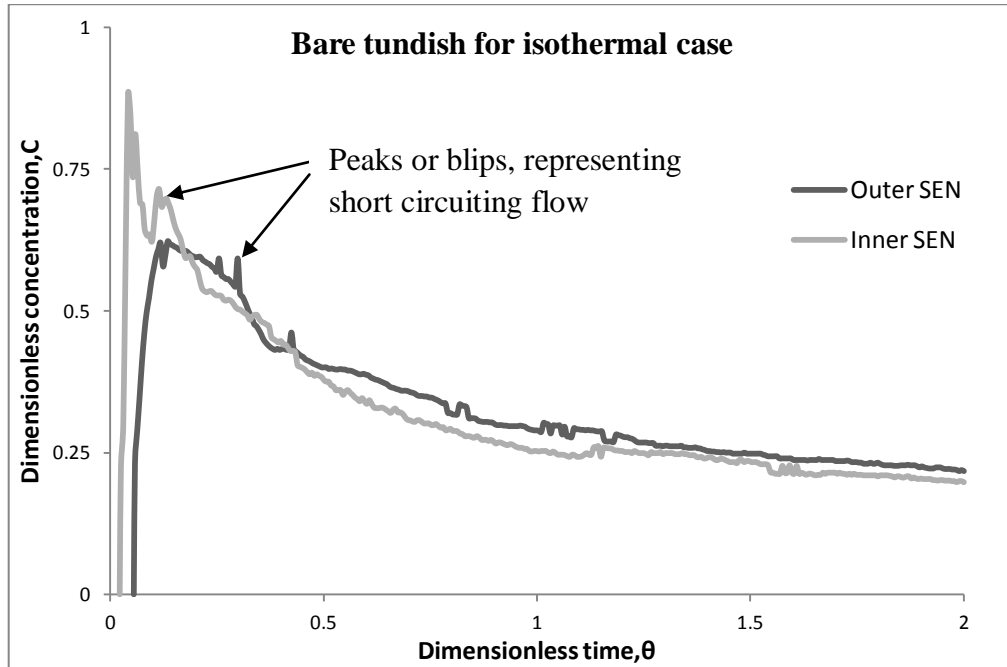


Figure 4.25. RTD curves for a bare tundish under isothermal conditions

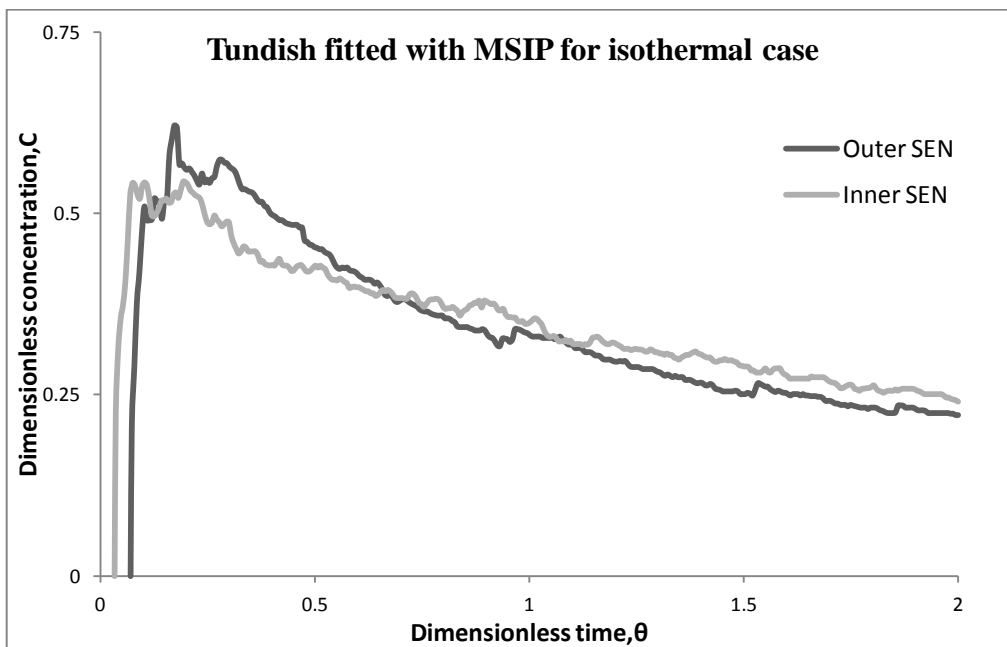


Figure 4.26. RTD curves for tundish fitted with MIIP under isothermal conditions

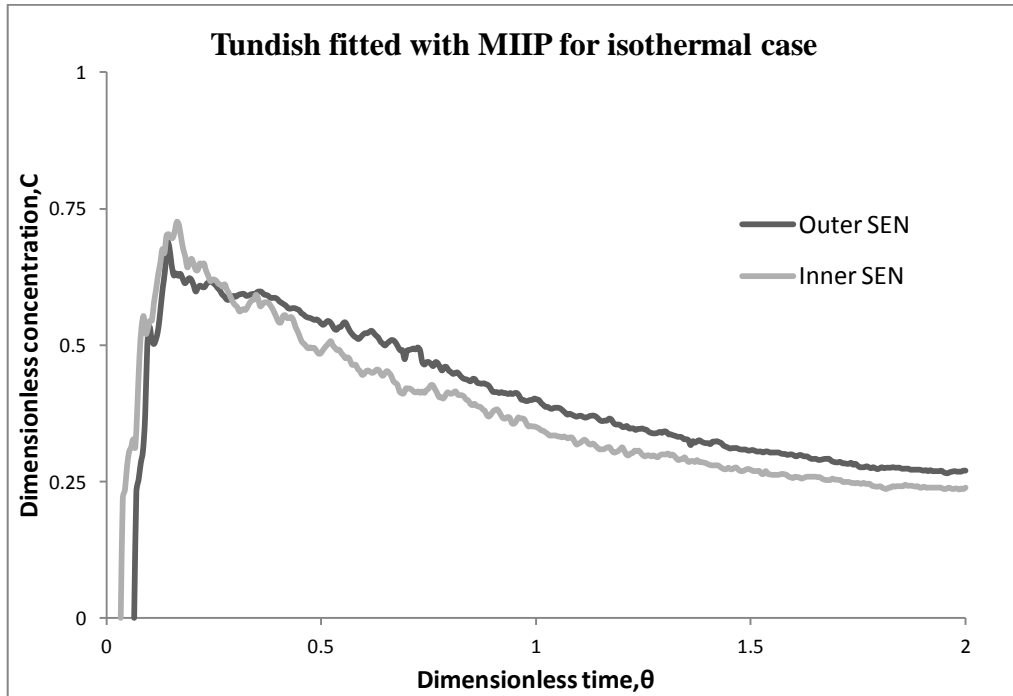


Figure 4.27. RTD curves for tundish fitted with MIIP under isothermal conditions

It has been suggested [54] that the optimum flow within the tundish should have large plug flow volume, high plug flow to dead volume ratio, comparatively large plug flow to mixed volume ratio and longer mean residence time. In the plug flow volume region, usually fluid particle mix in the transverse direction containing approximately identical residence time, as ladle shroud carrying incoming fluid located in the vertical plane. In the mixed volume region, maximum possible mixing is happened. In the dead volume zone, the fluid stays twice longer than the mean residence time, and is therefore treated as a slow moving region. The summation of plug flow region and well mixed region is termed as the active flow region.

The quantification of plug flow volume, mixed volume, dead volume, time for first appearance of tracer and time for maximum concentration of tracer are listed in Table-4.05. It is apparent that a tundish fitted with MIIP was observed to have the largest plug flow volume and longest mean residence time in the inner and outer strand. MSIP-tundish shown a less set of balance residence time in the both strands. Furthermore, tracer concentration of first appearance and maximum concentration of tracer are witnessed a

little later in a tundish equipped with a MIIP. However, the bare tundish exhibits a large difference in the volume fraction, attributing improper mixing of the fluid flow. This may result in more inclusions in the ingot. The inner strand, as a result of its closest position from ladle shroud, shows a higher short circuiting, and less plug flow volume and well mixed flow volume and in the outer strand, less short circuiting is depicted and increases the plug flow volume and well mixed flow volume, as it is located at a distant position from the entry shroud axes. The employment of the improved impact pad (MIIP) in a bare tundish significantly reduces the short circuiting, and exhibit higher plug flow volumes and well mixed flows both for the inner and outer strands. This is because of upward recirculation flows which are generated after fluid particles impact the side wall and front wall of the pad with higher momentum. In addition, a tundish furnished with MIIP holds fluid for more time before the observation of first and peak concentration is detected at the inner and outer SEN's.

Table 4.05: RTD parameters for different configurations of tundish under isothermal conditions

Tundish Configurations	SEN	t_{nominal} sec	t_{min} sec	t_{max} sec	t_{mean} sec	θ_c	Vp/V %	Vd/V %	Vm/V %
Bare tundish	Inner	355.5	8.4	13.6	163.5	0.46	3.10	65.32	31.57
	Outer	355.5	17.0	41.3	223.9	0.63	8.20	41.29	50.50
Tundish fitted with MSIP	Inner	355.5	13.2	17.6	181.3	0.51	4.33	58.61	37.05
	Outer	355.5	26.9	38.3	206.1	0.58	9.17	33.45	57.37
Tundish fitted with MIIP	Inner	355.5	14.9	21.4	191.9	0.54	5.12	48.63	46.25
	Outer	355.5	29.6	49.8	199.1	0.56	11.18	41.17	47.64

4.3.2 RTD curve in non-isothermal conditions of tundish with different flow modifiers

RTD curve were plotted for the non-isothermal step-up and non-isothermal step-down conditions, in order to analyze precisely fluid mixing phenomena within the tundish. These are discussed in the following sections.

4.3.2.1 Step up temperature of 10°C (+10°C)

Figure 4.29, 4.30 and 4.31 show the RTD curve that characterize the mixing of fluid within the tundish for different configurations. It is evident from tracer dispersion studies

discussed in the previous sections that non-isothermal step-up conditions can be beneficial due to density difference, as it enhances the upward forces generated within the impact pad region and delays the appearance of tracer in the SEN nozzles. However, during the RTD tests, a portion of the fluid elements with high concentration were observed at up to 0.25 times (approx.) of residence time (Figure 4.28) in the inner strand of a bare tundish, representing the existence of repeated short circuiting flows. There is also a secondary peak after 1.3 times (approx.) of the nominal residence time, which denotes inhomogeneity of fluid particle mixing within the tundish. Furthermore, incorporation of MSIP and MIIP didn't significantly reduce the short circuiting effect in this non-isothermal step up conditions, as shown in RTD curve illustrated in fig. 4.29 and 4.30. Since a tundish equipped with MSIP and MIIP form the short peak over the residence time in this non-isothermal condition that would drag some fluid elements towards the SEN without facilitating the unwanted particles to float in the free surface owing to inadequate residence time.

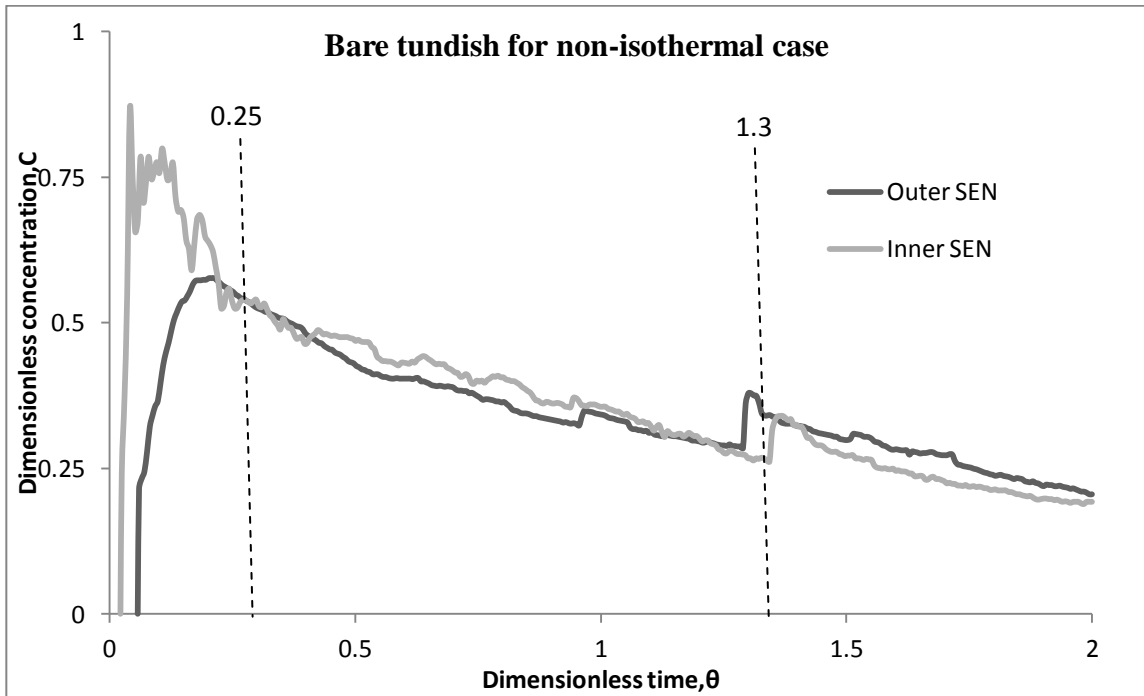


Figure 4.28. RTD curves for bare tundish under non-isothermal conditions with a step up temperature of $\Delta T = +10^{\circ}\text{C}$

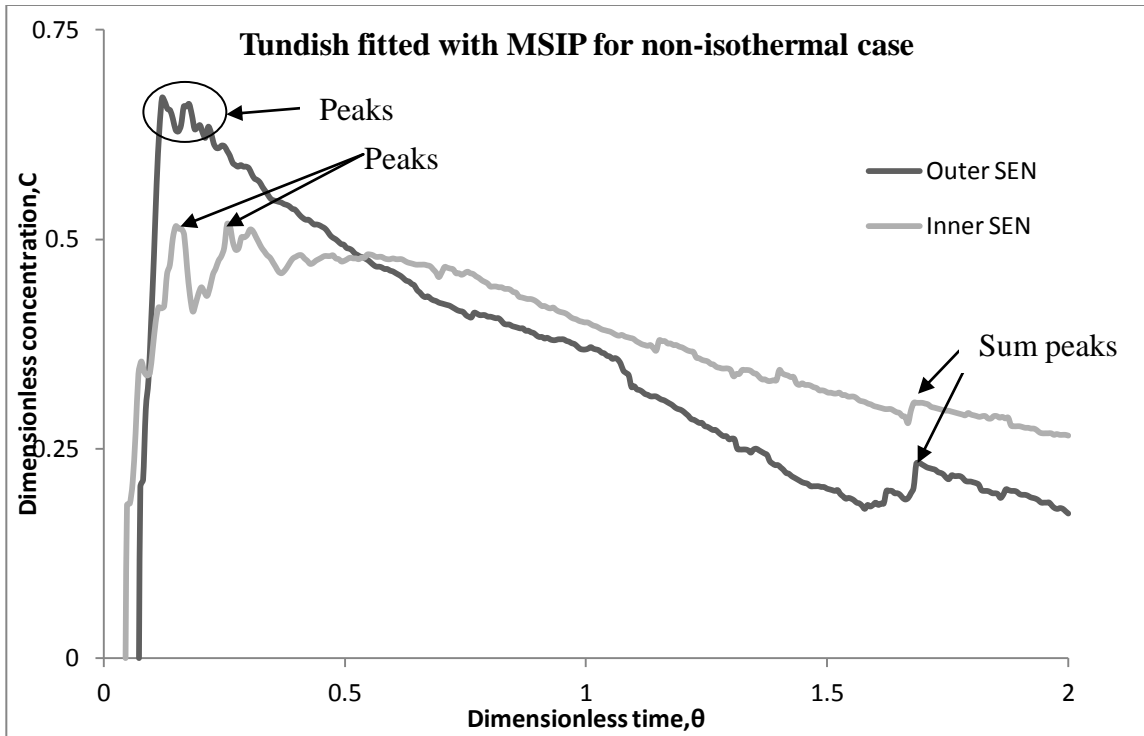


Figure 4.29. RTD curves for tundish fitted with MSIP under non-isothermal conditions with a step up temperature of $\Delta T = +10^{\circ}\text{C}$

Furthermore, a tundish employed with the MIIP depicts more peak concentration, attributing short circuiting effect in the outer strand compared to inner strand, as shown in Figure 4.30. This reason is that when lighter fluid hits the pad, the fluid particles redirect to the top surface and go towards the corner of the tundish. Hotter fluid loses heat in the cooler fluid through convective heat transfer process. Therefore, the outer strand, as a result of its distant position from the shroud axes records a higher short circuited flow, owing to density difference. Moreover, the incoming lighter fluid particle can't go directly towards inner strands due to the presence of the impact pad. So sharp peak is not observed for the inner strand RTD curve line. Finally it can be concluded that the non-isothermal condition of a step-up condition for a tundish could be beneficial so as to create a higher upward flow and a prolonged residence time. However, overall fluid mixing within the tundish is not quite as favorable in comparison with isothermal conditions, and this would undermine ingot quality containing inclusion, as tiny inclusions (size ranges from 20~100 μm) are enough for failure of any metal structure.

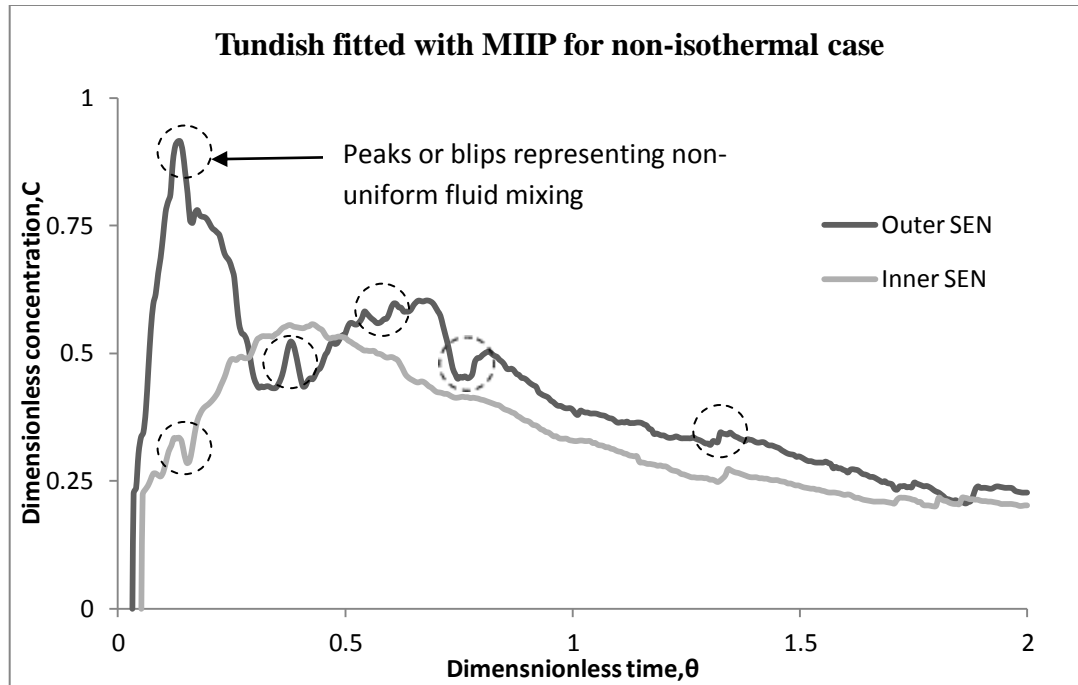


Figure 4.30. RTD curves for tundish fitted with MIIP under non-isothermal conditions with a step up temperature of $\Delta T = +10^{\circ}\text{C}$

4.3.2.1 Step down temperature of 10°C (-10°C)

Non-isothermal conditions of different tundish configurations (Bare tundish, tundish fitted with MSIP and MIIP) with 10°C temperature difference in between incoming fluid stream and existing fluid within the tundish were studied extensively with the help of the RTD curves. It was observed that there is a continuous peak and drop of concentration in the inner strands and outer strands, representing short circuiting flow or by pass flow in the RTD curve for all tundish arrangements (Fig. 4.31, 4.32 and 4.33). However, the interesting phenomenon is that the heavier incoming fluid did not change the overall fluid flow characteristics within the tundish soon after addition of cooler (low temperature) fluid.

When the bare tundish was considered, at approximately 20-25s, the heavier (colder) incoming tracer went down directly towards the SEN's without any impediment. This was confirmed by video analysis. In addition, continuous peaks of concentration and lower value of tracer concentration were noticed in the inner strands and outer strands, representing short circuiting flow in the RTD curve of all tundish arrangements (Fig.

4.31, 4.32 and 4.33). It seems that even generated upward velocity in the impact pad zone of the tundish-optimized impact pad (MIIP) configuration, might be unable to play enough role to prevent short circuiting flows in non-isothermal with negative temperature step input conditions. This is because, the upward flow can't overcome the downward force of the heavier incoming fluid. It also depends on the rate of transfer of the heat between the warmer and colder currents of liquid.

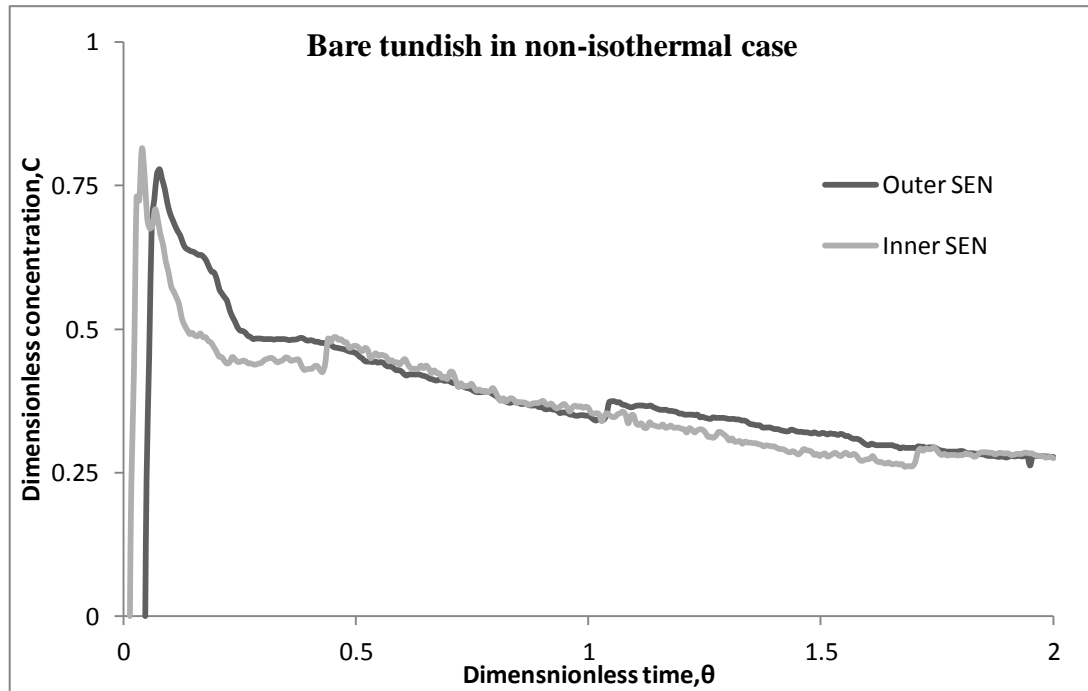


Figure 4.31. RTD curves for a bare tundish under non-isothermal conditions for a step down temperature of $\Delta T = -10^{\circ}\text{C}$

Moreover, this unfavourable mixing pattern has a severe effect on the inner strands, being the closest to the ladle shroud position, dragging more inclusions towards the SEN without proper filtration.

In a nutshell, non-isothermal condition with step down temperature of 10°C deteriorates the steel quality greatly, leading to more non-metallic particles in the ingot. So this case must be avoided in the plant, as this phenomena will reduce the flotation of inclusions, owing to, heavier incoming fluid dropping directly towards the SENs due to less residence time. If the temperature difference is higher than -10°C in the fluid

(water/steel) flow system, the effect on the extent fluid mixing will be even more catastrophic in terms of liquid metal cleanliness.

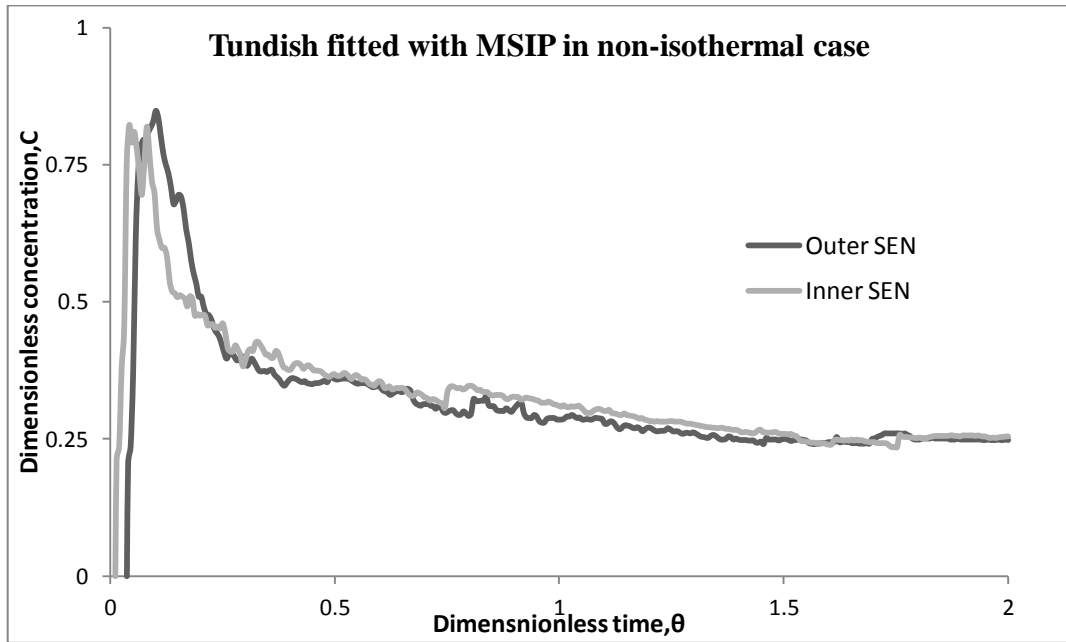


Figure 4.32. RTD curves for tundish fitted with MSIP under non-isothermal conditions for a step down temperature of $\Delta T = -10^{\circ}\text{C}$

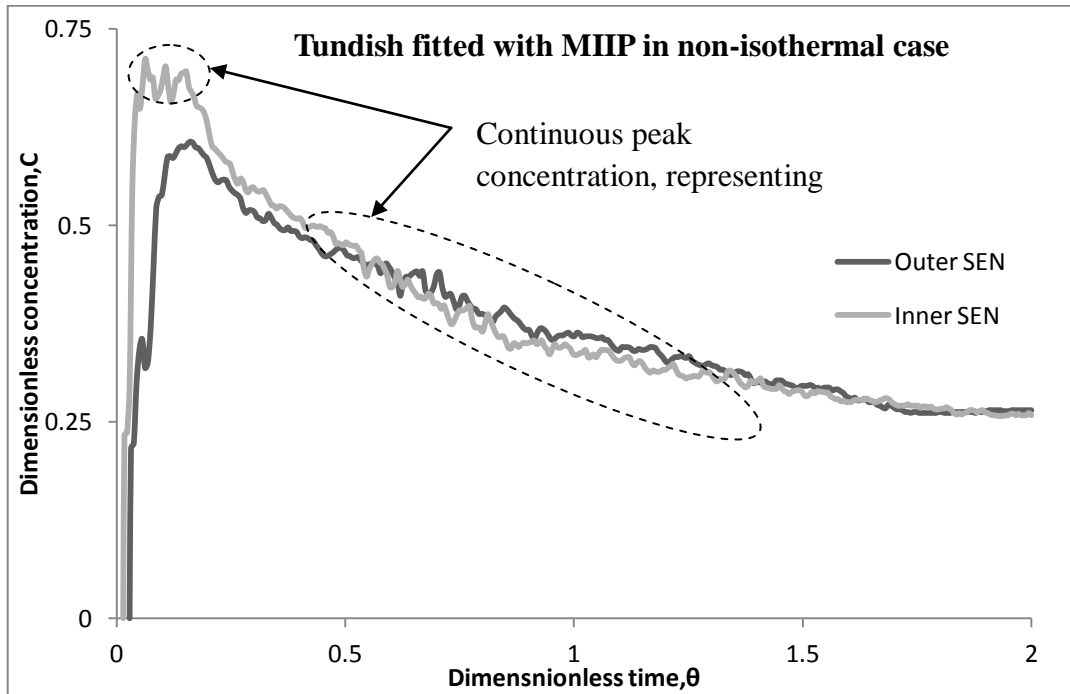


Figure 4.33. RTD curves for tundish fitted with MIIP under non-isothermal conditions for a step down temperature of $\Delta T = -10^{\circ}\text{C}$

Chapter 5.

CONCLUSIONS AND FUTURE WORK

5.1. Conclusions

Fluid flows in the 12 tonne tundish fitted with different flow modifiers were evaluated, using water model experiments, under isothermal and non-isothermal conditions. From the slag entrainment results, it has been observed that the 12t tundish fitted with an improved impact pad (MIIP) entrained lower amounts of slag in the SEN's, with a more even distribution of slag between the inner and outer nozzles, as compared to the tundish fitted the standard impact pad (MSIP). Furthermore, it was demonstrated that increasing the bath height of the tundish to raise the volume of liquid metal in a single heat could be beneficial in terms of lowering slag entrainment and liquid steel throughput .

From the red dye tracer experiments, it has been observed that a tundish without any flow modifiers (i.e.a bare tundish) generates strong recirculatory flows, especially to the inner nozzles. The best fluid flow pattern, which offer an even distribution of tracer to the four nozzles, was found for the tundish fitted with the optimized impact pad (MIIP). The vertical walls of the impact pad acts as a resistive wall to the flow, re-directing the fluid elements upwards to the surface. Under non-isothermal conditions, when incoming liquid steel with a higher temperature is charged into existing cooler steel in the tundish, upward buoyant force were generated that further facilitated inclusion flotation. In non-isothermal conditions, tundish fitted with MIIP could be a better option to improve steel cleanliness versus that observed in a bare tundish and in a tundish fitted with the MSIP. The buoyancy number could be introduced as a parameter to evaluate the significance of buoyancy forces that dominate the fluid flow behavior in a tundish, especially during non-isothermal conditions. Higher steel temperature differences (20°C) between the ladle and the tundish leads to a higher buoyancy number operating in the tundish. This can generate higher upward forces which are advantageous in terms of inclusion flotation. When temperature differences are in between 1-3°C, all the flow arrangements, including the increased capacity tundish, have practically equivalent buoyancy and inertial forces. At a low bath height (for a 12t capacity tundish), Bu increases very slowly with

temperature. Bu increases much faster at higher bath depths (18t and 20t capacity tundish), when the temperature difference between the incoming liquid steel and the existing cooler steel in the tundish is even smaller. So tundishes with a large volume of liquid metal should contain fewer inclusions exiting the SEN's, since the higher the upward recirculating flow, the higher is the tendency to drive some inclusions to the free surface that can be captured in the slag layer. However, when molten steel temperature within tundish is higher than that of incoming steel through the ladle shroud, the heavier incoming steel proceeds towards the SEN's, dragging more inclusions with it. This deteriorates the steel quality greatly, and the buoyancy forces become stronger with time.

By analyzing the residence time distribution (RTD) curves, it was possible to know details about the extent of fluid mixing within the tundish. It was found that the isothermal condition of tundish could provide higher mixing pattern than the extent of mixing patterns for the non-isothermal condition. This is because warmer fluid moves towards the free surface and cooler fluid drop down towards the bottom of tundish in the direction of SEN. A tundish fitted with the MIIP arrangement under non-isothermal conditions can provide better quality steel, as this types of impact pad generates strong upward flows. Moreover, severe short circuiting effects were depicted in the RTD curve for the non-isothermal step-down tundish condition and this was in good agreement with tracer dispersion experiments. So this condition must be avoided in the plant for improved quality steel. On the other hand, it can be concluded that a non-isothermal condition with step-up temperature inputs are beneficial, so as to create stronger upward flows and prolonged residence times. However, overall fluid mixing within the tundish is not as quite favorable in comparison with isothermal conditions, as some peaks existed in the RTD curves that would undermine ingot quality containing inclusion, as even tiny inclusions are enough for failure of any metal structure.

We repeated all experiments 3~5 times, so as to provide accurate data for further analysis. However, there was an experimental error, i.e. 5-7 % in our studies, caused by variations in the weights of entrained slag during slag entrainment tests, interfacing error of the reading of conductivity meter, thermocouple varying temperature, etc.

Nonetheless, all the experimental results were consistent and feasible enough for analyzing the metallurgical performance studies of the continuous casting tundish.

5.2 Future work

- The effect of flow modifiers on slag entrainment and RTD needs further investigation in the full scale tundish in order to achieve the processes for yielding better melt quality.
- Inclusion separation studies need to be performed using hollow glass microspheres in the ESZ PAS III instrument inclusion counter based on the electric sensing zone technique.
- For non-isothermal conditions in a tundish, plant data should be taken into consideration to evaluate the heat loss from the side wall, bottom wall and free surface of the tundish. Similarly, temperature variations between the different ladles of steel in the turret position to casting, must be evaluated by plant personnel.
- Visualizing instantaneous flows and velocity field measurement using PIV (Particle Image Velocimetry) in the water modeling experiment.
- Forward arching of the front vertical wall of the impact pad should be examined, as this is predicted to be an efficient technique to entrain smaller amounts of slag and inclusions in the SEN's, by dispersing the fluid along the tundish. This would increase the residence time of the fluid particles and redirect the flow towards the top free surface. In addition, an outwardly fitted horizontal sleeve near the top of the vertical wall would also be incorporated in the impact pad to evaluate the feasibility of the design, as it might provide better fluid flow within the tundish in terms of metal cleanliness, by uniformly distributing the melt flow across the tundish and would facilitate the inclusions flotation.
- Modeling the experimental results of tundish with a CFD study, using the commercially available Fluent code.

REFERENCES

1. Chatterjee, D., *Designing of a novel shroud for improving the quality of steel in tundish*, 2012: International Conference on Advanced Materials Processing - Challenges and Opportunities, AMPCO 2012. p. 359-363.
2. Thomas, B.G., "Continuous Casting," *The Encyclopedia of Materials: Science and Technology*. K.H. J. Buschow, R. Cahn, M. Flemings, B. Ilschner, E. J. Kramer, S. Mahajan, (D. Apelian, subject ed.) Elsevier Science Ltd., Oxford, UK, 2001. **Vol. 2, 2001**: p. 1595-1599.
3. Mazumdar, D. and R.I.L. Guthrie, *Physical and mathematical modelling of continuous casting tundish systems*. ISIJ International, 1999. **39**(6): p. 524-547.
4. Hou, Q., et al., *Modelling of inclusion motion and flow patterns in swirling flow tundishes with symmetrical and asymmetrical structures*. ISIJ International, 2008. **48**(6): p. 787-792.
5. Chattopadhyay, K., M. Isac, and R.I.L. Guthrie, *Physical and mathematical modelling of steelmaking tundish operations: A review of the last decade (1999-2009)*. ISIJ International, 2010. **50**(3): p. 331-348.
6. Sahai, Y. and T. Emi, *Tundish Technology for Clean Steel Production*. World Scientific Publication Co. Pte. 2008.
7. Kumar, R.S., *Water modeling studies to predict steel quality in a 4 strand delta-shaped tundish*. Masters Thesis, McGill University, Canada, 2006.
8. Guthrie, R.I.L., *Engineering in Process Metallurgy*. Oxford University Press, 1992.
9. Chatterjee, S.G.R.D.a.A., *Proc. of the Sixth Int. Iron and Steel Cong.* ISIJ.Tokyo, 1990. **3**: p. 197.
10. Zhang, L., et al., *Investigation of fluid flow and steel cleanliness in the continuous casting strand*. Metallurgical and Materials Transactions B: Process Metallurgy and Materials Processing Science, 2007. **38**(1): p. 63-83.
11. Mazumdar, D., et al., *Similarity considerations in the physical modelling of steel making tundish systems*. Steel Research, 1995. **66**(1): p. 14-19.
12. Yue, Q., et al., *Water Modeling of Swirling Flow Tundish for Steel Continuous Casting*. Journal of Iron and Steel Research International, 2009. **16**(5): p. 17-22.

13. Damle, C. and Y. Sahai, *A criterion for water modeling of non-isothermal melt flows in continuous casting tundishes*. ISIJ International, 1996. **36**(6): p. 681-689.
14. Sheng, D.Y., et al., *Water model study on convection pattern of molten steel flow in continuous casting tundish*. ISIJ International, 1998. **38**(8): p. 843-851.
15. Vargas-Zamora, A., et al., *Inertial and buoyancy driven water flows under gas bubbling and thermal stratification conditions in a tundish model*. Metallurgical and Materials Transactions B: Process Metallurgy and Materials Processing Science, 2004. **35**(2): p. 247-257.
16. Aguilar-Corona, A., et al., *Thermal stratification of steel flow in tundishes with off-centred ladle shrouds using different flow control designs*. Canadian Metallurgical Quarterly, 2003. **42**(4): p. 455-464.
17. Singh, S. and S.C. Koria, *Model study of the dynamics of flow of steel melt in the tundish*. ISIJ International, 1993. **33**(12): p. 1228-1237.
18. Levenspiel, O., *Chemical Reaction engineering*. Wiley International, New York, 1972.
19. Michálek K., V.V., Pindor J., Cieslar, *Application of physical modelling for optimisation of flowing at asymmetric tundish of CCM*. VŠB-Technical University Ostrava, Department of Metallurgy, Czech Republic.
20. Sahai, Y. and T. Emi, *Melt flow characterization in continuous casting tundishes*. ISIJ International, 1996. **36**(6): p. 667-672.
21. Sahai, Y. and R. Ahuja, *Fluid flow and mixing of melt in steelmaking tundishes*. Ironmaking and Steelmaking, 1986. **13**(5): p. 241-247.
22. Koria, S.C. and S. Singh, *Physical modeling of the effects of the flow modifier on the dynamics of molten steel flowing in a tundish*. ISIJ International, 1994. **34**(10): p. 784-793.
23. García-Hernández, S., et al., *Modeling study of the vortex and short circuit flow effect on inclusion removal in a slab tundish*. Steel Research International, 2010. **81**(6): p. 453-460.
24. García-Hernández, S., et al., *Modeling Study of the Vortex and Short Circuit Flow Effect on Inclusion Removal in a Slab Tundish*. steel research international, 2010. **81**(6): p. 453-460.

25. Mazumdar, D., G. Yamanoglu, and R.I.L. Guthrie, *Hydrodynamic performance of steelmaking tundish systems: A comparative study of three different tundish designs*. Steel Research, 1997. **68**(7): p. 293-300.
26. Sinha, S.K., et al., *Fluid flow behaviour in a water model tundish under open, submerged and modified inlet conditions*. Scandinavian Journal of Metallurgy, 2001. **30**(2): p. 103-107.
27. Chattopadhyay, K., M. Isac, and R.I.L. Guthrie, *Effect of flow modifiers on liquid metal cleanliness in four-strand delta shaped bille caster tundish*. Ironmaking and Steelmaking, 2012. **39**(6): p. 454-462.
28. Li, J., et al., *Study on geometric dimension design of multiheat teeming tundish for heavy steel ingots*. Ironmaking and Steelmaking, 2012. **39**(2): p. 140-146.
29. Zong, J.H., K.W. Yi, and J.K. Yoon, *Residence Time Distribution Analysis by the Modified Combined Model for the Design of Continuous Refining Vessel*. ISIJ International, 1999. **39**(1-2): p. 139-148.
30. Kumar, A., S.C. Koria, and D. Mazumdar, *An assessment of fluid flow modelling and residence time distribution phenomena in steelmaking tundish systems*. ISIJ International, 2004. **44**(8): p. 1334-1341.
31. Craig, K.J., et al., *Design optimization of a single-strand continuous caster tundish using residence time distribution data*. ISIJ International, 2001. **41**(10): p. 1194-1200.
32. Tripathi, A. and S.K. Ajmani, *Effect of shape and flow control devices on the fluid flow characteristics in three different industrial six strand billet caster tundish*. ISIJ International, 2011. **51**(10): p. 1647-1656.
33. Moumtez, B., A. Bellaouar, and K. Talbi, *Numerical Investigation of the Fluid Flow in Continuous Casting Tundish Using Analysis of RTD Curves*. Journal of Iron and Steel Research International, 2009. **16**(2): p. 22-29.
34. De Kock, D.J., K.J. Craig, and C.A. Pretorius, *Mathematical maximisation of minimum residence time for two strand continuous caster*. Ironmaking and Steelmaking, 2003. **30**(3): p. 229-234.
35. Kumar, A., D. Mazumdar, and S.C. Koria, *Modeling of fluid flow and residence time distribution in a four-strand tundish for enhancing inclusion removal*. ISIJ International, 2008. **48**(1): p. 38-47.

36. DeBlois, R.W., C.P. Bean, and R.K.A. Wesley, *Electrokinetic measurements with submicron particles and pores by the resistive pulse technique*. Journal of Colloid And Interface Science, 1977. **61**(2): p. 323-335.
37. Kim, H.B., *Modeling of Transport Phenomena in a Delta-shaped Four Strand Tundish*. . PhD thesis, McGill University, 2003.
38. Chattopadhyay, K. and M. Isac, *Dimensionless numbers for tundish modelling and the Guthrie number (Gu)*. Ironmaking and Steelmaking, 2012. **39**(4): p. 278-283.
39. Joo, S. and R.I.L. Guthrie, *Inclusion behavior and heat-transfer phenomena in steelmaking tundish operations: Part I. Aqueous modeling*. Metallurgical Transactions B, 1993. **24**(5): p. 755-765.
40. Joo, S., J.W. Han, and R.I.L. Guthrie, *Inclusion behavior and heat-transfer phenomena in steelmaking tundish operations: part III. applications-computational approach to tundish design*. Metallurgical Transactions B, 1993. **24**(5): p. 779-788.
41. Kouji Takatani, Y.S., Yoshihiko Higuchi ,Yoshinori Tanizawa, *Fluid flow, heat transfer and inclusion behaviour in continuous casting tundishes*. Modelling Simul Mater. Sci. Eng, 1993. **1**: p. 265-274.
42. Ray, S.K., M. Isac, and R.I.L. Guthrie, *Modelling performance of four-strand, 12 t, delta shaped continuous casting tundish fitted with different flow modifying arrangements for better steel quality*. Ironmaking and Steelmaking, 2011. **38**(3): p. 173-180.
43. Vargas-Zamora, A., et al., *Heat and mass transfer of a convective-stratified flow in a trough type tundish*. International Journal of Heat and Mass Transfer, 2003. **46**(16): p. 3029-3039.
44. Chattopadhyay, K., M. Isac, and R.I.L. Guthrie, *Considerations in using the discrete phase model (DPM)*. Steel Research International, 2011. **82**(11): p. 1287-1289.
45. Miki, Y. and B.G. Thomas, *Modeling of inclusion removal in a tundish*. Metallurgical and Materials Transactions B: Process Metallurgy and Materials Processing Science, 1999. **30**(4): p. 639-654.
46. Zhang, L., S. Taniguchi, and K. Cai, *Fluid flow and inclusion removal in continuous casting tundish*. Metallurgical and Materials Transactions B: Process Metallurgy and Materials Processing Science, 2000. **31**(2): p. 253-266.

47. López-Ramirez, S., et al., *Modeling study of the influence of turbulence inhibitors on the molten steel flow, tracer dispersion, and inclusion trajectories in tundishes*. Metallurgical and Materials Transactions B: Process Metallurgy and Materials Processing Science, 2001. **32**(4): p. 615-627.
48. Jha, P.K., P.S. Rao, and A. Dewan, *Effect of height and position of dams on inclusion removal in a six strand tundish*. ISIJ International, 2008. **48**(2): p. 154-160.
49. Solorio-Diaz, G., et al., *Modeling study of turbulent flow effect on inclusion removal in a tundish with swirling ladle shroud*. Steel Research International, 2009. **80**(3): p. 223-234.
50. Solorio-Díaz, G., R.D. Morales, and A. Ramos-Banderas, *Effect of a swirling ladle shroud on fluid flow and mass transfer in a water model of a tundish*. International Journal of Heat and Mass Transfer, 2005. **48**(17): p. 3574-3590.
51. Chattopadhyay, K., M. Isac, and R.I.L. Guthrie, *Physical and mathematical modelling to study the effect of ladle shroud mis-alignment on liquid metal quality in a tundish*. ISIJ International, 2011. **51**(5): p. 759-768.
52. Bul'ko, B., et al., *Influence of misalignment ladle shroud on tundish residence time*. Acta Metallurgica Slovaca, 2011. **17**(1): p. 51-57.
53. Chattopadhyay, K., M. Isac, and R.I.L. Guthrie, *Effect of submergence depth of the ladle shroud on liquid steel quality output from a delta shaped four strand tundish*. Ironmaking and Steelmaking, 2011. **38**(5): p. 398-400.
54. Singh, R.K., A. Paul, and A.K. Ray, *Modelling of flow behaviour in continuous casting tundish*. Scandinavian Journal of Metallurgy, 2003. **32**(3): p. 137-146.
55. Wen, G.H., et al., *Improvement of tundish shape and optimization of flow control devices for sequence casting heavy steel ingots*. International Journal of Minerals, Metallurgy and Materials, 2012. **19**(1): p. 15-20.
56. Yue, Q., Z.s. Zou, and Q.f. Hou, *Aggregation Kinetics of Inclusions in Swirling Flow Tundish for Continuous Casting*. JOURNAL OF IRON AND STEEL RESERACH -INTERNATIONAL-, 2010. **17**(5): p. 6-10.
57. Yang, S.F., et al., *Fluid flow in large-capacity horizontal continuous casting tundishes*. International Journal of Minerals, Metallurgy and Materials, 2010. **17**(3): p. 262-266.

58. Kam, D.H., et al., *Fluid flow analysis in horizontal continuous casting tundish*. Metals and Materials International, 2002. **8**(6): p. 535-541.
59. Merder, T. and J. Pieprzyca, *Optimization of two-strand industrial tundish work with use of turbulence inhibitors: Physical and numerical modeling*. Steel Research International, 2012. **83**(11): p. 1029-1038.
60. Rückert, A., et al., *Particle distribution and separation in continuous casting tundish*. Steel Research International, 2009. **80**(8): p. 568-574.
61. Joo, S., J.W. Han, and R.I.L. Guthrie, *Inclusion behavior and heat-transfer phenomena in steelmaking tundish operations: Part II. Mathematical model for liquid steel in tundishes*. Metallurgical Transactions B, 1993. **24**(5): p. 767-777.
62. Sheng, D.Y. and L. Jonsson, *Two-fluid simulation on the mixed convection flow pattern in a nonisothermal water model of continuous casting tundish*. Metallurgical and Materials Transactions B: Process Metallurgy and Materials Processing Science, 2000. **31**(4): p. 867-875.
63. Morales, R.D., et al., *Mathematical simulation of effects of flow control devices and buoyancy forces on molten steel flow and evolution of output temperatures in tundish*. Ironmaking and Steelmaking, 2001. **28**(1): p. 33-43.
64. Alizadeh, M., H. Edris, and A. Shafyei, *Fluid Flow and Mixing in Non-Isothermal Water Model of Continuous Casting Tundish*. Journal of Iron and Steel Research International, 2008. **15**(2): p. 7-13,22.
65. López-Ramírez, S., et al., *Physical and mathematical determination of the influence of input temperature changes on the molten steel flow characteristics in slab tundishes*. Metallurgical and Materials Transactions B: Process Metallurgy and Materials Processing Science, 2004. **35**(5): p. 957-966.
66. Solhed, H. and L. Jonsson, *An investigation of slag floatation and entrapment in a continuous-casting tundish using fluid-flow simulations, sampling and physical metallurgy*. Scandinavian Journal of Metallurgy, 2003. **32**(1): p. 15-32.
67. Morales, R.D., et al., *Mathematical simulation of the influence of buoyancy forces on the molten steel flow in a continuous casting Tundish*. Modelling and Simulation in Materials Science and Engineering, 2000. **8**(6): p. 781-801.